1-1-1986

Scattering studies of swollen polymer networks/

Vivek K. Soni
University of Massachusetts Amherst

SCATTERING STUDIES OF SWOLLEN POLYMER NETWORKS

A Dissertation Presented

By

VIVEK. K. SONI

Submitted to the Graduate School of the
University of Massachusetts in partial fulfillment
of the requirement for the degree of

DOCTOR OF PHILOSOPHY

February 1986

Department of Polymer Science and Engineering

SCATTERING STUDIES OF SWOLLEN POLYMER NETWORKS

A Dissertation Presented

By

VIVEK K. SONI

Approved as to the style and content by :

Richard S. Stein, Chairperson of Committee

Richard J. Farris, Member

William J. MacKnight, Member

Robert W. Lenz, Member

Edwin L. Thomas, Head
Polymer Science and
Engineering Department

Dedicated to my mother Leela
and my father Balbir, for their
encouragement, love and support.

ACKNOWLEDGEMENT

It is a great pleasure to express my gratitude and deepest appreciation to Professor Richard S. Stein for his guidance throughout the course of this work. I also wish to thank my dissertation committee members, Professors Richard J. Farris, William J. Macknight and Robert W. Lenz for their suggestions and encouragement.

I appreciate the cooperation and assistance I recieved from Dr. George Wignall, at ORNL, and from Drs. C. C. Han, C. Glinka and W. Wu, at NBS, regarding the neutron scattering measurements. Appreciation is also extended to Professor K. Langley and Matt Bishop for their valuable advice and assistance with light scattering measurements.

Many thanks are extended to my colleagues Satish, Cam, Chunduri, Hsinjin, Ravi, Murthy, Paula, Herve, Ray, Bill, Bruce, Kevin, Peter, Mitsu, Thien, Will, Ping, Yang, Joanna and Meir Ben Aliz for their help and friendship.

Financial support for this work from the Center for University of Massachusetts Industry Research in Polymers (CUMIRP) is greatly appreciated.

Finally, I would like to express my gratitude to my family, especially to my wife Ameeta, my mother-in-law Dr. Uma Narula and my brother Inder for their love, help and encouragement.

ABSTRACT

Scattering Studies of Swollen

Polymer Networks

(February 1986)

Vivek K. Soni

B.Tech., Indian Institute of Technology, New Delhi

M.S., University of Massachusetts

Ph.D., University of Massachusetts

Directed by : Professor Richard S. Stein.

Scattering methods were used to study the network structure in crosslinked polymer systems in an effort to characterize their homogeneity of crosslinking. The networks were swollen with a diluent to enhance the contrast. The scattering from swollen networks was compared to that from solutions containing the linear polymer at equivalent concentrations in the same diluent. In all the cases, the scattering from swollen networks is considerably greater than for the solutions.

Initial experiments were performed on dicumyl peroxide crosslinked polybutadienes and simple epoxy thermosets. The studies were extended to model PDMS networks which

offer greater control on the network architectrure.

Bimodal PDMS were prepared by mixing specific amounts of short and long chain prepolymers. The networks were swollen in benzene and in toluene and studied by light scattering (LS) and by small angle neutron scattering (SANS).

The SANS results from unimodal and bimodal PDMS networks revealed correlation sizes larger than the dimension of a chain between two crosslinks in the networks. Light scattering experiments were performed on flat tilted samples. The intensity of scattered light was observed to be much smaller than that calculated on the basis of network composition.

These results indicate that the local fluctuations in the polymer concentration in swollen networks are smaller than those predicted on the basis of the macroscopic theories of rubber elasticity. This suggests the need for taking into account the network structure in describing the local properties of a crosslinked polymer. The results are consistent with the network unfolding hypothesis proposed by Bastide for the deformation of network polymers.

TABLE OF CONTENTS

LIST OF TABLES

LIST OF FIGURES

C H A P T E R I

INTRODUCTION

Rubber elasticity is a property that is unique to polymers consisting of long, flexible chains. No substance otherwise constituted will sustain, without rupture, the high deformation that is typical of rubberlike materials, while simultaneously retaining the capacity to recover its original dimensions. Achieving recoverability requires preventing the chains from irreversibly sliding by one another. This is accomplished by joining different chains with crosslinks. Covalent crosslinks serve to bind the long chains into a permanent network structure.

It was recognized half a century ago [1] that rubber elasticity originates in the capacity of randomly coiled long chain molecules to adopt diverse configurations. Recovery from deformation is a manifestation of the chains to assume the most probable distribution of configurations. The retractive force is therefore considered to originate primarily in terms of the entropy of the chains rather than the forces of attraction between chains and their neighbors in the space they share. The elastic free energy of an elastomeric network is usually treated as the sum of the contributions of its individual chains. Therefore, the most important parameter describing the properties of a

network is the molecular weight of the chain between two crosslinks M_c.

Theories have been developed to describe the mechanical properties of amorphous networks and their swelling behavior in terms of an average M_c [2,3]. Over the years, there have been modifications in the theories to account for the fluctuation of the junction points, the role of network defects such as dangling chains and loops and the role of trapped entanglements in determining the equilibrium elasticity of a network [4].

Until recently, most of the polymer networks were prepared by random crosslinking processes. It was not easy to control the distribution of chain lengths between crosslinks in such networks. Recently, due to advances in synthesis procedures, it has been possible to prepare "model" networks by reacting end functional chains with small molecules of specific functionality.

Therefore, in principle, it is possible to prepare such networks with controlled M_c and functionality ϕ. Mark and coworkers [5-11] have performed extensive studies on model networks to test the various theories of rubber elasticity. A lot of their work has involved polydimethyl siloxane (PDMS) networks. In the case of unimodal networks, they have found that the macroscopic properties such as the stress and strain behavior could be described

reasonably well using the current theories [4].

In the case of bimodal PDMS networks, they obtained some very interesting results. The bimodal networks were prepared by mixing a predetermined fraction of short chains [M_n = 1000] with long chains [M_n = 20,000]. For high mole fractions of short chains, typically 90%, they found marked increases in modulus at high elongations [9-11]. This behavior is quite unexpected on the basis of affine deformation of gaussian chains. Affine deformation means that the macroscopic deformation ratio and the deformation ratio at the molecular level are equal.

On the basis of affine deformation, the short chains in the bimodal network are expected to reach their limit of extensibility and then break. However, in reality, the short chains are highly non gaussian. The deformation process seems to be such that the long chains take up most of the elongation resulting in large extension ratios and a high modulus at break. Therefore, the work by Mark and his coworkers has established the significance of the distribution of crosslink densities in determining the behavior of a network. The sketch of an inhomogeneously crosslinked network is given on Figure 1.

Although the theories of rubber elasticity work reasonably well at the macroscopic level, there are big discrepancies when they are tested at the molecular level

i.e., at the level of a chain length between crosslinks. Picot and coworkers [12,13] and Bastide [14,16] have used small angle neutron scattering (SANS) to measure the dimensions of a few labelled chains in networks.

In uniaxial deformation and swelling measurements, they find a molecular extension ratio much less than the macroscopic deformation ratio. For labelled paths which involve several crosslinks, they find that the deformation ratio is still less than affine although it is greater than the deformation ratio for a single chain between crosslinks.

Based on the SANS results, Bastide has proposed that network deformation takes place involving unfolding of chains or topological rearrangements such that the network chains do not have to deform significantly at a molecular level to still allow large macroscopic deformation. This implies that the network topology plays an important role in determining the overall properties.

It is the purpose of this work to study network topology with an emphasis on the homogeneity of crosslink density i.e., distribution of M_c. The study will primarily involve scattering methods. Different structural levels in a network can be probed by choosing radiations of different wavelengths such as light (λ = 5000 Å) and neutrons (λ = 5 Å). Usually, there is not enough contrast

in dry amorphous networks. Therefore, it is necessary to enhance the contrast for scattering. Since we are interested in the overall network structure, the contrast for this work is enhanced by swelling the network in a diluent which has a scattering power significantly different from that of the polymer comprising the network. Initial experiments were performed on randomly crosslinked polybutadiene networks. Studies were then extended to model PDMS networks. Preliminary studies of epoxy thermosets were also undertaken.

C H A P T E R II

REVIEW OF RUBBER ELASTICITY THEORIES

An understanding of the elasticity of rubber networks has developed over the years largely on the basis of the kinetic theories of rubber elasticity. It was realized that, in the case of non-crystallizable rubbers, the elastic free energy was determined primarily by the reduction in entropy of network chains upon extension. Thermoelastic measurements revealed that the contribution of internal energy was, except at small extensions, insignificant in comparison to the entropic term [17].

Affine Deformation

One of the earliest theories to be developed was that by Kuhn [1]. This is known as the " affine deformation " theory. In this theory, there are two major assumptions :

1) Each junction point may be fixed at its mean position in either the strained or unstrained state within a small volume element. The volume element is independent of the state of the strain.
2) The effect of the deformation is to change the components of the vector length of each chain in the same ratio as the corresponding dimensions of the bulk rubber

The expression for the stress of a particular state of deformation is developed by estimating the change in the Helmholtz free energy or the work of deformation. This involves the change in the entropy of the network chains which is obtained by adding together the contributions of the individual chains. The stress f in the case of the uniaxial deformation is given by:

$$f = v\,k\,T\left(\alpha - \frac{1}{\alpha^2}\right)$$

$$= \frac{\rho\,R\,T}{M_c}\left(\alpha - \frac{1}{\alpha^2}\right) \qquad (1)$$

where α is the deformation ratio, v is the number of chains per unit volume, ρ the density of the network, M_c the molecular weight between crosslinks and T is the temperature. Therefore, it is possible to measure M_c by measuring the modulus of a network.

Equilibrium Swelling

Another common method of estimating the crosslink density is by equilibrium swelling measurements. The equilibrium swelling of a network, immersed in a diluent, results from a balance between a free energy of dilution and a restoring elastic free energy. Flory and Rehner [18] developed the theory for equilibrium swelling assuming that

the free energy for dilution and the elastic free energy are additive.

$$\Delta F = \Delta F_{dil} + \Delta F_{el} = 0$$

$$= R\,T\left(\ln(1-v_2) + v_2 + \chi\, v_2^{\,2} + \frac{\rho\, \overline{V}_1\, v_2^{\,1/3}}{M_c}\right) \qquad (2)$$

where v_2 is the volume fraction of polymer in the swollen network, χ is the polymer solvent interaction parameter and $\overline{V}_1$ is the partial molar volume of the diluent.

Equation (2) is rearranged to give

$$M_c = \frac{-\rho\, \overline{V}_1 v_2^{\,1/3}}{\ln(1-v_2) + v_2 + \chi\, v_2^{\,2}} \qquad (3)$$

For high degrees of swelling , (small v_2)

$$v_2^{\,5/3} = \frac{\rho\, \overline{V}_1}{M_c\,(1/2 - \chi)} \qquad (4)$$

Using the Flory and Wall expression [19] for the elastic free energy of the network :

$$M_c = \frac{\rho\, \overline{V}_1 (v_2/2 - v_2^{\,1/3})}{[\ln(1-v_2) + v_2 + \chi\, v_2^{\,2}\,]} \qquad (5)$$

This equation differs from equation (3) by an additional term $v_2/2$ in the numerator. The difference is caused by taking into account the dispersions of the junctions over the volume of the deformed (swollen) network.

Phantom Network Model

In the affine deformation theory, it was assumed that the junction points were fixed. In reality, the junction points were not fixed, but take part in the micro-brownian motion of the chain elements. To take into account the fluctuation of the junction points, James and Guth [20] developed a theory which is now called the "Phantom network theory" of rubber elasticity. The main features of their theory are:

i) The junctions are allowed to fluctuate about their mean positions and the magnitude of the fluctuations is independent of the strain. Only the functions on the surface are fixed.

ii) The mean positions of the junction points are deformed affinely.

iii) The average forces exerted by the network are the same as would be produced if each chain was replaced by a classical elastic spring exerting a tension proportional to its length.

The theory gets its name due to the third assumption which implies that the chains move freely through each other (no entanglements). This, however, would suggest that in the absence of other forces, a network should collapse to zero volume. According to James and Guth, the network collapse is prevented by the internal pressure

developed in the network by the interatomic forces of the same kind as those existing in an ordinary liquid.

The prediction of the Phantom network theory for the modulus G is:

$$\begin{aligned} G_{ph} &= (\nu - \mu) \; R \; T \\ &= \Lambda \; R \; T \\ &= \nu \; R \; T \; (1 - 2/\phi \;) \end{aligned} \qquad (6)$$

where ν and μ are the number of chains and the number of junctions per unit volume, and ϕ is the network functionality. Λ is called the cycle rank of the network. The cycle rank of a network is defined as the number of chains that have to be cut to reduce the network to an acyclic structure or tree. Flory [21] realized that there may be defects such as loops or dangling chains in networks. The dangling chains can be accounted for in estimating the number of elastically effective chains. According to Flory

$$\nu_a = \nu_o \; (1 - 2 \; M_c/M) \qquad (7)$$

where ν_a and ν_o refer to the number of elastically effective and the total number of chains respectively. M is the molecular weight of the molecules before crosslinking. Such an expression holds for random crosslinking where M is large and a sufficient number of crosslinks are formed.

Flory's New Molecular Theory

Experimental measurements of the stress versus the macroscopic deformation ratio α in uniaxial extension have revealed that the behavior of the real networks is between the affine and the phantom limits. A common way to represent the data is in terms of the phenomenological Mooney-Rivlin equation [22]:

$$\frac{f}{(\alpha - 1/\alpha^2)} = [f^*] = 2C_1 + \frac{2C_2}{\alpha} \qquad (8)$$

The constants $2C_1$ and $2C_2$ have been obtained for several systems, but no convincing molecular explanation had been found until recently. In the recent molecular theory due to Flory [23-25], restrictions on the fluctuations of junctions due to the neighboring chains are represented by domains of constraints. At small deformations, the fluctuations of the junction points are suppressed due to the constraints imposed by the trapped entanglements. Therefore, the stress is enhanced relative to that exhibited by a phantom network. At large strains or at high dilation, the effects of the restrictions on fluctuations vanish and the stress becomes equal to that expected for a phantom network.

The reduced stress is therefore expressed as :

$$[f^*] = f_{ph} \left(1 + f_c / f_{ph} \right) \qquad (9)$$

where f_{ph} is the modulus for a phantom network and

f_c / f_{ph} is the ratio of the force due to the entanglement constraints to that for the phantom network. The ratio depends on two parameters κ and ζ. κ measures the severity of the entanglement constraints relative to those imposed by the phantom network. ζ takes into account the non affine transformation of the domains of constraints with strain. $\kappa = 0$ and $\kappa = \infty$ correspond to the phantom network and the affine model respectively.

In uniaxial extension :

$$\frac{f_c}{f_{ph}} = \frac{\mu}{\Lambda}\left(\frac{\alpha\, K_1(\alpha_1^2) - \alpha^{-2} K_1(\alpha_2^2)}{(\alpha - \alpha^{-2})}\right) \qquad (10)$$

where $\alpha_1 = \alpha$; $\alpha_2 = \alpha^{-1/2}$.

For a perfect network :

$$\frac{\mu}{\Lambda} = \frac{2}{(\phi - 2)}$$

The function $K_1(\alpha^2)$ is given by :

$$K_1(\alpha^2) = B\left[\frac{\dot{B}}{1+B} + g\,\frac{(\dot{g}B + g\dot{B})}{1+gB}\right] \qquad (11)$$

where

$$g = \alpha^2\,[(1/\kappa) + \zeta\,(\alpha - 1)]$$

$$B = \frac{(\alpha - 1)\,(1 + \alpha - \zeta\,\alpha^2)}{(1+g)^2}$$

and $\dot{g} = \dfrac{\partial g}{\partial \alpha^2}$ and $\dot{B} = \dfrac{\partial B}{\partial \alpha^2}$

The typical plot of [f*] vs α^{-1} is sigmoidal. This theory has had reasonably good success in fitting data for elongation and compression. Typically κ is found to be on the of the order 5-10. Erman and Flory [25] have suggested that $\kappa[f^*_{ph}]$ should be a constant.

Role of Entanglements

The molecular theory developed by Flory and Erman [26] suggests that the role of trapped entanglements is to basically restrict the fluctuations of the junctions about their mean positions. They claim that trapped entanglements do not contribute to the equilibrium elasticity of a network. There are several workers [27-32] such as Langley, Grassley, Ferry, Macosko and others who believe that trapped entanglements do contribute to the equilibrium modulus of a network.

The small strain modulus is expressed as a sum of two terms :

$$G = G_x + G_e T_e \qquad (12)$$

where G_x is the term due to the chemical crosslinks. The second term arises from the permanently trapped entanglements. G_x can be written as :

$$G_x = v\ R\ T\ (\ 1 - h\ \mu/v\ ) \qquad (13)$$

where h is an empirical parameter, such that h = 1 and h = 0 correspond to the phantom and affine deformation

limits respectively. T_e is the probability that the trapped entanglements are elastically active. G_e is a modulus thought to have a value close to the plateau modulus G_N^o for linear polymers with high molecular weight. It is possible to estimate T_e from branching theory [31] for networks prepared by end linking reactions (model networks). Equation (12) can be written as :

$$\frac{G}{T_e} = \frac{\nu R T}{T_e}\left(1 - \frac{h\mu}{\nu}\right) + G_e \qquad (14)$$

The Langley plot can be obtained by plotting the data as G/T_e vs $\nu RT/T_e$. h and G_e can be estimated from the plot. G_e is frequently found to be close to G_N^o, the plateau modulus in dynamic measurements, which is taken to suggest the existence of an entanglement contribution.

The parameter h in equation (13) and the parameter κ in the Flory theory deal with the severity of constraints on the junction points. Gottlieb and Macosko [33] have recently developed an analytical expression of h as a function of for a perfect network :

$$h = 1 - \frac{[(2 - \zeta)^2 (1 + 1/\kappa^2)]}{4 (1 + 1/\kappa)^4} \qquad (15)$$

Although, it is now possible to compare the parameters in the two theories, the major disagreement remains about the role of the G_e term in equation (12). Flory, Mark and coworkers feel that there should be no such term for

measurements made at equilibrium .

Crystallization and Non Gaussian Effects at Large Strains

The theories by Flory and Erman and by Grassley and coworkers are based on the assumption of Gaussian statistics for the distribution of the end to end vectors of the network chains. Such an assumption is usually reasonable for long chains with moderate extents of deformation. The non gaussian effects have to be taken into account for short chains and high extension ratios.

The non gaussian statistics result in an upturn in the force extension curve at large extensions [2]. The upturn can also be caused by strain induced crystallization as in the case of natural rubber. In general, the effect of crystallization, on the shape of the force - extension curve, will depend on the precise manner in which the measurements are made [2].

If a rubber is stretched to a given extension and the chains are allowed to relax to their equilibrium positions before crystallization begins (by raising the temperature), the process of crystallization will lead to a reduction in the tension. However, if crystallization takes place during stretching, the effects are more complex. First, there is the tendency for further crystallization leading to a reduction in tension, and secondly, there is an

increase in the effective crosslink density which will tend to increase the tension.

Flory [34] has developed a theory which yields expressions for the equilibrium degree of crystallinity and for the applied stress as functions of the amount of strain and the temperature. More recent theories have been developed by Smith [35] and by Ziabici et al [36] for the crystallization of stressed rubbers.

It is possible to study non gaussian effects at large extensions by working with the non crystallizable elastomers or by working well above the melting points of crystallizable rubbers. Recently Mark and coworkers [9-11] have studied bimodal model PDMS networks. These are prepared by mixing very short and long chains and crosslinking them at the end using a linking agent of a specific functionality.

For specific compositions of the short chains (90 mole %), they observed a marked increase in the ultimate properties as compared to the unimodal networks. The enhancement of the mechanical properties is not due to a filler effect due to the short chains. If this had been the case, segregating the short chains would have resulted in an enhanced modulus. Experimentally, it was found that significant segregation of the short chains actually caused a decrease in the force at rupture. The increased modulus

is believed to be caused by the limited extensibility of the short chains which causes the long chains to take up most of the deformation. The deformation in such networks is, therefore, highly non-affine.

Mark and Curro [37,38] have recently tried to theoretically predict the deformation in bimodal PDMS networks. They consider the average chain deformation to be affine. However, the deformation is partitioned non-affinely between the short and long chains to minimize the free energy. They used gaussian statistics for the long chains. The distribution function for the short chains is found from Monte Carlo simulations using the rotational isomeric state [39] model for PDMS. The results of the simulations are in qualitative agreement with their experimental results. The differences are possibly due to the assumption that the average deformation is affine.

Network Unfolding

Bastide, Picot and coworkers [12-16] have used small angle neutron scattering (SANS) to test the theories of rubber elasticity at the molecular level (Chapter 3). They found that the deformation of a labelled chain in between crosslinks was much less than the macroscopic deformation. This means that there is some kind of a threshold path length in a network below which the deformation is less

than affine. From SANS experiments involving long labelled paths, it seems that such a threshold path length must be several times longer than a single chain between two crosslinks.

The deformation process is visualized by Bastide [14-16] to involve large scale topological rearrangements. He suggests that the elastic free energy is determined by the entropy of all the chains and not by just a summation of the entropy of the individual chains.

These new findings by Picot and coworkers using SANS, have therefore, added a new dimension to the controversies in the theories of rubber elasticity . They seem to suggest that some of the most basic assumptions used in the theories, past or present, may not be correct.

C H A P T E R III

SCATTERING : THEORY AND EXPERIMENTS

When a beam of a particular radiation is incident on a sample some of it gets transmitted, some absorbed and some scattered. The scattered fraction depends on the type of radiation and the composition of the sample. Over the years, scattering methods have been used extensively to study the structure of materials. The commonly used types of radiation include light, x-rays and neutrons.

The intensity of the scattered beam for the three kinds of radiation listed above can be described in general as:

$$I(q) = K \sum\sum z_i \, z_j \exp (i\tilde{q}.\tilde{r}_{ij}) \qquad (16)$$

Here, one is concerned with the interference between scattering elements located at points i and j and having scattering powers z_i and z_j respectively. $\tilde{r}_{ij}$ is the vector connecting the two points. $\tilde{q}$ is the scattering vector, the magnitude of which is defined as:

$$q = [4\pi \sin(\theta/2)]/\lambda$$

where θ is the scattering angle and λ the wavelength of the radiation used. K is a constant which will depend on the type of radiation used and the experimental conditions. It is convienient to measure the scattered intensity in terms of a Rayleigh ratio R(q), which is

defined as:

$$R(q) = (I_s(q)\ S^2) / (I_o\ V) \qquad (17)$$

where the subscripts s and o refer to the scattered and incident beams. V is the scattering volume and S is the distance berween the sample and the detector.

The scattering power is different for different types of radiation. In case of neutron scattering, it is associated with the nature of the scattering nucleus and is called the scattering length. For x-ray scattering, the scattering power is the electron density and for light scattering it is the polarizability or refractive index. Since these three properties differ for a given system for the different sorts of radiation, various structural elements will be weighted differently through their use. In this work we have used neutron scattering and light scattering.

The description of the scattered intensity as a function of the scattering angle θ for a particular system involves the estimation of the double summation in Eqn. (16). Two approaches can be used to perform the calculations for the structure factor. These are :

a) Calculation of the structure factor analytically from a predetermined model for the system. Such an approach is most applicable for dilute random dispersions of particles wherein inter particle

interferences are negligible.

b) For non particulate systems or at high concentrations of inclusions, a statistical approach is preferable. In this method, one considers the scattering which arises from fluctuations in the scattering power throughout the material.

This is the approach that will be followed for most of this work.

If $\overline{z}$ is the average scattering power and z_i is the local scattering power, then the local fluctuation in the scattering power will be:

$$\eta_i = z_i - \overline{z} \qquad (18)$$

For isotropic, inhomogeneous materials one has the familiar Debye [40] result for the Rayleigh factor:

$$R(q) = 4\pi K \eta^2 \int_0^\infty \gamma(r) \frac{\sin qr}{qr} r^2 \, dr \qquad (19)$$

Here η^2 is the mean squared fluctuation in the scattering power. $\gamma(r)$ is a correlation function which is defined as :

$$\gamma(r) = \left[\frac{<\eta_i \ \eta_j>_r}{\eta^2}\right] \qquad (20)$$

where $<\ >_r$ represents averaging over all scattering elements i and j separated by a distance r. In terms of a material having a two phase structure, the correlation

function $\gamma(r)$ represents the probability that a rod of given length, r, will have both its ends in the same phase.

For $r = 0 \quad \gamma(0) = 1$ (21

$r = \infty \quad \gamma(\infty) = 0$

Therefore, such a function contains all the information regarding spatial correlations of scattering elements within the material under study. The scattering is then completely defined in terms of the mean squared fluctuation in the scattering power and the correlation function $\gamma(r)$.

The correlation funciton can be obtained from the scattering data by taking the inverse fourier transform of the scattered intensity as:

$$\gamma(r) = \frac{1}{2\,\pi^2 K\,\eta^2} \int_0^\infty q^2\, R(q)\, \frac{\sin qr}{qr}\, dq \qquad (22)$$

Typically, one needs scattering data over a reasonably wide q range to extract such a function.

The Exponential Correlation Function

In the case of random, isotropic, two phase systems with sharp boundaries, Debye, Anderson and Brumberger [41] have shown that the correlation function can be expressed as an exponential function:

$$\gamma(r) = \exp - r / a_c \qquad (23)$$

where a_c is a correlation size which is defined as :

$$a_c = 4V \phi_1 \phi_2 / S$$

where ϕ_1 and ϕ_2 are the volume fractions of the two phases and (V/S) represents the ratio of the volume to the internal surface. Substitution of eqn. (23) into eqn. (20) gives the Debye Bueche [40] result:

$$R(q) = \frac{8\pi K \eta^2 a_c^3}{(1 + q^2 a_c^2)^2} \qquad (24)$$

If the data is plotted as a Debye Bueche plot i.e. $R(q)^{-1/2}$ vs q^2, one can estimate:

a) a_c^2 = slope / intercept

b) η^2 from the intercept

For dilute dispersions of one component in another, a_c may be taken as a measure of the size of the dilute component. For concentrated dispersions, the correlation size is best interpreted in terms of the chord lengths as given by Porod and Kratky [42].

$$a_c = L_1 \phi_2 = L_2 \phi_1$$

$$\text{or} \quad \frac{1}{a_c} = \frac{1}{L_1} + \frac{1}{L_2} \qquad (25)$$

where L_1 and L_2 are the average lengths of the random chords passing through the two phases.

In eqn. (24), at large q, $R(q) \sim 1/q^4$ in agreement with Porod's law. Negative deviations from such a behavior can be used to estimate the finite size of the boundary thickness between the two phases [43,44].

Although the exponential form of the correlation

function is defined rigorously for a random, isotropic, two phase system with sharp boundaries, it can be used to adequately describe the scattering from random, isotropic, multicomponent systems without sharp boundaries. Then, the interpretation of a_c becomes some what ambiguous.

In certain cases, especially at moderate concentrations of inclusions or the second phase, it is found that a single correlation size is not adequate and the correlation function can be described by at least two correlation sizes [41,45]

$$\gamma(r) = u \exp(-r/a_1) + (1-u) \exp(-r^2/a_2^2) \qquad (26)$$

where the correlation sizes a_1 and a_2 are associated with intra - and inter - particle correlations. The choice of the gaussian term representing the inter particle interference is quite arbitrary and could have very well have been an exponential function. Yuen and Kinsinger [46] have listed several functions which satisfy the basic properties of correlation functions i.e. eqn (21) Therefore, the correlation function could be considered in terms of distribution of correlation sizes. This can be represented in terms of a discrete distribution as

$$\gamma(r) = \sum u_i \exp(-r/a_i) \qquad (27)$$

where u_i represents the fraction of terms with size a_i.

The correlation distribution can be alternately expressed in terms of a continuous distribution as :

$$\gamma(r) = \int_0^\infty u(a) \exp(-r/a)\, da \qquad (28)$$

Such a representation is analogous to the representation of the spectrum of relaxation times in polymer viscoelasticity [47] or in quasi elastic light scattering. Therefore, standard analytical methods can be used to obtain the distribution of correlation sizes if data is available over a wide q range.

Light Scattering

When an electric field E is incident on a material, it induces a dipole $\hat{m}$, whose magnitude depends on the polarizability p of the material. Since the frequency of visible light w is less than the resonant frequency w_o of electrons, the intensity of the scattered radiation is dependent on w and on wo in terms of the polarizability $p = e_o^2 / M_o w^2$. Here M_o is the mass of an electron of charge e_o. Due to the wavelength dependence of scattered light, light scattering is usually referred to as Rayleigh scattering after Lord Rayleigh who used the wavelength dependence to explain the colour of the sky.

The resonant frequency w_o is related to the force constant K which holds the electron in place ($w_o = K/M_o$). The distribution of electrons is anisotropic which results in an anisotropic value for the

force constant. The polarizability p is therefore a tensor quantity.

$$\hat{m} = \underline{\underline{p}}\ \tilde{E} \qquad (29)$$

For an anistropic material, the three principal polarizabilities p_1, p_2 and p_3 can be reduced to two p_1 and p_3 in the case of cylindrical symmetry. Let $\hat{d}$ be the unit vector along the principal axis denoted by subscript 1. The anisotropy δ is then equal to $(p_1 - p_2)$. For such a system the induced dipole moment will be

$$\hat{m} = \delta (\hat{d} . \tilde{E}) \hat{d} + p_2 \tilde{E} \qquad (30)$$

If $\tilde{o}$ is the unit vector in the direction of polarization of the scattered light after passing through the analyser, then the scattering amplitude can be described as:

$$E_s = K' \hat{m} . \tilde{o} \qquad (31)$$

The scattered intensity is given by the expression:

$$I_s = K E_s E_s^* = K (\hat{m} . \tilde{o})^2 \qquad (32)$$

where E_s^* is the complex conjugate of E_s.

Let us consider the case of scattering of light for a vertically polarized incident beam. If the analyser is horizontal, the scattering geometry will be referred to as H_v and scattering will arise due to the anisotropy in the material. However, if the analyser was vertical, the geometry will be referred to as V_v and will contain

contributions due to isotropic and anisotropic polarizability fluctuations.

Therefore equation (32) can be used to estimate the intensity of the scattered light from anisotropic molecules for the H_v and V_v geometries.

$$I_{H_v} = K E^2 \delta^2/15$$

$$I_{V_v} = K E^2 [\bar{p}^2 + 4 \delta^2/45] \qquad (33)$$

where $\bar{p} = (p_1 + 2p_2)/3$

The isotropic scattering for a system possessing some anisotropy can be obtained by rearranging equation (33) as follows:

$$I_{iso} = I_{V_v} - 4I_{H_v}/3 \qquad (34)$$

The isotropic scattering can then be analysed using the Debye Bueche approach as described in previous sections.

The analysis so far has an implicit assumption, that the direction of the incident field is unmodified in crossing the boundary of the scattering particle. This is the "Rayleigh-Gans approximation." This is a good approximation for x-rays and neutrons and applies for light provided that there is not too much polarizability or refractive index difference between the particle and its surrounding and / or that the size of the particle is not too large as compared to the wavelength of the radiation. More exact theories have been developed by Mie and others [48,49] to describe the situation when the Rayleigh Gans

approximation is no longer valid.

Light Scattering from Solutions and Swollen Networks

Pure Liquids : In a gas, each molecule can be considered as an incoherent, randomly located scattering center. The total scattered intensity from a gas is therefore the sum of the intensities from each molecule. This is no longer the case for a liquid in which the molecules are not completely incoherent, randomly located scatterers.

The local density in a liquid is not constant. The distribution of molecules in any given small volume element will vary with time because of the thermal motion. As in equation (18), the local density can be considered to consist of two contributions. The major part is the macroscopic or average density and this is uniform throughout the liquid; superimposed upon this is a fluctuation from the average which varies in an irregular manner. There is no light scattering from the uniform part.

If the density fluctuations in each volume element are random, they can be considered as incoherent scatterers and each volume element will contribute additively to the scattering like the gas molecules. This is called the

fluctuation approach and was developed by Einstein [50] to account for the phenomenon of critical opalescence. The magnitude of the density fluctuations will depend on the bulk compressibility β. Therefore the intensity of scattered light from a pure liquid will depend on and the refractive index n, both of which are functions of temperature. Since this scattering is due to density fluctuations only, we will denote it by a subscript d.

$$R_{Total} = C_F R_d$$

$$R_d = \frac{\pi^2 k T \beta [\rho (\partial \epsilon / \partial \rho)_T]^2}{\lambda_o^4} \qquad (35)$$

where λ_o is the wavelength in vacuo, k is the Boltzmann constant and ϵ is the optical dielectric constant $(=n^2)$. The Eykman expression [48,52] can be used for $\rho(\partial \epsilon / \partial \rho)_T$ which is

$$\rho(\partial \epsilon / \partial \rho)_T = \frac{[2n (n + 0.4) (n^2 - 1)]}{(n^2 + 0.8n + 1)} \qquad (36)$$

The term C_F in equation (35) is called the Cabannes factor which accounts for the anisotropy of the scatterers. For vertically polarized incident light

let $\rho_V = I_{H_V} / I_{V_V}$

Then

$$C_F = \frac{R_{Total}}{R_{iso}} = \frac{3}{(3 - 4 \rho_V)} \qquad (37)$$

Use of the Cabannes factor to get the isotropic

scattering is equvalent to using equation (34).

The measurement of scattering from pure liquids is one of the ways of obtaining absolute calibration of light scattering data.

Solutions : For a mixture of two liquids or for a polymer in a solvent, in addition to the scattering due to density fluctuations R_d, there will be scattering due to concentration fluctuations R_c. At low polymer concentrations, the density and concentration fluctuations can be assumed to be independent of each other and

$$R_{iso} = R_c + R_d \qquad (38)$$

The concentration fluctuation term is then given by

$$R_c = \frac{K_L R T c}{(d \Upsilon / dc)_T} \qquad (39)$$

where R is the gas constant, c is the polymer concentration, Υ is the osmotic pressure and K_L is the light scattering constant and is given by

$$K_L = \frac{4 \pi^2 n^2}{\lambda_o^4 N_A} \left[\frac{dn}{dc}\right]^2 \qquad (40)$$

where N_A is Avagadro's number and (dn/dc) is the refractive index increment. At low concentrations of polymer, equation (39) can be expressed in the familiar Zimm form [53]:

$$\frac{K_L\, c}{R_c} = \frac{1}{M_w\, P(q)} + 2\, A_2\, c + \ldots. \qquad (41)$$

where M_w is the weight average molecular weight of the polymer and A_2 is the second virial coefficient. $P(q)$ is the single chain scattering function and at small values of q i.e. $q\, R_g < 1$

$$\frac{1}{P(q)} = 1 + \frac{q^2\, R_g^{\,2}}{3} \qquad (42)$$

where R_g is the radius of gyration of the polymer chain.

At moderate concentrations, density and concentration fluctuations become interdependent and it becomes necessary to account for such an interdependence. Bullough [54] has proposed an amended form of the equation (38) which is:

$$R_c = R_{iso} - R_d\, (\, 1 + 4Y\,) \qquad (43)$$

where $Y = \dfrac{c\, n\, (dn/dc)_T}{\rho\, (\partial \epsilon / \partial \rho)_T}$

For concentrated solutions, one can use the Flory-Huggins equation [3] for osmotic pressure :

$$\Upsilon = -\frac{R\, T}{V_1} [\ln (1-v_2) + (1 - \frac{1}{X_W})\, v_2 + \chi v_2^{\,2}]$$

where v_2 is the volume fraction of polymer ($c=v_2\, \rho_2$). X_W is the weight average degree of polymerization for the polymer and χ is the polymer solvent interaction parameter. Using equation (44) in equation (39) we have the following expression for R_c :

$$R_c = \frac{K_L V_1 v_2 \rho_2^2}{\frac{1}{1 - v_2} + \frac{1}{X_W} - 1 - 2\chi v_2} \qquad (45)$$

Such an expression can account for a maxima in R_c as a function of concentration as was observed by Debye and Bueche [55]. The position of the maxima depends on the size of the chain, moving to lower concentrations for longer chain lengths.

$$(v_2)_{max} = \frac{1}{1 + \sqrt{X_W}} \qquad (46)$$

In equation (44), χ has been assumed to be independent of composition. However, one can consider a concentration dependent $\chi = \chi_1 + \chi_2 v_2$, which will result in an additional term in the denominator of equation (45).

Swollen Networks : For a network swollen at equilibrium, the osmotic pressure can be expressed in terms of the Flory Rehner theory [18] as :

$$\Upsilon = \frac{-R T}{V_1} \left[\ln(1-v_2) + v_2 + \chi v_2^2 + \frac{\rho V_1}{M_c} \left(v_2^{1/3} - \frac{v_2}{2} \right) \right] = 0 \qquad (47)$$

where M_c is the molecular weight between crosslinks. Therefore, for an ideal network the expression for R_c can be obtained by using equation (47) in equation (39) giving:

$$(R_c)_{ideal} = \frac{K_L V_1 \rho_2^2 v_2}{\frac{1}{1-v_2} - 1 - 2\chi v_2 + \frac{\rho_2 V_1}{6M_c}(3-2v_2^{-2/3})} \quad (48)$$

The scattering from real swollen networks is usually much more than that predicted by equation (48). This excess scattering is usually attributed to inhomogeneities in the network.

If a network is nonuniformly crosslinked, then, the swelling will be non uniform. If there is sufficient difference in the refractive index between the polymer and diluent, then, the non uniform distribution of solvent in the swollen network can be studied by light scattering to estimate the inhomogeneity in the crosslink density, This approach has been used by Stein [56], Bueche [57] and Wun and Prins [58].

Using the Flory-Rehner theory for network swelling, Stein [56] developed expressions to estimate the mean squared fluctuation in molecular weight between crosslinks $\langle \triangle M_c^2 \rangle$ from the excess scattering of light. His approach is as follows :

The local $(M_c)_i$ deviates from the mean $\overline{M}_c$ as

$$(\triangle M_c)_i = \overline{M}_c - (M_c)_i \quad (49)$$

the corresponding fluctuation in the local concentration of polymer will be $(\triangle v_2)_i$. Flory-Rehner equation or any other expression for the equilibrium

swelling of rubbers, can then be used to relate $(\ v_2)_i$ to $(\triangle M_c)_i$ as :

$$(\triangle v_2)_i = \frac{(\triangle M_c)_i}{M_c} Q(v_2) \qquad (50)$$

where $Q(v_2)$ in the Stein theory is $-3v_2/5$. This corresponds to the case of high degrees of swelling. For smaller amounts of swelling, i.e., higher crosslink densities, one can use the more complete swelling expressions. For the general Flory-Rehner equation, we have :

$$Q(v_2) = Q_1 / Q_2 \qquad (51)$$

where

$$Q_1 = (0.5\ v_2 - v_2^{1/3})[\ln(1-v_2) + v_2 + \chi v_2^{\,2}]$$

and

$$Q_2 = [\ \frac{(3-2v_2^{-2/3})}{6}\ln(1-v_2) + \frac{2v_2^{1/3}}{3} + \frac{(0.5v_2-v_2^{1/3})}{(1-v_2)} + \chi v_2(\frac{5v_2^{-2/3}}{3}-0.5)\ ]$$

The fluctuatuion in volume fraction of polymer can be related to a fluctuation in the refractive index :

$$(\triangle n)_i = (n_2 - n_1)\ (\triangle v_2)_i = (n_2 - n_1)\ \frac{(\triangle M_c)_i}{M_c}\ Q(v_2) \qquad (52)$$

The equation for the excess isotropic scattered intensity is then expressed as :

$$R_{iso} = R_{V_V} - 4\,R_{H_V}/3$$

$$= 4\,\pi\,K_E \int_0^{\infty} \gamma(r)\,\frac{\sin qr}{qr}\,r^2\,dr \qquad (53)$$

where

$$K_E = \frac{4\,\pi^2 n^2}{\lambda_o^4}\,(n_1-n_2)^2 < \frac{M_c^2>}{M_c^2}\,[Q(v_2)]^2$$

and $\gamma(r)$ is a correlation function defined as :

$$\gamma(r) = \frac{<(\triangle M_c)_i\,(\triangle M_c)_j>_r}{<\triangle M_c^2>}$$

$$= \frac{<(\triangle n)_i\,(\triangle n)_j>_r}{<\triangle n^2>}$$

The scattered intensity can be measured as a function of the scattering angle. Thus, the correlation size and $<\triangle M_c^2>$ can be estimated from the slope and intercept in the Debye Bueche plot by using equation (53).

With the use of endlinking reactions to form model networks, it is possible to vary $<\triangle M_c^2>$ systematically using various amounts of short and long chains to test the predictions of equation (53).

Wun and Prins [58] have also used a similar approach to describe the excess scattering from a swollen network. They introduced a non randomness index (NRI) which is defined as

$$NRI = \frac{\left[R_{V_V}(0)\right]_{exp}}{\left[R_{V_V}(0)\right]_{ideal}} - 1 \qquad (54)$$

where the ideal term can be calculated by equation (48).

They studied a series of poly (2-hydroxy ethyl methacrylate) (PHEMA) networks and tried to correlate the NRI with the mechanical properties. They concluded that a low NRI could be a quantitative criterion for superior mechanical performance of a rubbery material. This is not necessarily correct, since the work by Mark and coworkers [5] on bimodal PDMS networks has shown that bimodal networks with a large fraction of short chains can have mechanical properties superior to unimodal networks.

In estimating the scattering due to concentration fluctuations for swollen networks one has to subtract the term for density fluctuations from the total scattering. To estimate the density fluctuation scattering one needs to know the refractive index and the bulk comressibility. Although, the values of the bulk compressilility of a network and the linear chains of the same polymer should be similar, the presence of voids can drastically effect the compressibility of a dry network. For a swollen network, if one considers that the resultant β is a weighted sum of the individual pure components, it is useful to have an accurate value for β for the network. To avoid complications due to voids, the bulk compressibility for a network can be estimated by measuring β as a function of $1/M_n$ and extrapolating to $1/M_n = 0$. In any case, the magnitude of the density fluctuations term is very small

compared to the concentration fluctuation term and a lot of workers tend to ignore it.

Small Angle Neutron Scattering

In recent years, small angle neutron scattering (SANS) has developed into one of the most powerful methods to study polymer conformations in the whole concentration range from dilute solutions to the bulk [60-63]. Neutron scattering is the result of the interaction of the incident neutrons with atomic nucleii and hence different isotopic species may interact with neutrons quite differently [59]. In particular, hydrogen and deuterium have scattering power, or scatttering length b, that differ in both sign and magnitude. As a consequence a deuterated molecule in a protorated matrix will be visible to neutrons and vice versa.

The wavelength of thermal neutrons is in the range ($2\text{Å} < \lambda < 20$ Å) and combined with the use of small angle detectors has made it possible to cover q range from 0.001 to 1 Å^{-1}. This q range compares well with typical polymer dimensions. The combination of enhanced contrast, possibility of selective labelling and the suitable range of momentum transfer (or q) has made SANS a popular technique for the investigation of polymeric materials.

In SANS experiments one has to be concerned with perturbations caused by the substitution of deuterium for hydrogen in the system. Deuterated and hydrogerated polyethylene, which are miscible in the melt, undergo segregation when crystallized slowly from the melt. This is a result of the different melting temperatures of the two polymers. In the case of Polystyrene-Polyvinyl methyl ether blends, deuteration of the polystyrene is found to shift the phase diagram significantly [64]. Deuteration is also found to effect the theta temperature of polystyrene in cyclohexane. However, in most other cases, the effect of deuteration is not very significant.

Coherent and Incoherent Scattering

The scattered intensity for a system containing n identical nuclei will be given by equation (16) :

$$I(q) = K \sum\sum b_i b_j \exp (iq.r_{ij}) \qquad (55)$$

The way in which a neutron interacts with a nucleus depends on their relative spins. If the nucleus has a spin I, then the neutron can interact with the nucleus with spin up or down i.e. in total spin states, T, of I+1/2 and I-1/2. Associated with these total spin states are scattering lengths b^+ and b^- with the corresponding relative frequencies f^+ and f^-. The averages are then :

$$\bar{b} = f^+b^+ + f^-b^- \qquad (56)$$

$$\overline{b^2} = f^+(b^+)^2 + f^-(b^-)^2 \qquad (57)$$

In equation (55), separating the terms for i = j from those for i ≠ j gives :

$$I(q) = K\,[N(\,\overline{b^2} - \bar{b}^2\,) + \bar{b}^2 \sum\sum \exp\,(iq.r_{ij})]$$

The second term in equaion (57) is phase dependent as it corresponds to interference between nuclei. It is called the coherent contribution and is analogous to that measured by light or x-ray scattering. The first term which is called the incoherent contribution is unique to neutron scattering. It does not depend on the phase and leads to isotropic scattering.

Therefore coherent and incoherent cross sections σ are defined as :

$$\sigma_{coh} = 4\,\pi\,\bar{b}^2 = 4\,\pi\,b_{coh}{}^2 \qquad (58)$$

$$\sigma_{incoh} = 4\,\pi\,[\,\overline{b^2} - \bar{b}^2\,] = 4\,\pi\,b^2{}_{incoh} \qquad (59)$$

The scattering length $\bar{b}$ in general is complex. The real part may be positive or negative and the imaginary part is a measure of the neutron absorption that might occur. The cross section for absorption is σ_{ABS}. Table 1 lists the cross section data for common elements.

The coherent intensity in a SANS experiment is described by the cross section $d\Sigma/d\Omega$, which is the probability that a neutron will be scattered in a solid angle Ω per unit volume of the sample. This cross section is identical with the Rayleigh ratio R used earlier for

light scattering.

SANS from Polymer Solutions

In a light scattering experiment, dilute solutions of a polymer chain in a theta solvent are used to estimate the unperturbed dimensions. In the initial SANS experiments also, measurements were made using dilute concentrations of polymer in the theta solvent.

In the case of SANS, it is not necessary to work at low concentrations of labelled species to extract the single chain scattering behavior. Consider a mixture of polymers A and B of the same degree of polymerization X. Let A be the deuterated form of B and let D be the fraction of the deuterated chains. The scattering from such a system will consist of two terms as follows :

$$\frac{d\,\Sigma(q)}{d\,\Omega} = K\,X^2\,(b_A - b_B)^2\,D\,[P(q) + N\,D\,Q(q)] \qquad (60)$$

where N is the number of chains of type A. P(q) is the single chain interference function and Q(q) represents the inter chain monomer correlations. Using the incompressibility hypothesis, according to which the local fluctuations in the density of A and B cancel each other, it can be shown that $P(q) = - N\,Q(q)$ and equation (60) reduces to the form :

$$\frac{d\,\Sigma(q)}{d\,\Omega} = K\,X^2\,D\,(1-D)\,(b_A - b_B)^2\,P(q) \qquad (61)$$

Therefore, P(q) can be estimated at high concentrations of labelled polymer. The intensity is maximized at D = 0.5. The higher concentration of labelled species therefore results in an improved signal to noise ratio resulting in shorter experimental counting times.

The advent of SANS and the advances in theories of polymer solutions [66] have led to a considerable improvement in the understanding of polymer solutions.

Dilute Solutions : In dilute solutions, the R_g, M_w and A_2 can be measured using a Zimm plot as in equation (41). R_g is measured at small q i.e. qRg < 1. This is the Z average radius of gyration and will be denoted as R_g^z. If the molecular weight distribution is known, the parameters of a Flory Schulz distribution can be used to convert this to a weight average R_g^w.

For an unperturbed chain, Gaussian statistics hold and one has the relation :

$$R_g^w = C\,M_w^{0.5} \qquad (62)$$

where C is a constant.

In general one can express in terms of an exponent

$$R_g^w = C\,M_w^{\nu} \qquad (63)$$

In a good solvent for very good chains

$$\nu \sim 3/5 \text{ or } 0.6.$$

This is because in the presence of good solvent, there is the excluded volume effect caused by the mutual repulsion between the two monomer units sufficiently removed from each other along the chain resulting in an expansion of the chain. The expansion not only perturbs R_g ; it also effects the local conformation and gaussian statistics are no longer valid.

At larger q or at smaller distances, the structure factor is :

$$S(q)^{-1} \sim q^{1/\nu} \tag{64}$$

Therefore, the solvent quality can be estimated by examining the wide q data where $qR_g > 1$. The exponent ν = 3/5 is strictly valid for chains of infinite length. In more recent developments of the theory of polymer solutions [68,69], short sequences are presumed to be ideal whereas long sequences are fully swollen due to the excluded volume effect. The chain is viewed as a sequence of blobs or subchains each containing N_T bonds in an ideal (random flight) sequence. The critical parameter in this type of picture is N_T, the temperature dependent bond index which marks the transition from ideal to swollen behavior.

Semi Dilute Solutions : As the polymer concentration is increased, there is an overlap concentration c^*, at which the chains start overlapping. Above c^*, the chains interpenetrate each other and the properties of the system become independent of the size of of the single chain (for $M_w \longrightarrow \infty$).

According to the scaling approach [66], a semi dilute solution is imagined to consist of blobs. The size of each blob is ξ. Within the blobs, the monomers are expected to experience excluded volume interactions and at distances greater than ξ, the excluded volume effects are screened [70].

Therefore, at small q the structure factor has a Lorentzian form :

$$S(q) = \frac{K}{(1 + q^2 \xi^2)} \qquad (65)$$

Typically, a plot of $S(q)^{-1}$ vs q^2 is used to estimate ξ. According to the scaling laws :

$$\xi \sim c^{-3/4} \qquad (66)$$

and the osmotic pressure $\Upsilon \sim c^{9/4}$

$$\text{or } \frac{d\,\Sigma(0)}{d\,\Omega} = \frac{K\,c}{(d\,\Upsilon/dc)} \sim c^{-1/4} \qquad (67)$$

At small distances, i.e., inside a blob the excluded volume interaction causes the structure factor $S(q)^{-1} \sim q^{5/3}$.

As mentioned earlier, the scaling predictions are valid for the chains of infinite length. For the short chains, there can be deviations from the scaling predictions.

In the case of a poor solvent, the semi dilute solution can still be imagined to consist of blobs which represent the transient network structure. However, the correlation length ξ_p meaasured now in the small q range does not reflect the mesh size of the transient network. This is because excluded volume interactions which are binary interactions are now replaced by ternary contacts. Now it is expected that :

$$\xi_p \sim c^{-1} \tag{68}$$

and the osmotic pressure

$$\Upsilon \sim c^3 \tag{69}$$

SANS from Swollen Polymer Networks

Most theories of rubber elasticity are based on the molecular weight between crosslinks M_c as the central parameter in determining the behavior of the networks. SANS, therefore, can be very helpful in checking the validity of the macroscopic theories at the molecular level. One can adopt three approaches to study networks by SANS.

1) Labelling all the crosslinks and then deforming the network in tension or by swelling (Type A).

2) Labelling a few paths through the network. These paths may be just equal to a single chain between crosslinks or could involve several chains between crosslinks. (Type B).

3) Swelling the network consisting of all hydrogeneous chains with a deuterated solvent or vice versa (Type C).

In the first case where all crosslinks junctions are labelled, one can observe the spatial correlations for all the crosslinks. Typically, for any given network junction, inside the volume containing all the first topological neighbors, there would be other crosslinks which are spatial neighbours. Therefore, in such a case it becomes difficult to differentiate between spatial and topological neighbors. If the molecular weight distribution for the chains between crosslinks is narrow, the networks give rise to a scattering maxima. Such a maxima is also predicted using the R.P.A. for a melt of chains. All the chains are labelled at the ends. The maxima in the scattering curve is a reflection of a 'correlation hole' which is caused by the depletion of labelled species in the immediate vicinity of the labelled part. Benoit et al [71] have observed such a maxima in polysterene networks crosslinked with labelled divinyl benzene. On swelling the networks, the maxima was found to move to smaller q.

Recently Wu [72] has studied epoxy thermosets using a partially deuterated epoxy ; the diglydyl ether of Bisphenola (DGEBA). This was cured with di and tri amines based on poly propylene oxide chains. The system was studied at different stages of cure and prominent peaks were observed at the final cure. The initial prominent peak corresponds to the correlation hole and the higher order peaks are indicative of the spatial correlations associated with the stiffness of the network structure.

Bai [73] studied a slightly diferent epoxy system. He used the same epoxy DGEBA but used m-phenylene diamine to crosslink. The four hydeogen atoms on the phenylene ring were substituted by deuterium to give a labelled crosslink. He scanned a q range from 0.02 $Å^{-1}$ to 0.2 $Å^{-1}$. He observed that the scattered intensity was quite independent of q and concluded that the distribution of the labelled centers was uniform and that the epoxies were homogeneous.

Studies of the chain labelled (type B) networks allow the determination of the conformation of the elastic chains between crosslinks. For the different models of network deformation, one has the following predictions for the molecular extension ratio α_m in terms of the macroscopic deformation ratio α:

1) <u>Affine Deformation</u> : In such a model the junctions

are not allowed to fluctuate and the deformation is affine at the level of the statistical segement. ($\alpha = \alpha_m$)

2) Phantom Network : The junctions are free to fluctuate and their fluctuations are independent of the strain. The deformation of the mean position of the crosslinks is assumed to be affine [74].

$$\alpha_m = \left[\frac{\phi + 2 + (\phi - 2)\alpha^2}{2\phi} \right]^{1/2} \qquad (71)$$

where ϕ is the network functionality.

3) Junction Affine Model or the End to End pulling model : In such a model the network chains in the deformed state have a conformation such that their ends are seperated by a particular distance R. The deformation is applied affinely to the chain ends. For such a model [75]:

$$\alpha_m = \left[\frac{\alpha^2 + 1}{2} \right]^{1/2} \qquad (76)$$

Benoit et al [71] studied polysterene networks crosslinked by divinyl benzene. They found that on swelling to equalibrium, the expansion of the R_g was much less than that predicted by the affine deformation model. Uniaxial extension experiments by Hinkley et al [76] on model polybutadiene networks with a few labelled chains indicated that the deformation was less than affine. The

observed extension ratios seemed to be close to those predicted by the Phantom and Junction Affine models.

In recent years, Picot and coworkers [12,13] have performed an extensive set of experiments on model PDMS networks using labelled chains. Their results can be summarized as follows:

a) The conformation of the chains after crosslinking is gaussian in the dry state.

b) In uniaxial deformation experiments, the deformation at the mesh size could not be described by a unique model although the data was found to be close to the predictions of the Junction Affine and Phantom models.

c) In the case of networks swollen to equilibrium in a good solvent; the radius of the gyration of the elastic chain did not change significantly with a change in the macroscopic swelling ratio. R_g values for the swollen network chains were found, within experimental error to be equal to that for a corresponding free chain in a dilute solution.

Bastide [14] has recently studied polystyrens networks swollen in benzene using labelled chains. The networks were osmotically deswollen by the addition of large linear chains to the surrounding solvent. Although, the macroscopic swelling ratio varied by a factor of four;

R_g remained fairly constant. Based on these results, Bastide [14] has proposed a desinterspersion or network unfolding model which basically involves topological rearrangements in a network.

The deformation ratio of a single chain between crosslinks is expected to be less than the distance between spatial neighboring crosslinks. The latter involves a path through the network which is much longer than a single chain length. This suggests the notion of a threshold path length above which the deformation is affine. Experiments on labelled chains in polystyrene networks constraining several crosslinks have shown that the deformation is still less than affine.

Ullman [77] has suggested that one way to express such non affine deformation is to use the following relation between the molecular extension ratio and the macroscopic extension ratio

$$\alpha_m^2 = \alpha^2 (1 - A_f) + A_f \qquad (73)$$

where A_f is a non affineness parameter. If $A_f = 1$, there will be no molecular deformation inspite of the macroscopic deformation of the gel.

In the Type C networks, a hydrogeneous network is swollen with a deuterated solvent or vice versa. In such an experiment one is looking at the total spatial correlations in the swollen network. The volume fraction

of the polymer in a network swollen to equilibrium is typically in the range corresponding to a semi dilute solution in the case of linear polymer chains. Therefore, can the difference between the scattering of a swollen network and the corresponding semi dilute solution provide information about the network topology ? This is one of the questions raised in this piece of work.

In a good solvent, the correlation size for a semi dilute solution represents the mesh size of the transient network. Using similiar ideas, deGennes [66] has proposed that the only characterstic dimension in a swollen gel is the dimension of the chain between the crosslinks. He has therefore suggested that the correlation size in a swollen network is comparable to the radius of gyration of the chain between crosslinks. His notion is too idealistic as it does not take into account entanglements and the question of a distribution of crosslink densities. In the case of a semi dilute solution, the effect of polydispersity is not very serious since the chains can move with respect to each other resulting in an averaging of properties.

In a network, however, if there is a distribution of crosslink densities; it is quite unlikely that the local polymer concentration gets averaged out to the same extent as in the case of the semidilute solution of linear

chains. Therefore, the interpretation of the correlation size for a swollen network is not easy since it will be dependent on the distribution of crosslink density also. In addition to a distribution of crosslink densities, one can have long range correlations involved with the network unfolding process. Therefore, it is to be expected that the correlation size in networks is larger than the size of a chain between crosslinks.

Scattering Instrumentation

Light Scattering

The early light scattering experiments were performed using conventional light sources. However, these sources have almost entirely been replaced by lasers which can provide extremely intense, well collimated, monochromatic beams. The experiments in this work included small angle light scattering (SALS) and wide angle light scattering (WALS).

The SALS experiments were performed in the laboratory using a Spectra Physics (2mW) He-Ne laser ($\lambda = 6328$ Å) with a one dimensional optical multi channel analyzer (OMA1). The optical system consists of a set of neutral density filters to attenuate the beam and a set of lenses. The combination of lenses determines the scattering angle

range to be covered. The scattering pattern is scanned by a vidicon camera which is connected to a computer for data processing. The sample is held in between a glass slide and a micro slide cover. A special glass spacer was used for the polymer solutions. The main beam is prevented from entering the detector by using a beam stop. Details about the apparatus can be found elsewhere [78]. The angular range was calibrated using a diffraction grating.

The WALS experiments were performed in the Physics Department in Professor Langley's laboratory. The instrument used is basically a Quasi Elastic Light Scattering apparatus which can be used for total intensity light scattering measurements also. The source is a Spectra Physics 165 Ar Ion Laser, which provides a beam with a wavelength of 5145 Å. The beam passes through a polarizer (optional) and a beam monitor before being incident at the sample. The sample is held in a thermostated glass vat which contains excess of solvent. If necessary the beam can be focussed onto the sample using a lens before the vat. The scattered beam then passes through an analyzer, a pair of slits and onto the detector which is a photon counter. The detector is connected to a Langley Ford digital correlator which is run off a Tektronix Computer. A schematic diagram of such an instrument is given in Figure 2.

The detector is mounted on an arm which can be rotated about the sample position. The nominal scattering angles accessible are from 30° to 135°. Absolute intensity measurements are performed using the scattering from pure toluene for calibration. Pure solvents and solutions were studied using 10 mm diameter pyrex test tubes. As mentioned earlier, the vat contained excess of toluene or benzene to minimize stray light. For the swollen networks the samples were suspended into the vat containing excess of solvent. Experiments were performed using cylindrical and flat samples. The latter had to be tilted with respect to the incident beam and therefore a special sample holder was designed to allow different sample tilt positions.

Neutron Scattering

For SANS experiments, the common neutron sources are usually steady state nuclear reactors althought in recent years pulsed neutron sources are being developed. For this work, experiments were performed at the High Flux Isotope Reactor (HFIR) in the Oak Ridge National Laboratory (ORNL) under the auspices of the National Center for Small Angle Scattering Research (NCSASR) and at the National Bureau of Standards Research Reactor (NBSRR). Here a brief description of the neutron scattering experiment will be presented along with a comparision of the two facilities.

Detailed information about the two facilities can be found elsewhere [79].

In a typical reactor, fusion neutrons are produced in the core of the reactor. The energies of the neutrons are reduced by surrounding the core with D_2O which moderates the energies of the neutrons to thermal energies. A typical moderator temperature of 40°C will produce a Maxwellian distribution of neutron wavelenths peaking at about 1 Å with a long wavelength tail. By using a "cold source", it is possible to shift the wavelength distribution to produce a greater proportion of long wavelength neutrons. The Institure Lave-Langevin (ILL) at Grenoble France currently uses a cold source. There are plans to install a cold source at NBS in the near future.

The monochromation of the neutron beam may be achieved by using Bragg diffraction off graphite crystals or by using a mechanical helical velocity selector. Usually the latter results in a bigger wavelength spread. At Oakridge, the pyrolytic graphite crystals are used giving a wavelength of 2.37 Å or 4.75 Å. At NBS, the wavelength can be varied between 4-10 Å by changing the speed of the velocity selector.

Thermal neutrons are counted by detecting the recoil products of their reaction with certain nuclei. The products of these reactions can then be detected by the

ionization of a gas, such as BF_3. Since the spatial resolution of such two dimensional position sensitive detectors is low, it is necessary to use a large detector and therefore, a large sample to detector distance.

At Oakridge, the sample to detector distance (SDD) can be varied from about 1.5 m to 19 m. The q range that is accessible is from 0.003 to 0.6 $Å^{-1}$. At NBS, SDD is usually kept at 3.6 m and the detector can be swung around upto 15°. The q range at NBS is from 0.003 to 0.5 $Å^{-1}$. The power of the HFIR at Oakridge is 100 MW whereas at NBS it has recently been upgraded to 20 MW. For smaller q measurements, it is preferable to use the Oakridge facility.

For work involving swollen networks and solutions, the facility at NBS has the attractive feature that the sample changer is under ambient conditions, unlike Oakridge, where the sample changer is in a reduced pressure environment. The swollen networks are placed in special cells using quartz windows and are sealed to prevent the leakage of solvent during the experiment.

In addition to measuring the scattering from the samples being studied, one needs to measure the scattering from the pure components to estimate the incoherent level. One also needs to measure the transmission of each sample. Absolute intensity calibration may be performed using water

or Vanadium. These need long counting times. Therefore, it is convienient to use a precalibrated working standard which is usually a strong scatterer.

C H A P T E R I V

POLYBUTADIENE NETWORKS

The 1,4- polymers of isoprene and 1,3- butadiene and their copolymers comprise the largest group of elastomers. Commercial vulcanization is usually achieved by heating with sulphur. Vulcanization of a diene polymer by heating solely with sulphur is very inefficient and involves long polysulphide crosslinks. Commercial sulphur vulcanizations are carried out in the presence of various additives which greatly increase the rate and efficiency of the process [80]. The network finally has mono- or di- sulfide crosslinks. However, not all the reactions which take place in such a curing process are well understood. Moreover, the commercial vulcanizates usually contain several additives and reinforcing fillers to improve the properties.

Apart from the sulphur crosslinking, the other methods of crosslinking diene polymers are by using peroxides or by ionizing radiation. Dicumyl Peroxide (DCP) is the most commonly used peroxide in the cure of natural rubber (cis 1,4- polyisoprene) by dicumyl peroxide. The reaction is supposed to be quite simple and usually one crosslink is formed per molecule of peroxide [81,82]. At the cure

temperature, the dicumyl peroxide decomposes to yield two cumyloxy radicals :

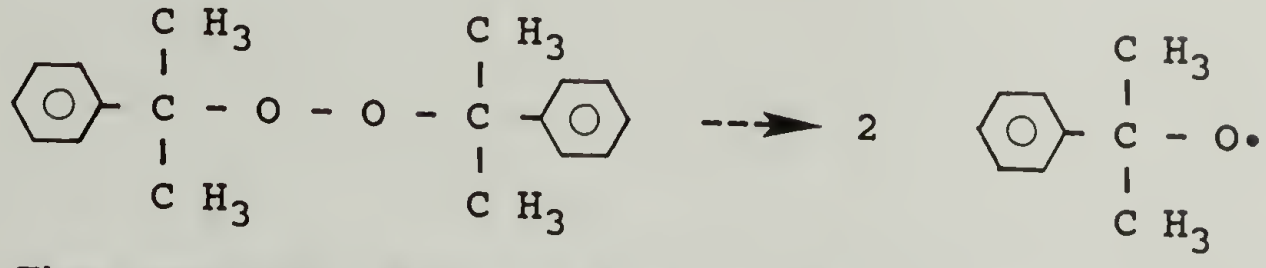

The cumyloxy radicals are not very stable and may decompose to form acetophenone and a methyl radical. Either the cumyloxy or the methyl radical then abstracts a hydrogen atom from the polymer. The polyisoprenyl radical formed is resonance stabilized and is therefore only weakly active towards double bonds. Crosslinks are formed by the recombination of the polyisoprenyl radicals.

In the case of curing of polybutadienes with DCP, it is found that more than one crosslink is formed per molecule of DCP [83-86]. The polybutadienyl radical is more reactive than the polyisoprenyl radical and can attack the double bonds of the polymer resulting in an addition polymerization step which gives several crosslinks per molecule of DCP.

The propagation of the polybutadienyl radical can be quantified in terms of the kinetic chain length. The kinetic chain length is defined as the number of propogation or transfer steps per radical from its generation to its termination. As in the case of polyisoperene curing, the kinetic chain length is zero

corresponding to one crosslink per DCP molecule.

In the DCP cure of polybutadienes, the kinetic chain length is found to be very sensitive to the microstructure of the polymer [85,86]. Polybutadiene can have three isomers : trans 1,4-, cis 1,4- and vinyl 1,2-. By varying the polymerization conditions it is possible to prepare a polymer with a specific microstructure. High 1,2- content polymers undergo more crosslinking than the polymers with a majority of 1,4- units. The kinetic chain lengths for high 1,2- content polymers have been reported to be as high as 40-50 compared to about 10 for the high cis 1,4- polybutadienes. Although the exact magnitudes of the kinetic chain length is questionable, the relative crosslink efficiencies are :

1,2-polybutadiene >> 1,4-polybutadiene >> 1,4-polyisoprene

The uniformity of the cure will also depend on the quality of the mixing of DCP in the polymer. Commercially, blending or compounding is usually accomplished by using mechanical mixers. Such a mixing can result in degradation of the chains and hence an alteration of the molecular weights and the molecular weight distribution of the polymer. More efficient mixing can be achieved by solvent blending using a common solvent. However, such a process is not very convenient on large scales. Therefore, in the case of crosslinking of polybutadiene with DCP, non uniform

mixing and unequal reactivities, depending upon the microstructure, can result in a complex network structure.

Ionizing radiation such as γ- rays or electron beams are also used to crosslink polybutadienes. In addition to the formation of crosslinks, chain scission can also take place. The relative amounts of crosslinks versus chain scissions depends on the chemical structure of the polymers and the radiation conditions [87,88]. The yields are usually expressed in terms of G values - G(x) and G(s) expressing the number of crosslinks and scissions per 100 eV of absorbed energy respectively. G(X) and G(S)are usually determined by sol - gel analysis. Pearson et al [89] used a modified Charlesby - Pinner approach. They took scission and chain reactions into account to estimate the G(X) values for the polybutadienes. They assumed the polymer was a random copolymer of cis, trans and vinyl isomers and studied polymers of different micro-structures to obtain the following results :

$G(X)_{cis} = 2.22$

$G(X)_{trans} = 1.09$

$G(X)_{vinyl} = 3.90$

Although the G(X) values seem to be dependent on the microstructure of the polymer, the difference is not as large as in the case of dicumyl peroxide curing of polybutadienes. One possible explanation could be a

radiation induced cis - trans isomerization. Such an isomerization is much more rapid in solution, especially when sensitized by bromine atoms. Moreover Golub et al [90] have estimated that in the solid state 14-15 double bonds are isomerized per 100 eV in cis 1,4- polybutadiene compared to 3.6 isomerizations in the case of all trans 1,4- polybutadienes. The kinetic chain lengths estimated in the case of radiation curing of polybutadiene are of the order of 1-2. Therefore, if a sample is uniformly irradiated, it is expected that electron radiation will result in more homogeneous curing of polybutadienes as compared to peroxide curing.

Sample Preparation and Characterization

Randomly crosslinked networks were prepared by crosslinking polybutadiene with dicumyl peroxide (DCP). A high cis 1,4- polybutadiene polymer DURAGEN 1203 ® (GenCorp, Akron, Ohio) was used. The molecular weights were determined by GPC to be

M_W = 401,000 and M_N = 149,000.

The microstruture of the polymer was examined by IR using the extinction coefficients reported by Hampton [91] listed in Table 2.

The polybutadiene was found to have the following microstructure

cis	1,4-	92%
trans	1,4-	4%
vinyl		4%

The polymer was purified prior to crosslinking. It was dissolved in benzene and the solution was filtered and precipitated into methanol. The precipitated polymer was redissolved in benezene and filtered again. The solutions typically had a concentration of 5 gm of polymer / 100 ml of solvent. Seven different weights of DCP were dissolved in benezene. These solutions were mixed with seven different solutions of polybutadiene in benezene. The concentration of DCP in terms of parts per hundered parts of polybutadiene (phr) in the different solutions was then 2,4, 7.7, 11, 15.3, 20.3 and 30. One phr of the anti-oxidant, 2.2' methylene bis (6-tert-butyl-p-cresol) was added to each solution. The solutions were poured into Teflon lined containers and the solvent was allowed to evaporate. The remaining solvent was stripped under vacuum at room temperature.

The dried polymer containing the DCP and antioxidant was then placed in Teflon lined molds using a 1mm spacer. The samples were cured at 140°C for 40 minutes under a pressure of about 2000 psi. The seven networks

corresponding to the different amounts of DCP i.e. different crosslink densities were numbered But 21 - But 27. The networks were extracted for five days at room temperature in benzene. The networks were then dried by slowly reducing the solvent quality and by adding methanol to the sample container. The degree of swelling and the sol fraction were estimated by comparing the final dry weight of the network to the swollen weight and the dry unextracted weight. These are listed in Table 3.

Using the Flory-Rehner theory for equilibrium swelling of networks (equation 5), the crosslink densities were calculated from the swelling measurements. Corrections for dangling ends were made by using the molecular weight of the starting polymer (equation 7). The crosslink functionality was assumed to be four and the value of χ for polybutadiene - benzene interaction at 25°C was taken to be 0.387, as suggested by Rowland and Labun [92]. The calculated values of M_c for the different networks are listed in Table 3.

The mass densities of the dry networks were measured by a floatation method using methanol as the fluid being displaced. The solubility parameters of the polymer and methanol are 8.6 and 14.5 $(cal/cm^3)^{1/2}$ respectively. Therefore, it is very unlikely that there is any significant swelling of the networks in methanol.

The measured values of the densities ρ are listed on Table 3. The glass transition temperatures of the networks were determined using a Perkin Elemer DSC II at a heating rate of 20 C/min. These are listed on Table 3.

Light Scattering

The networks were studied by small angle light scattering (SALS) using the OMAI described in chapter III. Experiments were performed on the swollen networks and the polymer solutions corresponding to the same volume fraction of polymer as in the swollen network at equilibrium. The swollen films were placed on microscope slides and excess solvent was added using a dropper. The film was then covered with a slide cover and placed in the path of the laser to obtain the scattering pattern. The solutions were placed in a special cell made by sticking a glass spacer (2mm high) onto a microscope slide and covering with a slide cover.

The V_V scattered intensities for the networks and solutions are shown in Figure 3. The networks scatter light considerably more than the solutions. The magnitude of the H_V scattering was small and was therefore neglected. The excess scattering from the swollen networks as compared to the solutions was then analysed using a Debye Bueche plot. Figure 4 represents such a plot.

The correlation size a_c and the mean squared scattering power η^2 are estimated from the slope and intercept of such a plot. The correlation sizes for the different results are given in Table 4. These correspond to distances of the order of 5000 Å. Bueche [57] also observed such large dissymetries in swollen PMMA and polystyrene gels. For the crosslink densities studied, one would expect the dimension of a chain between two crosslinks to be in the range of 30 - 75 Å. The measured a_c values are two orders of magnitude higher, reflecting long range correlations.

A precise interpretation of the correlation size is possible only in the case of two phase systems with sharp boundaries in terms of

(a) the average size of an inclusion for low concentrations of the inclusion

(b) the ratio of the volume to the surface (V/S) for non-particulate systems at moderate concentrations.

Swollen networks are most likely to be multi component systems with no sharp boundaries. Therefore, there is no simple interpretation of the correlation sizes. One possible interpretation of the large values of a_c is that they correspond to large range variations in the crosslink densities. However, the correlation size a_c should not

be considered to be the size of a region of crosslink inhomogeneity.

The intensity measurements in these experiments were not in absolute units. Therefore, only relative comparisions are made in arbitrary units. Using the Stein theory for the excess scattered intensity (equation 53); the values of $<\triangle M_c^2>$ were obtained from the intercept of the Debye Bueche plots for the various swollen networks. Figure 5 shows the relative root mean squared fluctuation in the molecular weight between crosslinks $<\triangle M_c^2>^{1/2}$ for the various networks. It can be seen that $<\triangle M_c^2>^{1/2}$ increases as M_c is increased [93].

The SALS results can be summarized as follows :

a) The distribution of solvent in the swollen polybutadiene networks is not uniform and these concentration fluctuations give rise to scattering of light several orders of magnitude larger than that for corresponding solutions.

b) The non uniform distribution of solvent is attributed to variations in the local crosslink density. Relative values of $<\triangle M_c^2>^{1/2}$ or $\triangle M_c$ are calculated for the various networks by using the Stein theory for scattering from inhomogeneously crosslinked networks. These values of $\triangle M_c$ are found to increase on increasing M_c.

c) The large correlation sizes on the order of 5000 Å suggest that there may be large regions of crosslink unhomogeneity distributed in a relatively uniform matrix. Non uniform mixing of dicumyl peroxide could possibly account for such a hypothesis.

Neutron Scattering

To probe the networks at smaller dimensions, the swollen networks were studied by SANS. The experiments were performed at ORNL using 30m instrument. Dr. George Wignall, of the NCSASR, assisted with the experimental details.

The polymers studied were hydrogeneous. Therefore, the networks were swollen in deuterated benzene to improve contrast. The swollen networks and the solutions were placed in special cells for the experiment. The cells had quartz windows and were sealed with Teflon O-rings. A more complete description of the cells is given in Chapter III. The sample changer at the 30 m facility at Oakridge is in a reduced pressure environment. The cells were checked for leakage in a vacuum oven before being placed in the sample changer.

Depending on the desired q range, the beam collination and beam stop alignment were performed as per the

guidelines in the manual . For the beam stop alignment and the transmission measurements a strong scatterer, such as a glassy carbon was placed at the sample stage. For the transmission measurements, the sample was placed at the initial collimating slit with the strong scatterer at the sample position. In addition to the scattering from the samples, the scattering from the pure solvent and the dry network were also measured to account for the incoherent background. Absolute intensity calibration was performed using a precalibrated aluminium standard. AL-5 is an irradiated aluminium sample with a small concentration of voids (<1%). The forward scattering cross section for this sample is 170 $\pm$ 10 cm^{-1} and the linear Guinier plot gives an R_g value of 210 $\pm$ 5Å.

The q range can be changed by changing the sample to detector distance (SDD). Measurements were made at SDD's of 18.9 m and 4.89 m to cover a reasonably wide q range and the data was combined to give an effective q range of 0.005 - 0.1 $Å^{-1}$.

Three dicumyl peroxide crosslinked networks swollen in deuterated benzene were studied. The sample characteristics are:

Sample	v_2	M_c
But 10	0.17	6600
But 35	0.26	2750
But 27	0.45	650

Scattered intensities for the swollen networks and the corresponding solutions were measured for both the geometries. Figure 6 shows the scattered intensities for But 35 and the corresponding solution after incoherent subtraction.

The coherent scattered intensity of the solution was subtracted from the intensity for the swollen networks to give the excess scattering due to the presence of the crosslinks. Figures 8 and 9 show the excess scattered intensity for But 27 and But 35. Clearly the excess scattered intensity indicates at least two correlation sizes. This suggests that there may be different correlation sizes corresponding to different size levels of inhomogeneity of solvent distribution.

Using a continous distribution for the correlation function $\gamma(r)$ as in equation (28), it is possible in general to solve for the distribution of correlation sizes u(a). One method involves using a histogram approach to directly fit the scattered intensity to obtain u(a).

However, for the SANS data from the swollen

polybutadiene networks, it is sufficient to use two correlation sizes a_1 and a_2. Using the approach of Stein, Wilson and Stidham [94], the large size a_1 corresponds to an average size of the inhomogeneity or inclusion and the small size a_2 corresponds to the internal fluctuations. The internal fluctuations and the large scale inhomogeneity are assumed to be uncorrelated.

The total correlation function will then be a sum of two correlation functions:

$$\gamma(r) = \frac{< \eta_i \ \eta_j >_r}{\eta_o^2 \ [\ 1 + \eta_1^2 \ ]}$$

$$= \frac{\gamma_o(r) \ [\ 1 + \eta_1^2 \ \gamma_i(r) \ ]}{[\ 1 + \ \eta_1^2 \ ]} \qquad (74)$$

Let $\gamma_o(r) = \exp \ (-r/a_1)$

$\gamma_i(r) = \exp \ (-r/a_2)$

Then

$$\frac{d \ \Sigma(q)}{d \ \Omega} = 8 \ \pi \ \eta_o^2 \left[\frac{a_1^3}{(1+q^2 a_1^2)^2} + \frac{\eta_1^2 \ a_3^2}{(1+q^2 a_3^2)^2} \right] \qquad (75)$$

where $a_3 = \frac{a_1 a_2}{a_1 + a_2}$

Therefore, such an expression for the scattered intensity has 4 parameters η_o^2, η_1^2, a_1 and a_2 which can be obtained using a simple fitting routine. The data for the excess scattering from the swollen networks was fit to equation (75) to obtain the two correlation

sizes a_1 and a_2, the mean squared fluctuation in scattering power η_o^2 and η_1^2. η_1^2 represents the enhancement of the fluctuaions observed at a local level. The fitted curves are shown in Figures 8 and 9 and Table 5 lists the parameters of the fit.

Although the fit of the data to two correlation sizes is quite good, it is not a unique solution. Therefore, the interpretation of the parameters becomes ambiguous. The large size (a_1) fluctuation is considered to correspond to regions of fluctuating crosslink density. The Stein theory (equation 53) is used to estimate $<\triangle M_c^2>$ from η_o^2. The results are:

Sample	M_c	$\triangle M_c/M_c$
But 10	6600	0.19
But 35	2750	0.14
But 27	650	0.10

The small correlation size a_2 is of the order of 20-30 Å. It corresponds to local fluctuations of the solvent concentration in the swollen network as compared to a solution of linear chains. One way to account for local fluctuation in solvent concentration is to consider the possibility of solvent exclusion in the immediate vicinity of a crosslink. For very bulky crosslink junctions, such as those of very high functionality, solvent exclusion near the center of the crosslink is expected. Daoud and

Cotton [95] and Miyake and Freed [96] have predicted such a solvent depletion in the case of high functionality star polymers in solution.

It is possible to have some addition polymerization type of reactions during crosslinking for polybutadiene networks crosslinked with DCP. These reactions give rise to a few regions of high crosslink functionality. If it is assumed that a_2 corresponds to the size of a region depleted in solvent, then an estimate of the degree of solvent exclusion is required to estimate the number of such regions. In the case of the total exclusion of the solvent, the number of such regions is calculated to be on the order of 0.1% of the number of tetra functional crosslinks in the network. In the case of partial exclusion of solvent, if a concentration gradient away from the center of a crosslink is assumed, the model becomes too complicated to make an estimation of the number of such regions.

Remarks

The objective in this project is to try to understand network structure using scattering methods. The experiments on the polybutadiene networks constitute the preliminary part of the work. The excess SANS data for the

swollen networks can be represented reasonably well in terms of the two correlation sizes. However, it has not been possible at this stage to provide a satisfactory interpretation of the scattering data in terms of a molecular model for the network structure. The reasons for this are:

i) Real network structures are very complex. At present, there are no theories which adequately describe the spatial correlations in swollen networks.

ii) The dicumyl peroxide crosslinking of polybutadiene can result in complicated structures due to non uniform mixing of DCP and the tendency to form regions of high functionality.

It is possible to have a better control on the molecular weight between the crosslinks and the functionality by using model networks. This will result in better defined networks as compared to the randomly crosslinked polybutadiene networks.

Therefore, it was decided to use model networks for the rest of the project. The model networks used were those based on polydimethyl siloxane (PDMS), and the experiments and results of those networks are discussed in Chapter VI.

C H A P T E R V

EPOXY THERMOSETS

Highly crosslinked epoxy thermosets are of considerable commercial importance as adhesives and as matrices for composites. It is usually believed that cured epoxy resins are highly inhomogeneous [97-103]. Mechanical properties, such as tensile strength, show large discrepancies between theoretical and measured values. The main cause for the inhomogeneous structure is believed to be inhomogeneous crosslinking. The system is supposed to consist of segregated regions of high and low crosslink densities.

Most of the evidence for a non uniform network structure in epoxies is based on electron microscopy results [97-100]. The materials have been observed to contain spherical entities with a size distribution in the 50-500 Å range. Evidence based on DSC measurements is also cited [102] to indicate crosslink inhomogeneities. Epoxy resins annealed below T_g have an endothermic peak, which is supposed to indicate a phase separation of the higher and lower crosslinked regions. Inhomogeneity has also been inferred on the basis of sorption and swelling measurements [103].

Possible causes for inhomogeneous crosslinking in

epoxies are :

i) Unequal reactivity of the reactants during the course of the reaction.

ii) Phase separation (microsyneresis) in the case of curing in solution.

iii) Intramolecular cyclization reactions.

In addition to these factors, cure history is of concern in the curing of epoxies. Vitrification can occur if curing is carried out below the T_g of the fully cured material. Initial curing at high temperatures can be harmful because of degradation or side reactions which can take place due to the large exotherm caused by a very fast reaction.

Luttgert and Bonart [98] claim that the decisive factor determining the morphology of cured epoxy resins is the number of microgel particles formed during the very early stages of the curing process. The microgels are assumed to be formed due to cyclization reactions resulting in local regions of high crosslink density. As the curing process proceeds, these gel particles grow in size in the liquid resin until they meet and the bulk of the material gels. Consequently, the final size of the globular domains in the cured resin depends on the ratio of two rates, the rate of microgel formation (nucleation) and the rate of growth of the gel particles. At high curing temperatures, the rates

of nucleation will be fast and the great number of microgels formed permits growth only to a small size. Low curing temperatures initiate only a small number of gel particles and the cured resin will show large globular inhomogeneities. These authors proposed such a curing mechanism based on results obtained from electron microscopic investigations of fracture surfaces of resins cured at different temperatures.

Dusek et al [104] feel that the curing of simple epoxy resins with amines does not offer any special opportunity for microgel formation. They argue that significant cyclization will occur only in the case of crosslinking chain polymerization (as in the case of DCP cure of polybutadiene). Consequently, for stoichiometric amounts of the reactants, they do not expect the cured resin to contain regions of high and low crosslink densities. They are critical of the methods used to suggest crosslink inhomogeneities. Regarding DSC methods, they correctly suggest that enthalpic effects observed with annealed epoxies are associated with the non equilibrium character of the glassy state and are related to excess thermodynamic properties. With reference to the electron microscopy results, they indicate that the nodular structure observed in epoxies is similar to that observed in linear amorphous glassy polymers such as polystyrene and PMMA.

Recently Gupta et al [100] have investigated an epoxy resin based on DGEBA, the diglycidyl ether of bispherol A (Epon 828, Shell) using electron microscopy. The epoxy was cured using m-phenylene diamine. Using different techniques of sample preparation and examination, they observed nodular structures in the cured resin. The sizes of the nodules measured by the different techniques were reasonably consistent and were of the order of 50-300 Å.

Small angle scattering techniques such as SANS and SAXS can be used to study spatial correlations on the scale of the observed noular structures. Initial SAXS experiments on dry networks were not very successful due to the lack of contrast in the system. Contrast can be enhanced by swelling in a diluent with a different scattering power. This approach had been adopted to study the randomly crosslinked polybutadiene networks (Chapter 3). Therefore, an attempt was made to study the homogeneity of epoxy thermosets by swelling them with a deuterated diluent and using SANS.

The epoxy system chosen was the diglycidyl ether of bisphenol A (Epon 825) cured with meta phenylene diamine (MPDA). The T_g of the fully cured sample is 160°C. At room temperature the weight per cent uptake of water is about 2 per cent. Professor Karasz and coworkers in our department have been studying the effect of diluents

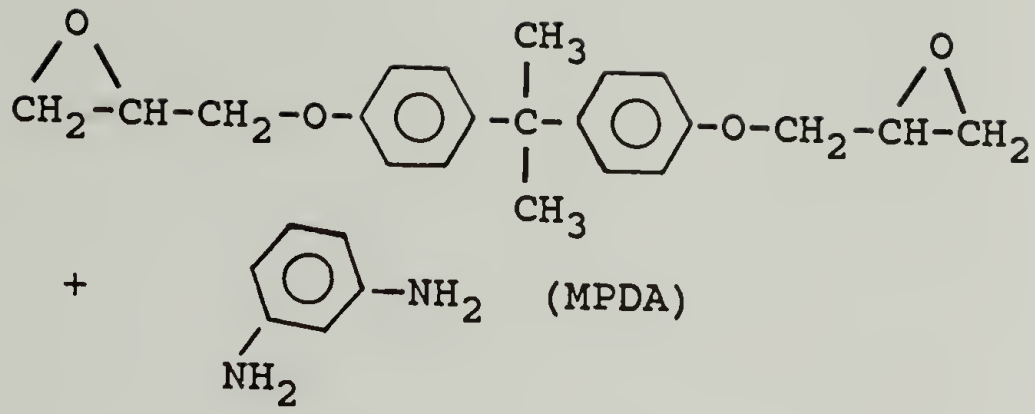

(EPON 825)

(MPDA)

such as, water on the T_g of cured epoxy systems. They observed that each percent take up by weight of water could reduce the T_g of the epoxy by about 20°C [118].

An initial experiment was performed on a sample obtained from Professor Karasz's group. A 2mm thick sample was immersed in D_2O for a week. The container was kept at a temperature of 80°C to enhance the take up. It had been observed that the weight of the sample was fairly constant after 5 days of swelling at 80°C. The SANS experiment was performed at ORNL using the 30m instrument. The experiment was performed by Dr. George Wignall of the NCSASR. The scattering was measured from an epoxy sample swollen with D_2O (2% water takeup) and a dry epoxy sample. The samples were contained in the scattering cells described in the previous chapters.

The scattering curves for the swollen and unswollen samples are given in Fig. 10. It can be seen that the swollen sample shows considerable excess scattering in the small q region. At larger q, the scattering from the

swollen and dry samples is comparable. The incoherent contribution to scattering due to D_2O is negligible. Therefore, the excess scattering due to the presence of the diluent is obtained by subtracting the scattering of the dry sample from the swollen sample. The excess scattering was plotted on a Guinier plot i.e., ln $[d\Sigma(q)/d\Omega]$ vs q^2. For a Gaussian correlation function :

$$\gamma(r) = \exp(-r^2/a^2)$$

where a is the correlation size.

The scattered intensity has the form :

$$\frac{[d\Sigma(q)]}{d\Omega} = \pi^{3/2} a^3 \eta^2 \exp(-q^2 a^2/4) \qquad (76)$$

η^2 is the mean squared scattering power.

The results of the Guinier plot gave :

$a = 710 \pm 25$ Å and $[d\Sigma(0)/d\Omega] = 720 \pm 495$ cm^{-1}

Assuming a two phase structure, we can estimate $\langle \Delta v_D^2 \rangle$, which is the mean squared fluctuation in the concentration of D_2O in the epoxy.

$$\eta^2 = (N_A/V_D)^2 \langle \Delta v_D^2 \rangle (b_D - b_E^*)^2 \qquad (77)$$

where $b_E^* = b_E (V_D/V_E)$

N_A is Avogadro's number, subscripts D and E refer to D_2O and the epoxy respectively, b is the scattering length and V is the molar volume.

Using equation (77) we get :

$\Delta v_D = 0.0145 \pm 0.0057$

Since the take up of D_2O in the sample was 2%, this would indicate very large fluctuations in the concentration of D_2O in the sample.

$$(\Delta v_D/v_D) \simeq 0.725$$

Due to the considerable excess scattering observed in the epoxy resin with 2% of D_2O, it was decided to plan a detailed experiment to critically examine the micro gel model for inhomogeneities in epoxies. Epoxy samples were prepared using Epon 825 and MPDA. The procedure used for the preparation of the resins was as follows :

i) m-phenylene diamine was purified by sublimation at 60 °C.

ii) Epon 825 was preheated at 70 °C for 15 minutes.

iii) The stoichometric amount of MPDA (15.4 phr) was added to the reaction vessel. The reactants were allowed to mix at 70 °C under an Argon atmosphere for 5 minutes.

iv) The reactants were quickly transferred into preheated Teflon lined molds to be cured under the desired conditions.

Curing was tried under partial vacuum to prevent degradation. However, an inert atmosphere of dry nitrogen gas was used to minimize the loss of MPDA during the early stages of the cure. Different cure conditions were employed to test the validity of the micro gel models for

inhomogeneities in epoxies. The cure history for different samples is given as follows on Table 6.

The first and second stage cures were under a N_2 environment. For the 3rd stage cure, all the samples were placed simultaneously in the oven under vacuum. The temperature was raised from 75°C to 180°C by changing the temperature setting on the oven. Therefore, the rise in the oven temperature was gradual and typically took about half an hour to reach the upper setting.

The cured epoxy resin contains hydroxyl groups attached to the network chains. On swelling the epoxy in excess of D_2O, there is a deuterium exchange between the D_2O and the hydroxyl groups resulting in -OD groups on the chains. With this in mind, three different specimens were prepared for each cure cycle for the SANS experiments. These are as follows :

(A) Sample swollen in excess of D_2O at 80°C

(B) Sample swollen in excess D_2O, and then placed under vacuum at 80°C for 1 week to extract the free D_2O.

(C) The dry sample.

(B) - (C) gives the excess scattering due to the OD groups.

(A) - (B) gives the excess scattering due to concentration fluctuation of D_2O in the epoxy.

The SANS experiments were performed at ORNL using the 30 m instrument. The sample to detector distance was set at 18.9 m with a 8 cm beam stop. The scattering curves for the various samples are shown in Figures 11 and 12. Contrary to the results of the preliminary experiment, all the samples used in this study had very low scattered intensities. The qualitative nature of the absolute scattered intensities is as follows

$$A > B > C$$

The intensities were too low to perform a quantitative analysis. Consequently, it was not possible to make a reasonable comparision of the various thermal histories used for the preparation of the samples. Since D_2O was given sufficient time to diffuse into the samples (A), it can therefore be concluded that the samples did not have any significant density fluctuations in the range of the experiment i.e., sizes of the order of 500 Å or less.

The difference in the results of this study and those of the previous experiment may be due to a slight difference in the curing methods. The sample obtained for the preliminary experiment had been cured under vacuum and the samples used in the detailed study were cured under

nitrogen. As mentioned earlier, in case of cure under vacuum, there is a possibility of loss of a small amount of the crosslinker MPDA in the early stages. This results in a non stoichiometric reaction. Therefore, when such a thermoset was swollen with D_2O, a few voids may have been formed resulting in a large concentration fluctuation of D_2O. Such an explanation could account for the large value of $(\Delta v_D/v_D)$. It is quite unlikely that there were any voids in the dry samples because the scattered intensity is quite flat even at small q. Also, the absolute scattered intensity from the dry unswollen samples is about the same in both the experiments.

Coherent scattering contrast for SANS was quite low in the swollen epoxy system studied. Contrast could have been enhanced by incorporating a larger amount of deuterated diluent. In the EPON 825 system, the crosslink density is high resulting in a high T_g and therefore a small take up of water or D_2O.

Epoxies can be studied by SANS by using deuterated junction points instead of a deuterated solvent. Recently, Bai [105] has studied epoxies based on EPON 828 cured with deuterated MPDA (D_4). The system was similar to the one studied by Gupta et al [100] by electrom microscopy. In the SANS experiments covering the real space range 30-400 Å, he observed that the deuterium labelled epoxies

consistently produced a constant excess intensity over the unlabelled epoxies. Therefore, Bai concluded that the crosslinks are uniformly distributed. This is in direct contradiction to the conclusion by Gupta et al [100].

The epoxy thermosets studied by Bai are fairly highly crosslinked ($M_c \sim 370$). In his experiments, the maximum q values covered were about 0.22 $Å^{-1}$ corresponding to 30 Å in real space. Since he had labelled crosslinks, if he had covered a wider q range, say upto 0.8 $Å^{-1}$, it is quite likely that he would have observed a peak corresponding to the correlation hole [66]. Recently Wu and Bauer [72] have used diamines based on poly propylene oxide (PPO) and partially deuterated DGEBA to make epoxies with labelled junction points. In the fully cured epoxy resins, they observed prominent scattering peaks over the q range within 1.2 $Å^{-1}$. By quenching the cure reaction at different stages, they were able to observe the development of the final network structure.

The PPO based epoxies, used by Wu et al [72], swell substantially in acetone. Therefore, by using deuterated acetone, it is possible to study such systems with SANS without having deuterated chains or junction points. Yang and Wu [111] have recently started studying unimodal and bimodal PPO based epoxies swollen in deuterated acetone by

SANS. These swollen epoxies have their T_g below room temperature. Therefore, the experiments do not involve any of the nonequilibrium effects which are usually associated with glassy systems.

C H A P T E R V I

PDMS NETWORKS

To critically evaluate the molecular theories of rubber elasticity it is valuable to have information regarding the crosslink density and junction functionality. In the case of randomly crosslinked elastomers it is difficult to obtain independent quantitative estimates of these parameters. It has been possible in recent years to make "model networks" [5,6,105] by using specific reactions. This typically involves the reaction of a small molecule, of a specific functionality, with prepolymers having reactive groups at the ends. The prepolymers are usually linear but can even be star shaped polymers.

Characterization of the reactants can be done prior to the network formation to yield information about the length of the chains between crosslinks or M_c and the functionality of the junction points ϕ. It is possible to prepare networks with a controlled amount of dangling chains by varying the stoichiometry.

Commonly studied model networks have been polyurethane and polydimethyl siloxane (PDMS) networks [5,106,107]. Polyurethane networks may be prepared by endlinking hydroxyl terminated linear chains with a triisocyanate. PDMS networks are usually prepared by two methods.

i) Endlinking hydroxyl terminated chains with silicates.

ii) Endlinking vinyl terminated chains with silanes containing active hydrogen atoms.

In recent years the PDMS networks have been more extensively studied than polyurethane networks. The main reason for this is that a very wide range of prepolymers and crosslinkers are available in the case of PDMS unlike the polyurethanes.

Mark and coworkers [5-11] have used mechanical, swelling and birefringence measurements to evaluate the molecular theories of rubber elasticity. They have been able to study PDMS networks with functionalities upto 80 by using special crosslinking agents. Their results on unimodal networks are in good agreement with the predictions of the Flory-Erman theory of rubber elasticity [4,5]. They support Flory's notion that trapped entanglements do not contribute to the equilibrium elasticity of networks. They also studied bimodal PDMS networks which were prepared by mixing very short PDMS chains with long chains. For specific compositions (high mole fraction of short chains), they found enhanced mechanical behavior, before rupture, as compared to the unimodal networks [9-11]. The improvement in mechanical properties is attributed to the limited extensibility of

the short chains (non gaussian behavior), which causes the long chains to deform more than the short chains.

There were a few uncertainities regarding the crosslink density and junction functionality in our preliminary work on randomly crosslinked polybutadiene networks. Therefore, it was decided to study model networks which offered more control regarding the network architecture. The PDMS system was chosen because of the wide range of reactants available commercially and the wealth of information available in literature. Therefore, the scattering from swollen networks in terms of network inhomogeneities can be understood better by using networks of known distribution of M_c's.

Experimental

PDMS model networks were initially prepared by crosslinking dihydroxy terminated PDMS chains with tetra ethyl orthosilicate (TEOS) in bulk at room temperature. Stannous-2-ethyl hexanoate (0.3 wt % of polymer) was used as a catalyst. The reaction proceeds with the evolution of ethanol which has to be removed. In thick samples, the evolution of ethanol during the crosslinking usually resulted in bubbles being trapped in the final network. Therefore, it was decided to prepare networks by using

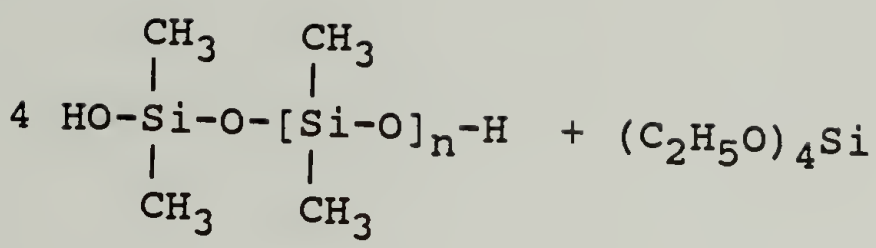

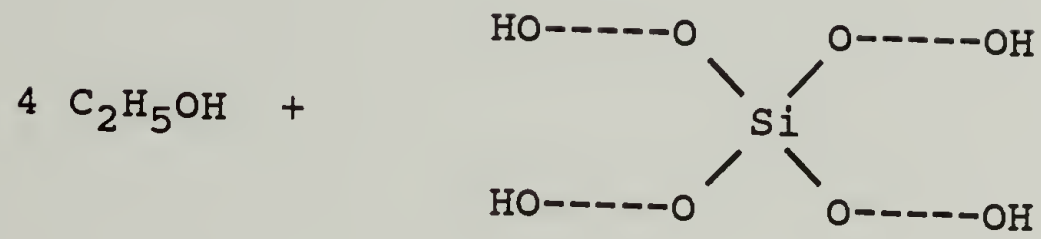

an addition reaction. This is accomplished by endlinking α,ω-divinyl PDMS with the active hydrogens on a silane crosslinking agent in the presence of a platinum catalyst. For a tetra functional network, a tetra silane such as tetra-kis dimethyl siloxy silane (TKDMS) is used.

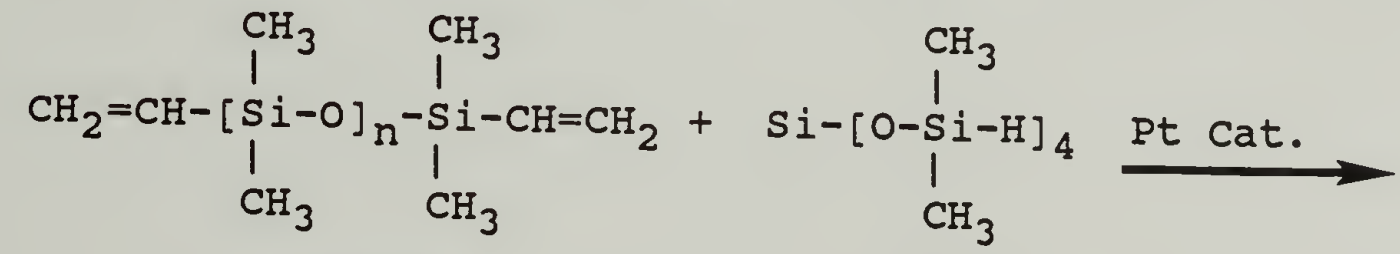

(PDMS) (TKDMS)

All the reactants are commercially available from Petarach Systems, Bristol, PA. The advantages of using such a PDMS system are:

i) Control on M_c and ϕ in the network.

ii) Simple and convenient chemistry.

iii) The prepolymers have a reasonably low viscosity compared to other polymers. This makes filtration fairly easy.

iv) Excellent optical clarity even in thick films.

v) The crosslinking agent is very similar to the chain repeat units.

The major drawbacks are:

i) A finite polydispersity ($M_W/M_N \sim 1.8$)

ii) The deuterated monomer is scarce. Therefore, it was not possible to get any labelled PDMS chains.

iii) The prepolymers usually contain approximately 3% non reactive, low molecular weight cyclics.

Myers et al [108] have observed that the cyclics account for a large fraction of the sol extracted from these networks. Macosko et al[109] have suggested that the cyclics may be removed by storing the open container under vacuum for at least one week.

The molecular weights of the prepolymers used were determined by using reference standards obtained from Dow Corning Corporation. These PDMS standards were provided by Dr.J.C. Saam. The charcteristics of these reference standards are given in Table 7 .

Petrarch Systems lists the PDMS prepolymers by their bulk viscosities. A similar approach has been adopted in naming the samples used in this study. The various prepolymers used in this study are listed on Table 8 in a similar manner.

The prepolymers were characterized for their molecular mass by the following methods:

i) End group analysis by NMR

ii) VPO

iii) GPC

iv) Light Scattering

v) Intrinsic Viscosity

M_N for PDMS 4-6 was determined by end group analysis and by VPO. The NMR measurements were made by Mr. Walt Bassett. The estimated value of M_n = 770, was obtained from the relative amounts of the methyl and vinyl groups present. The VPO measurements were made using a KNAUER No. 11 VPO in the Micro Analysis Laboratory. Measurements were made at 90°C using solutions in toluene. Benzil (M.W. = 210) was used for calibration. These measurements gave M_n = 783, which is in good agreement with the NMR results.

The light scattering measurements were made on dilute solutions in toluene at 25°C using Professor Langley's apparatus in the Physics department. The details of light scattering experiments on PDMS solutions are given at a later part in this chapter. Absolute intensity calibration was obtained by measuring the scattered intensity from toluene at an angle of 90°.

The GPC experiments were performed on a Waters GPC II

at the Polymer Central Facility at the Massachusetts Institute of Technology (M.I.T.) in Cambridge, MA. Prof. R.E. Cohen of the Chemical Engineering department at M.I.T. was in charge of that laboratory. Measurements were made by using toluene as the solvent with a flow rate of 1.5 ml/min. THF was not chosen as the solvent because of the small difference in refractive index between PDMS and THF. The PDMS reference standards obtained from Dow Corning were used for calibration. The results of the molecular mass measurements are listed on Table 8.

Meir Ben Aliz, a visiting scientist from Israel, made intrinsic viscosity $[\eta]$ measurements on these prepolymers. Toluene was used as a solvent at 25°C. The results are listed on Table 9.

$$[\eta] = K M_v^a \qquad (78)$$

The Mark-Houwink coefficients for PDMS in Toluene at 25°C are [110]

$$K = 2.15 \times 10^{-4}$$

$$a = 0.65$$

In Table 9, the values of the viscosity average molecular weight M_v were estimated by using the Mark-Houwink coefficients. Using the GPC data and the Mark Houwink coefficients, it is possible to estimate the intrinsic viscosity $[\eta]$. This is done by representing the molecular weight distribution by a Flory Schulz

distribution [67]. Let w_x be the weight fraction of species of mass x.

The polydispersity $x_W/x_N = 1 + 1/b$ (79)

$$w_x = [b/x_N\,\Gamma(b+1)]\,(bx/x_N)^b \exp-(bx/x_N) \quad (80)$$

where $\Gamma(A)$ is the gamma function of A

But

$$x_v = \left[\int_0^\infty w_x\, x^a\, dx\right]^{1/a}$$

$$x_v = \frac{x_N}{b}\left(\frac{\Gamma(a+b+1)}{\Gamma(b+1)}\right)^{1/a} \quad (81)$$

and $[\eta] = K\, x_v^{\,a}$

$$= K\left(\frac{x_N}{b}\right)^a \frac{\Gamma(a+b+1)}{\Gamma(b+1)} \quad (82)$$

Using the molecular weight data in Table 8 and equation (82); the intrinsic viscosity $[\eta]_{calc}$ was estimated and is listed in Table 9.

Sample Preparation and Characterization

Tetra functional PDMS networks were prepared by endlinking the divinyl terminated prepolymers with TKDMS. The reaction was catalyzed by a platinum catalyst PC072 purchased from Petrarch Systems. It consists of a complex of chloroplatinic acid in toluene and contains 3-3.5% Pt by weight. The solution was diluted further to give a concentration of 0.00858% Pt. The optimal amount of catalyst necessary was found to be 0.5 parts per million

(ppm) of Pt i.e. 2-3 drops of the catalyst solution per 5 gms of prepolymer.

The prepolymers were filtered and weighed. Usually, the weight of the network sample prepared was in the range of 20-30 gms. The required amount of the catalyst solution was added to the prepolymer and the two were mixed under vacuum for about one hour. The required amount of crosslinker was then added in an inert atmosphere of dry nitrogen. This was accomplished by placing the balance inside a glove bag which had the N_2 environment. The reactants were mixed for 15 to 20 minutes under N_2 and then poured into the mold. The reaction was allowed to proceed for one day at room temperature. The mold was then kept for one day in an oven at 60°C to ensure complete reaction.

Initially, the network samples were prepared in open faced Teflon lined molds. The molds were covered with Aluminum foil. The samples did not have a very uniform thickness and quite often did not have a perfectly flat top surface. A special mold was used to prepare films of uniform thickness and very smooth surfaces . This is a three part aluminium mold and is shown in Figure 13. It was made in the Chemistry Workshop by Richard Zinc. The top and bottom parts are attached to the middle part by screws, ensuring uniform thickness. The sample thickness

can be varied in the range 1-6 mm. by using spacers between the top and middle parts. The inside of the mold is lined with Teflon or mylar to prevent the network from sticking to the mold. The middle part is lined with Teflon. The surfaces of the top and bottom parts facing the inside are polished smooth. It is preferable to use mylar sheets on the smooth surfaces of the mold to get a very smooth surface on the network.

The networks were extracted in benzene for five to six days to remove the sol fraction. The sol fraction was typically about 3-4% in most of the networks. For a stoichiometric reaction the presence of a significant amount of sol suggests the possibility of network imperfections. Therefore, it is common practice to use a slight excess of the prepolymer. However, in the case of PDMS prepolymers it is known that the prepolymer contains a few percent of unreactive cyclics. The sol fraction from such PDMS networks usually consists largely of the unreactive cyclics.

The extracted networks were swollen in fresh benzene to measure the swollen weight. The networks were deswollen by slowly adding a non solvent like methanol to the system. The deswollen sample was dried by placing it in a vacuum oven at 60°C for a day. The sol fraction and degree of swelling were estimated from the initial dry weight,

the swollen weight, and the final dry weight. The swelling data for unimodal networks is given in Table 10.

v_2 is the volume fraction of polymer in the swollen network at equilibrium. F_ϕ is the front factor in the Flory-Erman theory and can be estimated from the swelling measurements.

$$M_c = \frac{F\phi \ \rho v_1 \ [\ (2v_2/\phi) - v_2^{1/3} \ ]}{\ln(1-v_2) + v_2 + \chi v_2^2} \qquad (83)$$

The value of the polymer-solvent interacton parameter χ is usually found to be concentration dependent. The value

$$\chi = 0.484 + 0.33 \ v_2$$

was used following Mark and coworkers [5].

The values of F_ϕ are sufficiently different from 1, indicating departure from the affine model of deformation. For tetra functional networks, Mark and coworkers have found $F_4 = 0.65 \pm 0.10$; which is in reasonable agreement with these values. For PDMS 100, it is found that $F_5 > F_4$. This is as expected, because as the functionality is increased, the deformation is expected to be closer to the affine model.

In addition to unimodal PDMS networks, bimodal networks were also prepared. PDMS 1000 (M_N = 22,500) was used as long chains and PDMS 4-6 (M_N = 770) as the short chains. Networks were prepared with varying mole fractions of short chains. The short and long chains were mixed

simultaneously and degassed for 1 hour before the crosslinker was added. This was done to minmize any segregation of the short chains. The bimodal networks were swollen in benzene and in toluene. The swelling results for the bimodal networks are given in Table 11.

If x is the mole fraction of the short chains, then the average M_C for a bimodal network will be

$$M_C = x\, M_S + (1-x)\, M_L \qquad (84)$$

where the subscripts $_S$ and $_L$ correspond to the short and long chains.

Based on the swelling measurements in benzene, F_4 was calculated using equation 83. Using these values of F_4 and the swelling results in toluene, the values of χ were determined for the various bimodal networks in toluene. These results can be expressed as :

$$\chi_{Tol} = 0.487 + 0.192\, v_2 \qquad (85)$$

Using light scattering from concentrated PDMS solutions in toluene, χ was estimated to be

$$\chi_{Tol} = 0.430 + 0.179\, v_2 \qquad (86)$$

Assuming a 3% error in the swelling measurements, the standard deviation in the value of χ is expected to be 15%. Therefore, the two values of χ seem to be consistent within experimental error.

SANS from PDMS Solutions

In this work, the focus is on the structure or spatial correlations in swollen polymer networks. It is, therefore, important to understand the correlations in solutions containing linear polymer chains at equivalent concentrations. The equlibrium degrees of swelling in networks typically correspond to polymer concentrations which are in the semi dilute and concentrated regimes for solutions with linear polymers. In these regimes, the correlations are typically in the order of 10 - 50 Å and therefore SANS is very convenient for such measurements.

The SANS experiments were performed on commercial PDMS polymers using deuterated benzene C_6D_6 to provide contrast. Other researchers have used long chain polymers to prepare the solutions for similar experiments in the semi dilute regime. The solutions for these experiments were prepared by using the same prepolymers which were used to prepare the networks. The motivation for this is as follows :

i) The expansion factor of a polymer chain in a good solvent depends on the size of the chain. Long chains expand more than short chains due to more excluded volume type or binary contacts per unit length of the chain.

ii) The SANS experiments by Picot and coworkers [13] on labelled chains have shown that the dimensions of a labelled chain between crosslinks in a swollen network is comparable to the dimension of a linear chain of the same mass of infinite dilution.

Therefore, to compare correlations in solutions and swollen networks, it is necessary to use the prepolymers to prepare the solutions rather than using long chains.

The SANS experiments were performed at NBS in collaboration with Dr. Charles C. Han. The solutions were placed in quartz couvettes with a 2mm path length. The measurements were made using a wavelength of 6Å and a sample to detector distance of 3.6 m. The q range covered was from 0.01 to 0.12 $\mathring{A}^{-1}$. Absolute intensity calibration was performed using a secondary standard, Vydac. This is essentially a silica gel which is a very strong scatterer. Its characterstics are:

$$\frac{d\Sigma(0)}{d\Omega} = 28.4 \text{ cm}^{-1} \text{ and } R_g = 44 \mathring{A}$$

Incoherent backgrounds were measured using the individual components. The coherent scattered intensities for different polymer solutions are given in Figure 14. The curves have a smooth Lorentzian type of decay. For small q, the data can be represented as a Lorentzian

function as in equation (65):

$$\frac{d\Sigma(q)}{d\Omega} = \frac{d\Sigma(0)}{d\Omega} \frac{1}{(1 + q^2 \xi^2)}$$

Therefore, the correlation distance ξ can be estimated for various unimodal PDMS solutions from a plot of the inverse intensity versus q^2 . The values of ξ are listed in Table 12. The values of x in Table 12 were obtained from wide q data as $\frac{d\Sigma(q)}{d\Omega}^{-1}$ vs q^x

Where $x = 1/\nu$

given $R_g \sim M^{\nu}$

The various limits of x are :

Good solvent	5/3
Gaussian	2
Rod	1

For PDMS 200 in C_6D_6; the dependence of on volume fraction of polymer is found to be:(see Figure 15).

$\xi = 4.36\ v_2^{-0.71}$

The exponent for the concentration dependence of ξ is fairly close to the value of -0.75 predicted by scaling laws for long chains in a very good solvent. This would normally suggest dominant binary interactions i.e., excluded volume effects. For such a case, $\nu = 3/5$ and x would be expected to be 5/3. In Table 12, it can be seen that for the PDMS 200 solutions, as the concentration of

polymer is increased, x decreases towards 1. $x = 1$ indicates correlations at the level of local rigidity of the chain. It also corresponds to the theta conditions in solutions. In this regime, excluded volume effects are weak and ternary intaeractions are dominant. For such a regime the osmotic pressure $\Upsilon \sim v_2^3$ which means

$$\frac{d\Sigma(0)}{d\Omega} \sim v_2^{-1}$$

For PDMS in C_6D_6, we find that

$$\frac{d\Sigma(0)}{d\Omega} \sim v_2^{-0.7}$$

This suggests that the system is approaching the theta limit.

Recently Schaefer [69] has presented what he calls a unified model for the structure of polymers in semi dilute solutions. It is expected that the scaling laws developed for infinetly long chains in good solvents are valid over only a small concentration range in real polymer systems. Schaefer has described the correlations in terms of the polymer solvent interaction parameter χ and the local rigidity of the chain. Figure 16 shows the representation of the correlation ranges. The various concentration regimes according to his model are :

i) $v_2 < v_2^*$ The dilute regime

ii) $v_2^* < v_2 < \tilde{v_2}$ The scaling regime.

The predictions of the scaling laws are valid only in this regime.

iii) $\tilde{v_2} < v_2 < v_2^+$. The marginal regime.

The existence of this regime in this model is a consequence of the local rigidity of the chains. In this regime, the chains are considered to be nearly ideal on all length scales. The binary contacts between monomers are too sparse to lead to any significant swelling of the chains.

iv) $v_2^+ < v_2 < v_{2b}$. The theta regime.

Here the three body effects dominate all other interactions. In this range, ν is still equal to 0.5, as in the marginal regime. However, $\xi \sim v_2^{-1}$. The upper limit of the theta regime is v_{2b} at which the correlation range becomes comparable to the persistence length b.

The transitions or crossovers from one regime to the another are predicted to be sharp. However, in real systems, the crossovers are expected to be smooth resulting in exponents intermediate between the different regimes.

The SANS results can be understood in terms of such a representation. The concentration ranges of interest, 0.1 to 0.5, correspond from marginal to the theta or even the concentrated regimes depending on the size of the chains.

This would mean that at most, the chains are only slightly swollen. Table 13 shows the SANS results for bimodal PDMS solutions in C_6D_6. PDMS 1000 was used for the long chains and PDMS 4-6 for the short chains.

For the bimodal solutions # 1-5, we have:

$$\xi = 4.25\ v_2^{-0.77}$$

This result is quite similiar to that found for unimodal solutions of PDMS 200.

In the lower part of the Table 13, comparisions are made for the 3 bimodal solutions containing the same volume fraction of polymers but different amounts of short and long chains. # 7 contains 50 mole % of short chains. The degree of polymerization N for the long and short chains are 10 and 300. $(N_S)^2 < N_L$

Therefore, according to the deGennes [66], it is expected that in the bimodal solutions the long chains are swollen by the short chains. Such a hypothesis is supported by the observation that the wide q exponent x is higher in the bimodal solutions as compared to the unimodal solutions with long chains.

SANS from Swollen PDMS Networks

These experiments were also performed at NBS at the same time as the solutions were studied. Hydrogeneous PDMS

networks were swollen in the deutero benzene C_6D_6. The swollen samples were placed in the aluminium cells with quartz windows. Figure 17 shows the scattering from a swollen network and the corresponding solution. The network was prepared by using PDMS 1000 and TKDMS. It can be seen that the intensity falls off more rapidly for the network indicating a larger correlation size as compared to the solution.

For small q, the correlation size ξ was estimated from a Lorentzian plot i.e., equation (65). Table 14 lists the correlation sizes for different unimodal networks.

To make ξ equivalent to a radius of a gyration type of measurement, we have

$$R_c = \sqrt{3}\ \xi \qquad (87)$$

This correlation size R_c is then compared with the radius of gyration R_g for a single chain between crosslinks. The value of R_g for the unperturbed chain is given by:

$$(R_g)_z^0 = 0.25\ M_z^{1/2} \qquad (88)$$

where M_z is the Z average molecular weight of the chain. The relation between R_g and M was obtained by Picot and coworkers [12] for labelled chains in a PDMS network. M_z can be estimated if we assume a Flory Schulz form of the molecular weight distribution function [67].

$$M_z = (1 + 2/b)\ M_N \text{ where } M_W/M_N = 1 + 1/b \qquad (89)$$

α is the macroscopic deformation ratio estimated from the degree of swelling :

$$\alpha = v_2^{-1/3}$$

Assuming a phantom network type of deformation, the molecular deformation ratio α_m will be (equation 71):

$$\alpha_m = \left[\frac{3 + \alpha^2}{4}\right]^{1/2}$$

For such a model, the expected radius of gyration for a chain between crosslinks in a swollen network is given by $(R_g)_{ph}^{sw}$ in Table 14. For all the networks it can be seen that :

$$R_c > (R_g)_{ph}^{sw}$$

Since $(R_g)_{ph}^{sw}$ is most likely an overestimate, the fact that it is still much less than R_c clearly indicates that in swollen networks correlations exist over distances greater than the distance between topologically neighboring crosslink junctions. The quantitiy Q_c in Table 14 is defined as :

$$Q_c = \frac{R_c}{(R_g)_{ph}^{sw}} \qquad (90)$$

There seems to be no systematic dependence of Q_c on crosslink density for the uinimodal networks. Values of Q_c will be compared for unimodal and bimodal networks.

The bimodal networks used in this work were prepared using PDMS 1000 as the long chains and PDMS 4-6 as the

short chains. The networks were swollen with C_6D_6 for the SANS experiments. The scattering curves for the bimodal networks and their corresponding solutions are given in Figures 18 and 19. The excess scattered intensity for various bimodal networks in comparision to the solutions are given in Figure 20.

As in the case of the unimodal networks, the correlation sizes ξ or R_c were estimated from the small q data. For the various networks these results are given in Table 15. In this Table x represents the mole fractions of short chains.

These networks were prepared by mixing the short and long chains prior to the addition of the crosslinker to avoid any spatial segregation of the short and long chains amongst themselves. For these bimodal networks, the value of R_c decreases as the average M_c is decreased. Moreover, the values of Q_c for these bimodal networks are comparable to those for the unimodal networks.

The fact that the correlation size in a swollen network is much larger than in the corresponding semi dilute solution has been taken by some workers [15] to be an indication of the presence of inhomogeneities in the network structure. However, the results from unimodal and bimodal networks seem to indicate that in the absence of non-random crosslinking, the distribution of crosslink

densities is not the dominant factor in determining spatial correlations in a swollen network.

According to Bastide and coworkers [14-16], the swelling of a network involves the desinterspersion of chains. This is imagined to involve the folding or unfolding of network strands by rearrangements of the conformations and the packing of the chains without significantly disturbing the end to end distances of a chain between croslinks. Therefore, for such a folding and unfolding mechanism to take place, it has to involve correlations in the network on a scale larger than just the distance between the two topologically neighboring crosslinks in a network. Even in an ideal or perfectly monodisperse unimodal network, correlations over distances greater than the R_g of a single chain between crosslinks are expected.

In addition to the network strand folding process, the overall correlations in a swollen network are also dependent on the distribution of crosslink densities and on network defects such as dangling chains and loops. The relative contribution of each factor will depend on the actual network structure. The role of crosslink inhomogeneities will be quite significant in determining the correlation in network structures possessing spatial hetrogeneities i.e., clusters of short or long chains.

Light Scattering Experiments

The wavelength of visible light is of the order of 6000 Å. Light scattering can therefore be used to study correlations of a larger size level than those possible by SANS. It is necessary to know the refractive index n of the material being studied, to obtain absolute intensity calibiration for light scattering.

Refractive Index Measurements : The refractive index of a binary system, such as a polymer solution or a swollen network will depend on the polymer concentration, the temperature, and the wavelength of the incident radiation. The refractive index measurements were made for PDMS solutions in benzene and in toluene and also for the pure individual components . These measurements were made on an American Optical Abbe Refractometer model 10450. A circulating water bath was used to maintain a constant temperature during the measurements.

The wavelength of the radiation used in the refractometer corresponds to the sodium line (λ = 5890 Å). However, the light scattering experiments were performed using an Argon Ion Laser which has λ = 5145 Å. Therefore, the refractive index was estimated at λ= 5145 Å.

For pure components, the refractive index at a particular temperature can be expressed in terms of the wavelength by the Cauchy dispersion formula :

$$n = A + \frac{B}{\lambda_o^2} + \frac{C}{\lambda_o^4} \qquad (91)$$

where λ_o is the wavelength of the incident radiation in vacuum. The Cauchy formula has no theoretical basis and is often used in its simplified form with just two terms A and B. Using the measurements and the values of n reported in the literature [51,52] at different wavelengths , A and B were estimated for toluene, benzene and PDMS at 25°C. These values are given on Table 16 along with the values of n at λ = 5145 Å.

For polymer solutions, the value of $n(\lambda = 5145\ \text{Å})$ was estimated using the Lorenz-Lorentz equation [48].

$$\frac{1}{\rho}\left[\frac{n^2 - 1}{n^2 + 2}\right] = \frac{W_1}{\rho_1}\left[\frac{n_1^2 - 1}{n_1^2 + 2}\right] + \frac{W_2}{\rho_2}\left[\frac{n_2^2 - 1}{n_2^2 + 2}\right] \qquad (92)$$

Here terms on the left hand side of the equation 92 refer to the solution and those on the right hand side refer to the individual pure components. W_i and ρ_i refer to the weight fraction and mass density of the species i. Using the results of the measurements at λ = 5890 Å, the value of ρ for that particular concentration of polymer can be estimated from equation 92. Using that ρ value and the values of $n_i(\lambda = 5145\ \text{Å})$

from Table 16 for the individual components, the refractive index at $\lambda = 5145$ Å for that particular solution can be estimated.

For PDMS solutions in toluene and in benzene, the refractive index was estimated as a function of polymer concentration at 25°C for $\lambda = 5145$ Å. The results are :

i) For PDMS in Toluene:

$$n = 1.5018 - 0.103v_2 \qquad (93)$$

ii) For PDMS in Benzene :

$$n = 1.5058 - 0.112v_2 \qquad (94)$$

The PDMS 1000 prepolymer was used for the refractive index measurements. Since the mass of density of this prepolymer ($\rho = 0.97$ gm/cc) is almost the same as the dry networks, the refractive indices for the swollen networks were estimated using equations 93 and 94.

Light Scattering from PDMS Solutions

The light scattering experiments on PDMS solutions and swollen networks were performed on a wide angle appratus shown in Figure 2 . The apparatus uses an Argon Ion Laser ($\lambda = 5145$ Å). The details of the instrumentation have been discussed in Chapter 3.

Pyrex test tubes with a 10 mm outer diameter were used as cells or sample holders for the PDMS and the individual components. The samples were filtered with Millipore

0.5 μm filters. The cells were mounted inside the thermostated vat which contained toluene to reduce stray light. The scattered intensity is measured using a photon counter. The intensity of the incident beam is monitored using a beam monitor. The output for the computer is the ratio A/B, where A is the counts per second at the detecter and B is the counts per second at the beam monitor. At low intensities, the dark currents for A and B are of concern. At high incident counts, one has to correct for the dead time τ in the beam monitor. If dA and dB are the dark currents for A and B, the correct measured intensity I at a given scattering angle will be :

$$I = \frac{K\,(A - d_A)\,[\,1 - \tau\,(B - d_B)\,]}{(B - d_B)} \qquad (95)$$

d_A and d_B are determined by closing the shutters. τ was estimated by varying the laser power so as to vary B. The typical values for the correction parameters are :

d_A = 20 counts per second.

d_B = 1800 counts per second.

τ = 100 nano second.

The dark current counts were found to be sensitive to the room temperature; therefore they were measured frequently.

At 25°C ,scattering was measurted in the angular range 45° to 135°. For all the samples, the measured intensity $I(\theta)$ was symmetrical about the scattering angle $\theta = 90°$.

Compared a scattering volume V at $\theta = 90^{\circ}$ for any arbitrary θ, the scattering volume will be $(V/\sin\theta)$. Therefore for any value of θ, the Rayleigh ratio will be :

$$R(\theta) = K\, I(\theta)\, \sin\theta \qquad (96)$$

Where K is the instrument constant.

For the solutions studied, the Rayleigh ratio $R(\theta)$ was independent of scattering angle. Therefore, all the measurements are reported corresponding to $\theta = 90^{\circ}$.

An analyser can be mounted onto the detecter arm. H_V scattering was measured by crossing the analyser so as to minimise the detecter output. V_V scattering was measured by maximizing the dectecter output. The scattering from toluene was used to locate the settings on the analyser for V_V and H_V scattering.

The total scattering from density fluctuations in toluene at $\theta = 90^{\circ}$ was used for absoulte intensity calibration. Kaye and McDaniel [119] have reported that for toluene at 23°C for $\lambda = 6328$ Å

$$R(\theta = 90^{\circ}) = 14.06 \times 10^{-6} cm^{-1}$$

converting to $\lambda = 5145$ Å and for 25°C we have

$$R(\theta = 90^{\circ}) = 32.85 \times 10^{-6} cm^{-1}$$

The total scattering from toluene contains a significant fraction of anisotropic contributions. For V_V scattering, the Cabannes factor C_F can be estimated from the depolarization ratio ρ_V as in equation 37.

For the pure components, toluene and PDMS, the bulk compressibility β was estimated from the scattering due to density fluctuations R_d using equation 35. The results are :

$$\beta_{Tol} = 9.6 \times 10^{-11} \text{ cm}^2 \text{ dyne}^{-1}$$

$$\beta_{PDMS} = 12.0 \times 10^{-11} \text{ cm}^2 \text{ dyne}^{-1}$$

For the solutions, the compressibility was approximated as a linear sum :

$$\beta = \beta_1 v_1 + \beta_2 v_2 \qquad (97)$$

Where v_i is the volume fraction of component i.

The Rayleigh ratio R_{sol} in absolute units is obtained for the solutions by comparing the intensity with that for toluene (Tol).

$$R_{sol} = \frac{I_{sol} \, n^2_{sol} \, R_{tol}}{I_{tol} \, n^2_{tol}} \qquad (98)$$

The refraactive index terms are included to correct for different solid angles due to refraction.

For solutions of PDMS 1000 in toluene at 25°C, Figure 21 shows the Rayleigh ratio for the total scattering as a function of the polymer correlation. It can be seen that the Rayleigh ratio for the solutions goes through a maxima as a function of concentration as predicted by equation (45). The position of the maxima is also in reasonable agreement with the prediction according to equation (46).

If we consider the interaction parameter to be concentration dependent as :

$$\chi = \chi_o + \chi_1 v_2 \qquad (99)$$

then equation (45) gets modified to :

$$R_c = \frac{K_L V_1 v_2 \rho_2^2}{\left[\frac{1}{(1-v_2)} - 1 - \frac{1}{X_w} - 2\chi_o v_2 - 3\chi_1 v_2^2\right]} \qquad (100)$$

Equation (100) can be rearranged to :

$$F(v_2) = \frac{1}{v_2}\left[\frac{1}{(1-v_2)} - 1 - \frac{1}{X_w} - \frac{K_L V_1 v_2 \rho_2^2}{R_c}\right]$$

$$= 2\chi_o + 3\chi_1 v_2 \qquad (101)$$

Therefore from a plot of $F(v_2)$ versus v_2 ; one can estimate $\chi(v_2)$. Figure 21 shows such a plot. The result for PDMS 1000 in toluene at 25°C is :

$$\chi = 0.43 + 0.179\, v_2$$

This value of χ was then used for networks swollen in toluene.

Light Scattering from Swollen PDMS Networks

Light scattering experiments were performed on swollen bimodal PDMS networks. By using networks of controlled hetrogeneity in crosslink density; it is possible to evaluate the analysis for the inhomogeneity of crosslinking as suggested by equation (53).

There are a number of concerns in performing light scattering experiments on swollen gels:

i) Trapped dust

ii) Shape of the gel sample

iii) Stray light at the sample-solvent interface

iv) Speckle patterns

The presence of dust particles and the scattering associated with them is of considerable concern in any light scattering experiment. In the case of gels great care has to be taken to make them dust free since trapped dust cannot be centrifuged or filtered out as in the case of solutions. One advantage of using relatively low viscosity prepolymers for the synthesis of the netorks is that they can be filtered without much difficulty prior to the crosslinking. The networks were extracted and swollen in filtered solvent after curing in bulk. It is possible to use two sample shapes for wide angle light scattering measurements :

i) cylindrical samples

ii) flat samples.

The flat samples have to be tilted with respect to the beam to measure scattering at wide angles. But, the cylindrical samples are easier to analyse since the volume correction is a simple $\sin\theta$ term as in equation (96). Therefore, initial experiments were attempted on

cylindrical samples. Two approaches are possible in the case of cylindrical samples.

i) to place the swollen sample inside the pyrex test tubes used for the solutions

ii) to use a special holder to suspend the cylindrical samples into the vat containing the excess solvent.

Several interfaces are involved in the first approach which result in considerable amount of stray light. The stray light problems in general can be minimized by having the maximum possible seperation of the interfaces across which there is change in refractive index. Therefore, it is necessary to have the largest possible diameter for cylindrical samples which were suspended into the vat.

An aluminium sample holder was designed to be attached to the thermostated vat. It was black anodized to avoid reflections. Its inner diameter was 17 mm. A Teflon plug was attached at the bottom of the holder to hold up the sample. The plug was kept in place with a Teflon pin.

It is necessary to have as small a clearance as possible between the sample and the sample holder to obtain perfect alignment. Therefore,it is desirable to have the swollen sample with a diameter as close as possible to 17 mm. It is necessary to prepare samples of different starting diameters as samples with different crosslink densities swell to different amounts with the same

diluent. Molds of varying diameters are needed to accomplish this. Teflon tubes were used as molds. Initially thick walled tubes were used. They did not give a very smooth surface; therefore, thin walled Teflon tubing, which gave a much smoother surface, was used.

Depending on the sizes of the Teflon tubing avaiable it was possible to prepare two network samples which would fit the sample holder with the least amount of clearance. These were networks with 100% long chains and 5% long chains. To allow measurements on samples of other crosslink densities; in principle, one could have used the same starting molds but used sample holders of different inner diameters or varied the temperature to change the swelling ratio. However, this was not necessary since the results from the two samples used suggested that this method was not suitable. The reasons for this are discussed in detail.

In the detector arm there are two circular apertures which are used to control the amount of light incident on the detector. A speckle pattern is formed when the laser beam is incident on the swollen gel.The size of the speckles depends on the size of the front aperture. The larger the aperture, the smaller is the speckle. If the speckle pattern is large then there are large fluctuations in the intensity. This makes it necessary to average over a large enough scattering volume to get a true average

intensity. In order to minimize fluctuations associated with speckle patterns it was necessary to use the largest possible front aperture (5 mm) and the largest possible scattering volume. The unfocussed beam was used to get a large scattering volume. There are large fluctuations in the intensity due to speckles if focussed beams are used. Although, an unfocussed beam has advantages as far as speckles are concerned; but it is disadvantageous for cylindrical samples. When an unfocussed beam is incident on a swollen cylindrical gel and the solvent;the sample acts as a cylindrical lens and results in $R(\theta)$ being independent of scattering angle.

The problem arises due to the finite curvature of the sample-solvent interface where the unfocussed beam is incident. The problem can be avoided by either using a focussed beam or by using a flat surface with a unfocussed beam. Since a focussed beam has problems associated with speckle patterns; the only alternative is to use a flat sample.

Flat samples are easy to prepare. But it is necessary to have uniform thickness and very smooth surfaces. To reduce stray light at the two surfaces; the samples were prepared in such a way that the thickness of the swollen sample was atleast more than 5.5mm. Flat bimodal PDMS network samples of ralatively uniform thickness were

prepared in bulk using the mold which is shown in Figure 13 and was described earlier. The mold was lined with MYLAR to give very smooth surfaces. It is not necessary to be concerned about multiple scattering in these relatively thick films because of their high optical clarity.

It is necessary to tilt the sample with respect to the incident beam to measure scattering from flat films at wide angles. A special holder was used to perform experiments on flat films. This was made by Richard Zinc in the chemistry workshop. This holder is shown in the Figure 23. It essentially consists of two parts-- a base and a stem. The base is attached to the vat and can be rotated to allow specific tilt angles. The sample is mounted on to the stem in between two windows. The windows are designed to grip the samples firmly but still provide opening for the incident or scattered beams to pass. The windows are seperated by a spacer which is about 5 mm thick. The samples of any thickness more than 5 mm can be held securely between the windows. The stem is attached to the base and can be moved up and down so as to expose different regions of the sample to the beam. The sample holder was black anodized to minimize the stray reflections.

Experiments were performed on bimodal PDMS networks swollen in toluene and benzene at 25°C. It was possible to obtain data over a wide angular range by using various tilt

angles. Let the tilt angle Φ_t be defined by the angle between the incident beam and the normal to the surface. This is shown in Figure 24. The positive and the negative angles are shown in Figure 24. For the different tilt angles Φ_t; the nominal scattering angles were :

i) Φ_t = 0 θ = 30 - 50

120 - 130

ii) Φ_t = + 30 θ = 35 - 80

iii) Φ_t = - 30 θ = 110 - 130

Three fixed tilt angles were used for the present design of the sample holder. The holder, however, could be modified to allow all the possible tilt angles by using a gear assembly. At each scattering angle, the sample holder was rotated by 180 (in terms of tilt), to get an average value.

There is concern about specular reflections for the backscattered light. For a tilt of Φ_t = -30 ; one expects a specular reflection at a scattering angle θ = 120 . One can observe the specular reflection when the stem in the sample holder is vertical. The narrow width of the specular reflection, in terms of θ, as shown in Figure 25 indicates that the surface of the sample is fairly smooth. Specular reflections in the plane of the detecter can be eliminated by a slight tilt of the sample holder stem in the vertical plane.

Light Scattering Correction Factors

To obtain the Rayleigh factor for the flat tilted samples; it is necessary to correct for tilt and refraction. Stein and Keane [112] have reported all the necessary corrections for scattering of light from flat, tilted, and thin films. Their analysis has been modified here for the case of thick samples. The Rayleigh factor $R(\theta)$ is then expressed in terms of measured intensity $I(\theta)$ and the various correction factors as :

$$R(\theta) = \frac{K\, I(\theta)\, C_n\, \Xi}{I_o\, V_s} \qquad (102).$$

where C_n is the refraction correction for the solid angle; Ξ is the correction for reflection; I_o is the incident intensity; V_s is the correction of the scattering volume for refraction and tilt; K is the instrument constant which includes the size of the apertures, the width of the incident beam, transmission of the attenuators and the analyser etc. The ratio (K/I_o) can be used as the absolute intensity calibration factor by measuring the scattering from the swollen samples with the same apertures, attenuatons, and beam monitor setting as for scattering from toluene. The various correction factors used are :

True Scattering Angle : Due to refraction and tilt the true scattering angle θ_T in the sample is not the same as the nominal scattering angle θ at which the intensity is measured. For a case of + ve sample tilt, as shown in the Figure 24, the true scattering angle is given by :

$$\theta_T = \arcsin\left\{\frac{\sin\Phi_t}{n}\right\} + \arcsin\left\{\frac{\sin(\theta - \Phi_t)}{n}\right\} \qquad (103)$$

where n is the ratio of the refractive indices of the swollen network and the solvent :

$$n = \frac{n_{GEL}}{n_{SOL}}$$

In all the equations here; Φ_t represents the magnitude of the tilt angle. For the case of - ve tilt, the true scattering angle is :

$$\Phi_T = 180 - \arcsin\left\{\frac{\sin\Phi_t}{n}\right\} - \arcsin\left\{\frac{\sin(180 - \theta - \Phi_t)}{n}\right\} \qquad (104)$$

Solid Angle Correction : The solid angle containing the scattered light flux reaching the detecter is different from that in the sample due to refraction. For the case of cylindrical samples; the correction factor was $C_n = n_{SAM}^2$ as in equation (98), where n_{SAM} is the refractive index of the sample. According to Stein and Keane [112] ,for flat tilted samples (+ ve tilt)

$$C_n = n_{SAM}^2 \frac{\left[1 - \left(\frac{\sin(\theta - \Phi_t)}{n}\right)^2\right]^{1/2}}{\cos(\theta - \Phi_t)} \qquad (105)$$

Scattering Volume Correction : A simple sin correction is not sufficient to correct for different scattering volumes at different scattering angles due to tilt and refraction in flat tilted samples. The scattering volume correction for the case of + ve tilt is :

$$V_s = \frac{\cos(\alpha)\ \cos(\Phi')}{\cos(\theta - \Phi_t)\ \sin(\alpha + \Phi')\ \cos(\Phi_t)} \qquad (106)$$

where $\Phi' = \arcsin[(\sin\Phi_t)/n]$

and $\alpha = \arcsin([\sin(\theta - \Phi_t)]/n)$

The correction factor for the case of - ve tilt is :

$$V_s = \frac{\cos\beta'\ \cos\Phi'}{\cos\beta\ \cos\Phi_t\ \sin(\beta' + \Phi')} \qquad (107)$$

where $\beta = (180 - \theta - \Phi_t)$

and $\beta' = \arcsin[(\sin\beta)/n]$

Reflection Correction : In the case of flat samples; it is necessary to account for the loss of intensity of the of the incident and scattered beams due to reflection at the interfaces where there is change in refractive index. The loss of intensity at a particular interface is corrected by dividing the measured intensity by the transmittance T_i at that interface :

$$\Xi = \frac{1}{T_i} = \frac{1}{(1 - r_i)} \qquad (108)$$

r_i is the reflectance at interface i. The reflectance is estimated by using the Fresnel equations for reflection.

Corrections were made for reflections at two interfaces referred to as A and B. A is the surface of the sample at which the laser beam is incident and B is the surface from which the scattered beam exists. The incident beam is treated as being vertically polarized and the scattered beam as containing H_v and V_v components. The reflectance r_A at the interface A is given by :

$$r_A = \frac{\tan^2(\Phi_t - \Phi')}{\tan^2(\Phi_t + \Phi')} \qquad (109)$$

Reflections at B will have two components. For V_v scattering :

$$r_B = \frac{\tan^2(i - r)}{\tan^2(i + r)} \qquad (110)$$

and for H_v scattering :

$$r_B = \frac{\sin^2(i - r)}{\sin^2(i + r)} \qquad (111)$$

In equations 110 and 111 we have for :

i) + ve tilt $i = \alpha$ and $r = (\theta - \Phi_t)$

ii) - ve tilt $i = \beta'$ and $r = \beta$

Therefore, for a particular scattering geometry, the total reflection correction is :

$$\Xi = \frac{1}{(1-r_A)\ (1-r_B)} \qquad (112)$$

Light Scattering Results

For the bimodal PDMS networks swollen in toluene and in benzene, the contributions of density fluctuations was estimated using equations (35) and (43). The isotropic intensity was obtained by using equation (34). The H_V scattering in the swollen networks was typically on the order of a few percent of the V_V scattering. Figure 26 shows the measured V_V and H_V intensities for a PDMS 1000 network (100% LC) swollen in toluene. This is the raw data and has not been corrected or converted into absolute units. H_V scattering in swollen networks arises from strains in the sample. Therefore, it is necessary to have the sample at equilibrium swelling. Strains and considerable H_V scattering can result if the samples are cut in the swollen state. The least amount of H_V scattering was obtained when the samples were cut in the dry state and then allowed to swell in the diluent for at least a week.

The contribution to the scattering due to concentration fluctuations in an ideal network having the same degree of

swelling and crosslink density as the network being studied was estimated by using equation (48). From the measured isotropic scattered intensity (Rayleigh ratio) ; their contributions due to density fluctuations and due to concentraion fluctuations in an ideal network were subtracted so as to obtain the excess scattered intensity which are supposed to correspond to inhomogeneity of crosslinking. For the different bimodal PDMS networks swollen in toluene and in benzene; the excess scattering data is shown in Figures 27 and 28. The excess scattering data was plotted in terms of a Debye -Bueche plot as shown in Figures 29-31. The correlation size a_c was obtained from the slope and the intercept. The mean squared fluctuations in scattering power can be obtained from the intercept of the plot and which can be related to $<\Delta M_c^2>$ as in equation (53). Therefore for each network it is possible to calculate a hetrogeneity index H which is defined as :

$$H = \frac{<\Delta M_c^2>^{1/2}}{M_c} \qquad (113)$$

Since the bimodal networks were prepared by endlinking prepolymers of known molecular weights; one can calculate as to what H should be for a particular composition of short and long chains. If we assume perfect mixing of the short and long chains; no clustering and equal reactivity

throughout the curing process; then a simple calculation for $<\Delta M_c^2>$ is possible. For mono disperse short and long chains

$$<\Delta M_c^2> = x\,(1-x)\,(M_L - M_S)^2 \qquad (114)$$

where x is the mole fraction of short chains. Equation (114) suggests that $<\Delta M_c^2>$ and H should be zero for x equal to zero or one. Therefore, for a mono disperse unimodal network one would not expect any excess scattering of light. However, this is not true for a unimodal network prepared from a prepolymer having a finite poly dispersity.

The Flory Schulz distribution function equation can be used to represent the molecular weight distribution of a polydisperse prepolymer i. Let the poly dispersity be:

$$\left[\frac{M_w}{M_n}\right]_i = 1 + \frac{1}{b_i}$$

Therefore, for a bimodal network containing short and long chains both of which are polydisperse; one has the following expression for $<\Delta M_c^2>$

$$<\Delta M_c^2> = \frac{xM_S^2}{b_S} + \frac{(1-x)M_L^2}{b_L} + x(1-x)(M_L - M_S)^2 \qquad (115)$$

In equation (115) M_S and M_L refer to the number average molecular weights for the short and long chains.

Table 17 lists the results for a_c and H obtained from the Debye - Bueche plots for the swollen bimodal networks. The experimentally determined values of H are

compared with the values of H calculated by using equation (115):

There are two important observations regarding this data :

i) H_{CAL} is about two orders of magnitude larger than H_{EXP}.

ii) For x = 0 or 1 , H_{CAL} is not a function of the molecular weight of the chains between crosslinks although H_{EXP} definitely is.

The motivation for using model bimodal networks was to evaluate our methods for the determination of homogeneity of crosslinking in polymer networks. The light scattering results on bimodal PDMS networks clearly indicate that there is a big difference in the measured and the expected value of the hetrogenity index H.

The scattering of light results due to local fluctuations in the refractive index of a material. In the analysis for H from the excess scattered intensity, a macroscopic theory, such as the Flory Rehner theory, has been used to relate the local molecular weight between crosslinks to the local fluctuations in the refractive index by equation 52. The excess scattering is then expected to arise due to such fluctuations in the refractive index. In such an approach; the presence of neighbouring chains and their role in determining the local polymer concentration is neglected. This has the effect of

exaggerating the local fluctuations in the polymer concentration and consequently results in an over estimation of the predicted value of the excess scattered intensity.

Analytically, it is not easy to account for the effect of the neighboring chains in determining the spatial correlations in swollen networks. By using a three dimensional computer simulation it may be possible to evaluate spatial correlations and thereby estimate the scattered intensity from swollen networks. However, to simulate a real swollen network; there is a need to understand as to how the dry network swells at the molecular level.

The SANS experiments by Bastide and Picot have revealed that the deformation of a labelled chain between crosslinks is much less than that predicted according to the affine deformation model. According to Bastide, the swelling of the network is assumed to involve the rearrangement of network chains, such that, on changing the swelling ratio the distance between the first topological neighboring crosslinks does not change. There will be four topological first neighbours for any given crosslink point in a tetra functional network represented by an open circle in Figure 32. These are connected to the central crosslink point by a single chain and are indicated by crossmarks on

Figure 32. In the volume, about the central junction point, containing the topological neighbors in a dry network there will be other junction points. These junction points are connected to the central junction point by a path through the network which is longer than the single chain length. These are called spatial neighbors of the central junction point and are shown as filled circles in Figure 32.

Picot and coworkers observed that the R_g of a labelled chain between the crosslinks in a swollen netwrok was comparable to the R_g of the same free chain at infinite dilution in the same solvent. Bastide [16] observed, that, when swollen networks were osmotically deswollen, R_g of a labelled chain did not change significantly although the macroscopic swelling ratio did. The swelling process is therefore assumed to involve a network folding or unfolding mechanism such as that the distance between the spatial neighbors is changed without altering the distance between first topological neighbors.

The ease with which the network rearrangement can take place depends on the size of the chain between crosslinks. Each junction point will have ϕ topological neighbors for a perfect network of functionality ϕ. The volume containing these ϕ topological neighboris will contain n total neighbors.

Therefore :

$$< n / \phi > = \frac{\text{\# of total neighbors}}{\text{\# of topological neighbors}}$$

For a network chain with degree of polymerization N, the ratio $< n / \phi >$ has been shown to be [14] :

$$< n / \phi > = \frac{8\ N^{1/2}}{\phi^2} \qquad (116)$$

According to Picot and coworkers [13,113], this ratio is the central parameter which can be used to describe the deformation in networks. There is greater ease of rearrangements of network strands for larger values of $< n / \phi >$. Therefore the molecular deformation is expected to be closer to the macroscopic deformation for smaller values of $< n / \phi >$. The experimental results are consistent with such a prediction.

The desinterspersion model developed by Bastide can be applied to account for the present light scattering results. The driving force for the topological rearrangements is lower elastic free energy when the chains are deformed to a lesser degree. This can be accomplished by the displacement of spatial neighbours rather than topological neighbours. The ease of the rearrangements of the network strands increases as the ratio $< n / \phi >$ is increased. This means that there will be bigger fluctuations in the local polymer concentration as the

ratio $< n / \phi >$ is increased. Therefore, as $< n / \phi >$ is increased, there will be greater excess scattering of light from swollen networks. The analysis has to be modified to include scattering of light due to concentration fluctuations caused by network strands rearrangements. The factors responsible for scattering from swollen networks are:

i) Density fluctuations

ii) Concentration fluctuations corresponding to an ideal network with no junction folding.

iii) Concentration fluctuations due to unfolding and rearrangement of network strands.

iv) Concentration fluctuations due to crosslink homogeneities.

In equation (116), $< n / \phi >$ is given for what may be considered the case of a monodisperse unimodal network. The expression for a unimodal system with a finite polydispersity is

$$< n / \phi > = \frac{8 \; b^{1/2} \; \Gamma(b+0.5) \; N^{1/2}}{\phi^2 \qquad \Gamma(b+1)} \qquad (117)$$

where $\frac{M_w}{M_n} = 1 + \frac{1}{b}$

Therefore for a bimodal network :

$$< n / \phi > = \frac{8}{\phi^2} \sum x_i \; F(b_i) \; N_i^{1/2} \qquad (118)$$

where $F(b_i) = b_i^{1/2} \dfrac{\Gamma(b_i+0.5)}{\Gamma(b_i+1)}$

Though it is not possible at this time to quantify concentration fluctuations in terms of the network strand unfolding model; it is reasonable to expect that the magnitude of the concentration fluctuations is proportional to $< n / \phi >$. Therefore the intensity of scattered light is proportional to $< n / \phi >^2$.

The intercept of a Debye Bueche plot gives the mean squared fluctuations in the scattering power η^2. The values of η^2 for different degrees of swelling can be normalized for networks of different crosslink densities as

$$K = \eta^2 / v_2^2 = \frac{R(0)\ \lambda_o^4}{32\ \pi^3\ n^2\ (n_p-n_s)^2\ v_2^2\ a_c^3} \qquad (119)$$

The total normalized mean squared scattering power K will contain contributions due to network strand folding and due to crosslink inhomogeneities. The ratio of K to the contributions due to the network unfolding mechanisms will then be :

$$\Omega = K / < n / \phi >^2 \qquad (120)$$

The value of Ω for the network made from 100% short chains is found to be least for a given diluent for the bimodal network studied. The values of Ω can be normalized to the value of Ω corresponding to 100% short chains for a

particular diluent. Let this ratio be called .

$$W = \frac{[\ \Omega\ ]_{sam}}{[\ \Omega\ ]_{100\%\ SC}} \qquad (121)$$

Table 17 gives the value of $< n / \phi >$, K, Ω and W for various bimodal networks in toluene and benzene. It can be seen that the values of W are about the same for measurements in benzene and in toluene. W can be seen to represent a relative measure of the total concentration fluctuations due to network unfolding, crosslink inhomogeneities,and other factors in comparison to the concentration fluctuations just due to the network unfolding. It is noted that W has larger values for bimodal networks than for 100% long chain or 100% short chain networks. Figure 33 shows a plot of W vs $< n / \phi >$ for the varoius networks. Figure 34 shows the plot of H^2 vs $< n / \phi >$ for the same bimodal networks. H was estimated using equation (115) for $<\Delta M_c^2>$. It is noted that Figures 33 and 34 are quite similiar and have a maximum at about the same value of $< n / \phi >$. It is very interesting to note that magnitudes of W and H^2 are comparable in the two Figures.

These results seem to indicate that the excess scattering in swollen networks arises due to concentration fluctuations caused by network strand folding or rearrangement, and, by inhomogeneous crosslink densities.

Therefore, this suggests that the current molecular theories of rubber elasticity are inadequate. An effort should be made to include the concepts of network strand folding and rearrangement as suggested by Bastide to understand the local swelling in a network.

The current molecular theories of rubber elasticity estimate the change on the free energy of a network on deformation by summing the contribution of all the individual chains. According to Bastide [114] one needs to consider the entropy of all network chains simultaneously to appreciate the consequences of network strand unfolding and rearrangement.

The description of the entropy of all the chains simultaneously, in a network is not a trivial task. There are several factors which determine the behaviour of a network and it is not possible to account for all of them. Network strand unfolding can be incorporated into a relatively simple network model if we consider a cell approach similiar to the four chain model of Flory and Rehner [115]. Let us consider a triangular prism with seven chains as shown in Figure 35; instead of a tetrahedral cell with four chains. As in Flory and Rehner model, the cell can be considered as a representative unit of the network structure. These cells can interpenetrate the same region of space. Therefore, the network structure

is not treated as a lattice of the individual cells.

The cell contains a central chain with ends 1 and 2 inside the prism. Each of these ends are connected by three other chains to the corner of the prism A, B, C, and A',B',C', respectively. The junction points 1 and 2 are allowed to fluctuate wheras all the corners of the prism are considered fixed. Initially it can be assumed that all the chains are of the same end to end distance $<R^2>^{1/2}$. Therefore, if there is a macroscopic deformation ratio α ; corresponding to the displacement of the sides of the prism, then the deformation ratio corresponding to the ends of the chains 1,2 is α^* . Due to the junction fluctuations and network unfolding α^* will be less than α. The relation between α^* and α will be determined by a parameter Θ^* which will determine the amount of unfolding. Therefore, Θ^* will be a function of $< n / \phi >$.

The change in the entropy of the chains can be determined by estimating the difference in the structural entropy of network formation in the undeformed and deformed states. Uptil now Bastide and coworkers have discussed the phenomenon of junction unfolding without considering the effects of trapped entanglements. Clearly, entanglements will reduce the number of conformational rearrangements possible for network strands. It may be possible to

consider the effect of entanglements on the ease of strand folding and unfolding following the Flory and Erman [25,26], treatment for the effect of trapped entanglements on the junction fluctuations.

Recently Stein [116] has proposed a cluster or branching approach to describe the local structure in networks. He developed the method essentially to describe the bimodal networks consisting of short and long chains in a predetermined ratio. This approach initially involves the identification of the various clusters of different sizes. The simplest cluster would involve four chains in the case of tetrafunctional network. The average properties of each cluster can be described once the various clusters and their probabilities are determined. It is expected that as the cluster size is increased; the properties of that cluster will become closer to the macroscopic properties. Following Ullman [77], one can express the local deformation ratio α^* in terms of the macroscopic ratio α as in equation 73.

$$\alpha^{*2} = \alpha^2 (1-A_f) + A_f$$

For $\alpha^* = \alpha$, $A_f = 0$

$\alpha^* = 1$, $A_f = 1$

Therefore, as the cluster size is reduced from the macroscopic down to the level of a few network strands; A_f increases from 0 to a value between 0 and 1.

In the cell model shown in Figure 35; if the chain 1 2 is replaced by clusters of different sizes; one may be able to develop an understanding for the parameter A_f in terms of number of strands in the cluster. It may be necessary to use a computer to compute the entropy of network formation for clusters involving more than a few strands. One may be able to obtain a very thorough description of the properties of a polymer network by incorporating the effect of entanglements on junction fluctuations and network strand rearrangements.

C H A P T E R V I I

DISCUSSION

Conclusions

Swollen polymer networks were studied by SANS and light scattering (LS) in an effort to characterize their homogeneity of crosslinking. In these experiments, the overall spatial correlations are observed by using a diluent with a scattering power sufficiently different from that of the polymer. In all the cases, it is observed, that swollen networks scatter more strongly than solutions of equivalent concentration. This clearly suggests that large scale concentration fluctuations give rise to the observed excess scattering.

The initial experiments were performed on dicumyl peroxide crosslinked polybutadiene. This crosslinking can result in inhomogeneous structures possibly due to non uniform mixing of the peroxide and / or due to a distribution of junction functionalities. Ambiguities regarding the crosslinking process and the resultant network structure made it difficult to have a satisfactory interpretation of the scattering results for these randomly crosslinked networks. Therefore, experiments were then performed on the model PDMS networks.

The volume fractions of polymer in networks swollen to equlibrium typically correspond to concentrations in the semi-dilute regime for linear polymer solutions. In this concentration regime SANS experiments on solutions of the linear PDMS prepolymers in C_6D_6, indicated weak swelling of the chains. A major reason for the weak excluded volume effects is that the chains are quite short.

In such a polymer solvent system, the chains are almost ideal at all levels and spatial correlations are not very significant. Therefore, the Flory Huggins type of analysis should work quite well in this regime. In fact, it is found that the Flory Huggins treatment, using a concentration dependent χ parameter, can be used to adequately describe the concentration dependence of the scattered light from PDMS solutions in toluene at 25°C.

The SANS results from swollen PDMS networks revealed correlation sizes R_c larger than the radius of gyration of a chain between two crosslink points R_g. The ratio R_c/R_g defined as Q_c in Tables 14 and 15 is found to be similiar for unimodal and bimodal PDMS networks. The bimodal networks had been prepared by mixing together the long and short chains prior to the addition of the crosslinker. Therefore, R_c is determined by correlations other than those due to random crosslink inhomogeneties. In view of Bastide's network desinterspersion model, these

values of R_c can be seen to be related to sturctures involved in network strand folding and rearrangements.

The network folding hypothesis is also supported by the light scattering experiments on bimodal PDMS networks swollen in toluene and in benzene. The excess scattered intensity from different swollen networks were obtained after correcting for density fluctuations and for concentration fluctuations corresponding to an ideal network. From the excess scattered intensity, a network hetrogeneity index H ($=\Delta M_c/M_c$) was estimated using equation 53. The measured value of H was found to be about two orders of magnitude less than that estimated from the composition of the network i.e. equation 115. This discrepancy could not be explained by any of the current theories of rubber elasticity.

Using $< n / \phi >$, the central parameter in the network unfolding model, it is possible to show that the excess light scattering can be accounted for by concentration fluctuations due to junction unfolding and due to crosslink inhomogenities. Although no quantitative analysis is possible at this time, the qualitative agreement is very encouraging.

A cell model is outlined for describing the properties of a network. Such a model can be used to combine the

features of junction unfolding into the framework of the current theories of rubber elasticity.

Suggestions for Future Work

The results of this study indicate that the theoretical developments are necessary to have a better understanding of the local behavior in polymer networks. A cell model could possibly be used to examine the validity of Bastide's hypothesis regarding network strand unfolding and rearrangements. Various cluster sizes could also be incorporated to get a more realistic model.

Most of the SANS experiments to date on labelled chains in a network have involved unimodal networks. The deformation is expected to be highly non affine in the case of bimodal networks. Therefore, by selectively labelling the short and long chains, one can evaluate the local deformation in bimodal networks.

The selectively labelled chains can also be studied by IR dichroism to obtain the local orientation functions in uniaxial deformation experiments. Recently Hrabowska and Stein [117] have studied the deformation of unlabelled bimodal PDMS networks by IR. Their preliminary results do indicate that the deformation in such networks is non affine.

The main problem in trying to perform such experiments is the availability of the labelled prepolymers for SANS. In the case of PDMS, the deuterated monomer is fairly expensive. Other possibilities include poly - tetrahydrofuran diols. One can use deutero THF as the monomer.

Bimodal networks can also be prepared to possess spatial inhomogeneities in addition to crosslink inhomogeneities. Mark and coworkers have prepared such networks by prereacting a few of the short chains to form small clusters. They found that the macroscopic properties such as swelling and mechanical response were not very sensitive to the presence of hetrogeneities. However, if such networks are swollen with a diluent having a different scattering power as in these experiments, it is expected that the scattered intensity will be quite dependent on the non-randomness of the structure. These swollen networks can therefore be studied by SANS and LS. Their results can be compared with the results of this study for bimodal networks having random mixing. To have a better understanding of the scattering from such non random networks, it may be helpful to characterize the clusters formed in the prereaction stage.

Instead of using a bimodal distribution of M_c, it is possible to study networks with a distribution of junction

functionalities. At high junction functionalities, one has to be concerned about the solvent exclusion in the immediate vicinity of the crosslinks. Such a phenomenon could be studied using model star polymers of controlled functionality and arm lengths.

In principal, a variety of network structures can be visualized and possibly even be synthesized. However, satisfactory description of the scattering from the networks will require advances in the current understanding of rubber elasticity at the level of the network chains.

FOOTNOTES

1. W. Kuhn, Kolloid Z., 76, 258 (1936); Angew. Chem., 51, 640 (1938)
2. L.R.G. Treloar, The Physics of Rubber Elasticity, 3rd ed., Clarendon, Oxford (1975)
3. P.J. Flory, Principles of Polymer Chemistry, Cornell University Press, Ithaca, New York (1953)
4. J.P. Queslel and J.E. Mark, Adv. Polym. Sci., 65, 135 (1984)
5. J.E. Mark, Adv. Polym. Sci., 44, 1 (1982)
6. J.E. Mark and J.L. Sullivan, J. Chem. Phys., 66, 1006 (1977)
7. M.A. Llorente and J.E. Mark, Macromolecules, 13, 681 (1980)
8. M.A. Llorente and J.E. Mark, J. Chem. Phys., 71, 682 (1979)
9. M.A. Llorente, A.L. Andrady and J.E. Mark, J. Polym. Phys., Ed., 19, 621 (1981)
10. M.A. Llorente, A.L. Andrady and J.E. Mark, Colloid. Polym. Sci., 259, 1056 (1981)
11. J.E. Mark, in Elastomers and Rubber Elasticity, Ed., J.E. Mark and J. Lal, Am. Chem. Soc., Washington D.C. (1982)

12. M. Beltzung, C. Picot, P. Rempp and J. Herz, Macromolecules, 15, 1594 (1982)

13. M. Beltzung, J. Herz and C. Picot, ibid, 16, 580 (1983); ibid, 17, 663 (1984)

14. J. Bastide, C. Picot and S. Candau, J. Macromol. Sci., Phys., B19, 13 (1981)

15. S. Candau, J. Bastide and M. Delsanti, Adv. Polym. Sci., 44, 27 (1982)

16. J. Bastide, R. Dupplesix, C. Picot and S. Candau, Macromolecules, 17, 83 (1984)

17. K.H. Meyer and C. Ferri, Helv. Chem. Acta., 18, 570 (1935)

18. P.J. Flory and J. Rehner Jr., J. Chem. Phys., 11, 521 (1943)

19. F.T. Wall and P.J. Flory, J. Chem. Phys., 19, 1435 (1951)

20. H.M. James and E. Guth, J. Chem. Phys., 15, 651 (1947)

21. P.J. Flory, Chem. Revs., 35, 51 (1944); Ind. Eng. Chem., 38, 417 (1946)

22. M. Mooney, J. Appl. Phys., 11, 582 (1940)

23. P.J. Flory, Proc. R. Soc. London, Ser. A, 351 (1976)

24. P.J. Flory, Macromolecules,12, 119 (1979)

25. B. Erman and P.J. Flory, Macromolcules, 15, 806 (1982)

26. P.J. Flory and B. Erman, Macromolcules, 15, 800 (1982)

27. N.R. Langley, Macromolcules, 1, 348 (1968)

28. N.R. Langley and K.E. Polmanteer, J. Polym. Sci., Polym. Phys. Ed., 12, 1023 (1974)

29. L.M. Dossin and W.W. Graessley, Macromolecules, 12, 123 (1979)

30. R.L. Carpenter, H.-C. Kan and J.D. Ferry, Polym. Eng. Sci., 19, 266 (1979)

31. D.R. Miller and C.W. Macosko, Macromolcules, 9, 206 (1976)

32. M. Gottlieb, C.W. Macosko, G.S. Benjamin, K.O. Meyers and E.W. Merrill, Macromolecules, 14, 1039 (1981)

33. M. Gottlieb and C.W.Macosko, Macromolcules, 15, 535 (1982)

34. P.J. Flory, J. Chem. Phys., 15, 397 (1947)

35. K.J. Smith Jr., in Elastomers and Rubber Elasticity, Ed, J.E. Mark and J. Lal, Am. Chem. Soc., Washington D.C. (1982)

36. M. Kosc and A. Ziabicki, Macromolecules, 17, 678 (1984)

37. J.E. Mark and J.G. Curro, J. Chem. Phys., 79, 5705 (1983)

38. J.G. Curro and J.E. Mark, J. Chem. Phys., 80, 4521 (1984)

39. P.J. Flory, Statistical Mechanics of Chain Molecules, Interscience, New York (1969)

40. P. Debye and A.M. Bueche, J. Appl. Phys., 20, 518 (1969)

41. P. Debye, H.R. Anderson Jr. and H. Brumberger, J. Appl. Phys., 28, 679 (1957)

42. G. Porod, Kolloid Z., 124, 83 (1951); O. Kratky, Pure and Appl. Chem., 12, 483 (1966)

43. J.T. Koberstein, B. Morra and R.S. Stein, J. Appl. Cryst., 13, 34 (1980)

44. U. Siemann and W.Ruland, Colloid Polym. Sci., 260, 999, (1982)

45. M. Moritani, T. Inoue, M. Motegi and H. Kawai, Macromolecules, 3, 433 (1970)

46. H.K. Yuen and J.B. Kinsinger, Macromolecules, 7, 329 (1974).

47. A.V. Toblosky, Properties and Structures of Polymers, John Wiley and Sons, New York (1960)

48. M. Kerker, The Scattering of Light and other Electromagnetic Radiation, Academic Press, New York (1969)

49. H.C. van de Hulst, Light Scattering by Small Particles, John Wiley and Sons, New York (1957)

50. A. Einstein, Ann. de Physik., 33, 1275 (1910)

51. M.B. Huglin, Light Scattering from Polymer Solutions, Academic Press, London (1972)

52. M.B. Huglin and M.B. Sokro, Polymer, 21, 651 (1980)

53. B.H. Zimm, J. Chem. Phys., 16, 1093 (1948)

54. R.K. Bullough, J. Polym. Sci., 46, 517 (1960)

55. P. Debye and A.M. Bueche, J. Chem. Phys., 1423 (1950)

56. R.S. Stein, J. Polym. Sci., Polym. Lett., 7, 657, (1969)

57. F. Bueche, J. Colloid Interface. Sci., 33, 61 (1970)

58. K.L. Wun and W. Prins, J .Polym. Sci., Polym. Phys., Ed, 12, 533 (1974)

59. G.E. Bacon, Neutron Diffraction, 3rd Ed., Oxford University Press, London (1975)

60. J.S. Higgins and R.S. Stein, J. Appl. Cryst., 11, 346 (1978)

61. A. Maconnachie and R.W. Richards, Polymer, 19, 739 (1978)

62. C. Picot, in Static and Dynamic Properties of the Polymeric Solid State, R.A. Petheric and R.W. Richards, Eds., D. Reichel Publishing Company (1979)

63. L.H. Sperling, Polymer. Eng. Sci., 24, 1 (1984)

64. H. Yang, Ph.D. Thesis, Univ of Massachusetts, Amherst (1984)

65. A.Z. Akasu, G.C. Summerfield, S.N. Jahshan, C.C. Han, C.V. Kim and H. Yu, J. Polym. Sci., Polym. Phys., Ed., 18, 863 (1980)

66. P.G. de Gennes, Scaling Concepts in Polymer Physics, Cornell University Press, Ithaca, New York (1979)

67. G.V. Schulz, Z. Physik. Chem., B43, 25 (1939)

68. D.W. Schaefer, J.F. Joanny and P. Pincus, Macromolecules, 13, 1280 (1980)

69. D.W. Schaefer, Polymer, 25, 387 (1984)

70. S.F. Edwards, Proc. Phys. Soc., 88, 265 (1966)

71. H. Benoit et al, J. Polym. Sci., Polym. Phys. Ed., 14, 2119 (1976)

72. W. Wu and B.J. Bauer, Polym. Comm., 26, 39 (1985)

73. S.J. Bai, Polymer, (in press)

74. D.S. Pearson, Macromolecules, 10, 696 (1977)

75. S. Levy, Thesis, Universite Louis Pasteur, Strasbourg (1964)

76. J.A. Hinkley, C.C. Han, B. Mozer and H. Yu, Macromolecules, 11, 836 (1978)

77. R. Ullman, Macromolecules, 15, 582 (1982)

78. J.T. Koberstein, Ph.D. Thesis, University of Massachusetts, Amherst (1979)

79. Manual for users of the 30m SANS instrument, NCSASR, Oakridge TN; NBS SANS users manual, NBS, Gaithersburg MD.

80. R.W. Lenz, Organic Chemistry of Synthetic High Polymers, Interscience, New York (1967)

81. C.G. Moore and W.F. Watson, J. Polym. Sci., 19, 237 (1956)

82. C.R. Parks and O. Lorenz, J. Polym. Sci., 50, 287 (1961)

83. L.D. Loan, J. Appl. Polym. Sci., 7, 2259 (1963)

84. B.M.E. Van der Hoff, Appl. Polym. Symp., 7, 21 (1968)

85. M. Morton and J.C. West, Paper presented at the 100th meeting, Rubber Division, Am. Chem. Soc., Cleveland (1971)

86. L.O. Malotky and M. Morton, Polymer Preprints, 15(1), 714 (1974)

87. A.R. Schultz, in Chemical Reactions of Polymers, E.M. Fettes, Ed., Interscience, New York (1964)

88. M. Dole, The Radiation Chemistry of Macromolecules, Academic Press, New York (1973)

89. D.S. Pearson, B.J. Skutnik and G.G.A. Bohm, J. Polym. Sci., Polym. Phys. Ed., 12, 925 (1974)

90. M.A. Golub, J. Polym. Sci., 25, 373 (1957)

91. R.R. Hampton, Anal. Chem., 21, 923 (1949)

92. T.J. Rowland and L.C. Labun, Macromolecules 14, 1468 (1981)

93. R.S. Stein, R.J. Farris, S. Kumar and V. Soni, in Elastomers and Rubber Elasticity, J.E. Mark and J.Lal, Ed, Am. Chem. Soc., Washington D.C. (1982)

94. R.S. Stein, P. Wilson and S.N. Stidham, J. Appl. Phys 34, 46 (1963)

95. M. Daoud and J.P. Cotton, J. Phys., Paris, 13, 531 (1982)

96. A. Miyake and K.F. Freed, Macromolecules, 17, 678 (1984)

97. W. Funke, W. Beer and U. Seitz, Progr. Colloid & Polym. Sci., 57, 48 (1975)

98. K.E. Luttgert and R. Bonart, ibid, 64, 48 (1975)

99. J.P. Bell, J. Appl. Polym. Sci., 27, 3503 (1982)

100. V.B. Gupta, L.T. Drazal and W.W. Adams, J. Mat. Sci. (in press)

101. T. Takahama and P.H. Geil, Die Makromol. Chemie, Rapid Commun., 3, 389 (1982)

102. U.T. Kreibich and R.J. Schmid, J. Polym. Sci., Polym. Symp., 53, 177 (1975)

103. A.S. Kenyon and L.E. Nielson, J. Macromol. Sci. (A), 3, 275 (1969)

104. K. Dusek, J. Plestil, F. Lednicky and S. Lunak, Polymer, 19, 393 (1978)

105. J. Hertz, P. Rempp and W. Borchard, Adv. Polym. Sci. 26, 105 (1978)

106. P.-H Sung and J.E. Mark, Polym. J., 12, 835 (1980)

107. P.-H Sung and J.E. Mark, J. Polym. Sci., Polym. Phys. Ed., 19, 507 (1981)

108. K.O. Meyers, M.L. Bye and E.W. Merrill, Macromolecules, 13, 1045 (1980)

109. E.M. Valles and C.W. Macosko, Macromolecules, 12, 521 (1979)

110. J. Brandrup and E.H. Immergut, Ed., Polymer Handbook John Wiley (1975)

111. H. Yang, R.S. Stein and W. Wu, private communication

112. R.S. Stein and J.J. Keane, J. Polym. Sci., 17, 21 (1955)

113. C. Picot, private communication

114. J. Bastide, private communication

115. R.S. Stein, private communication

116. P.J. Flory and J. Rehner Jr., J. Chem. Phys., 19, 512 (1943)

117. J. Hrabowska and R.S. Stein, results to be published

118. T.S. Ellis and F.E. Karasz, private communication

119. W. Kaye and J.B. McDaniel, Appl. Opt., 13, 1934 (1974)

Table 1

NEUTRON SCATTERING CROSS SECTIONS FOR COMMON ELEMENTS

Element	I	b $\times 10^{12}$ cm	σ_{inc} $\times 10^{24}$ cm^2	σ_{ABS} $\times 10^{24}$ cm^2
H^1	1/2	-0.374	79.7	0.19
H^2	1	0.667	2.0	0
C^{12}	0	0.665	0.0	0
N^{14}	1	0.940	0.3	1.1
O^{16}	0	0.580	0	0
Si^{28}	0	0.420	0	0.06
Cd		0.37+0.16i		2650

Table 2

POLYBUTADIENE ISOMERS INFRA RED DATA

Isomer	Frequency (cm^{-1})	Extinction Coefficient
cis 1,4-	724	0.608
trans 1,4-	967	2.608
vinyl	911	3.285

Table 3

CHARACTERISTICS OF POLYBUTADIENE NETWORKS

Sample	DCP phr	% sol	v_2	M_c	T_g K	ρ gm/cc
But 21	2.0	4.7	0.165	7900	166.7	0.91
But 22	4.0	3.5	0.196	5350	167.7	0.91
But 23	7.7	8.8	0.222	4000	167.5	0.91
But 24	11.0	8.0	0.230	3700	169.5	0.91
But 25	15.3	9.4	0.250	3000	170.0	0.91
But 26	20.3	14.5	0.376	1100	173.0	0.93
But 27	30.0	13.6	0.446	650	179.5	0.95

Table 4

LIGHT SCATTERING CORRELATION SIZES FOR SWOLLEN POLYBUTADIENE NETWORKS

Sample	a_c Å
But 22	4300
But 23	10750
But 24	8325
But 25	7775
But 26	6235
But 27	6150

Table 5

RESULTS OF 4 PARAMETER FIT (EQUATION 75)
OF SANS DATA FROM SWOLLEN POLYBUTADIENE NETWORKS

Sample	η^2 x10^{-17} cm^{-4}	η_1^2	a_1 Å	a_2 Å
But 10	3.8	10	450(8)	32(2.0)
But 35	4.0	27	620(17)	20(2.5)
But 27	3.7	40	580 (8)	19 (1.0)

Numbers in brackets indicate the standard deviations.

Table 6

CURE HISTORY OF EPOXY SAMPLES FOR SANS

SAMPLE #	STAGE 1	STAGE 2	STAGE 3
8	75°C for 15 min	180°C for 5 hrs	185°C for 24 hrs
10	75°C for 30 min	180°C for 5 hrs	185°C for 24 hrs
9	100°C for 15 min	180°C for 5 hrs	185°C for 24 hrs
11	100°C for 30 min	180°C for 5 hrs	185°C for 24 hrs

Table 7

CHARACTERISTICS OF PDMS REFERENCE STANDARDS

Sample #	M_N	M_W	$\left[\frac{M_W}{M_N}\right]$	$[\eta]^a$	η^b
1	2840	3465	1.22	0.0401	45
2	6650	8180	1.23	0.0707	160
3	14400	18144	1.26	0.1183	720
4	20800	23296	1.12	0.1513	1600

a : Intrinsic viscosity in Toluene at 25°C

b : Bulk viscosity in centistokes

Table 8

CHARACTERISTICS OF PDMS PREPOLYMERS USED

Sample Name	η (cstks)	M_N	M_W	$\left[\frac{M_W}{M_N}\right]$
PDMS 4-6	5	770	1450	1.88
PDMS 100	100	5200	8112	1.56
PDMS 200	200	7000	11900	1.70
PDMS 1000	1000	22500	40600	1.80
PDMS 5000	5000	52815	77610	1.47

Table 9

INTRINSIC VISCOSITIES OF THE PDMS PREPOLYMERS

Sample	$[\eta]_{meas}$	M_v	$[\eta]_{calc}$
PDMS 200	0.0870	10254	0.0916
PDMS 1000	0.1800	31381	0.2023
PDMS 5000	0.2660	57228	0.3131

$[\eta]_{calc}$ calculated using equation 82

Table 10.

SWELLING DATA UNIMODAL PDMS NETWORKS

(IN BENZENE AT 25°C)

Sample	M_c	ϕ	v_2	F_ϕ
PDMS 1000	22500	4	0.200	0.61
PDMS 100	5200	4	0.304	0.51
	5200	5	0.333	0.71
PDMS 4-6	770	4	0.535	0.68
	770	4	0.553	0.79

Table 11

SWELLING DATA BIMODAL PDMS NETWORKS AT 25°C

X	M_c	V_2^*	F_4	V_2^+	$\chi_{Tol.}$
0	22500	0.200	0.61	0.161	0.511
25	17068	0.230	0.69	0.192	0.520
50	11635	0.276	0.79	0.251	0.547
75	6203	0.330	0.81	0.301	0.554
90	2943	0.380	0.64	0.339	0.550
95	1857	0.439	0.71	0.402	0.563
100	770	0.535	0.68	0.504	0.581

* : volume fraction of polymer in benzene

\+ : volume fraction of polymer in toluene.

Table 12

SANS RESULTS UNIMODAL PDMS SOLUTIONS AT 25°C

M_n	Solvent	v_2	ξ Å	x
7,000	C_6D_6	0.010	25.1	1.66
		0.154	16.5	1.44
		0.201	13.9	1.28
		0.254	11.5	1.08
		0.301	10.3	1.00
7,000	C_7D_8	0.201	11.9	1.15
		0.300	8.9	0.85
22,500	C_6D_6	0.166	16.6	1.68
5,200	C_6D_6	0.333	8.9	1.10

x : wide q exponent

Table 13

SANS RESULTS BIMODAL PDMS SOLUTIONS AT 25°C

#	v_2	v_L	ξ Å	x
1	0.178	0.178	16.0	1.55
2	0.206	0.202	14.3	1.36
3	0.207	0.198	14.3	1.29
4	0.238	0.220	13.2	1.28
5	0.349	0.287	9.5	
1	0.178	0.178	16.0	1.55
7	0.177	0.168	17.4	1.62
8	0.177	0.0	7.4	

v_2 : total volume fraction of polymers in solution.

v_L : volume fraction of long chains in solutions.

Table 14

SANS RESULTS FOR UNIMODAL PDMS NETWORKS AT 25°C

#	Sol-vent	v_2	ξ Å	R_c Å	$(Rg)_{ph}^{sw}$ Å	Q_c
1000	4 B	0.19	76.1	131.8	74.2	1.78
1000	4 B	0.19	73.9	128.0	74.2	1.73
1000	4 T	0.16	86.6	150.0	76.4	1.96
100	4 B	0.30	42.8	74.1	30.0	2.47
100	5 B	0.33	35.7	61.8	29.6	2.08
4-6	4 B	0.54	9.3	16.1	12.2	1.32

B : Benzene

T : Toluene

Table 15.

SANS RESULTS FOR BIMODAL PDMS NETWORKS SWOLLEN IN BENZENE AT 25°C

x	v_2	R_c Å	M_Z	$(Rg)_{ph}^{sw}$ Å	Q_c
0	0.19	128	58500	74.2	1.73
25	0.23	124	44406	62.6	1.98
40	0.26	114	35950	55.4	2.06
60	0.29	100	24675	45.2	2.21
80	0.34	90	13400	32.4	2.78
100	0.54	16	2125	12.2	1.32

x : mole % short chains

Table 16

CAUCHY DISPERSION FORMULA COEFFICIENTS AND REFRACTIVE INDEX RESULTS FOR THE INDIVIDUAL COMPONENTS AT 25°C

Sample	A	B	n (λ =5145 Å)
Toluene	1.4680	8942.8	1.5018
Benzene	1.4702	9439.0	1.5058
PDMS	1.3898	4676.9	1.4074

Table 17

DEBYE BUECHE PLOT RESULTS OF THE LIGHT SCATTERING DATA FROM BIMODAL PDMS NETWORKS

Sample x %	a_c in Å In Tol	a_c in Å In Benz	H_{EXPT} In Tol	H_{EXPT} In Benz	H_{CAL}
0	320	380	0.0492	0.0424	0.89
50	372	433	0.0403	0.0429	1.54
90	364	352	0.0260	0.0320	3.10
95	345	356	0.0267	0.0295	3.54
100	383	373	0.0071	0.0080	0.94

Standard Deviations :

a_c $\pm$ 10 %

H_{EXPT} $\pm$ 20 %

Table 18

NETWORK FOLDING ANALYSIS RESULTS OF THE LIGHT SCATTERING DATA FROM SWOLLEN PDMS NETWORKS

x	$\langle n/\phi \rangle$	TOLUENE			BENZENE		
% sc		K $\times 10^6$	Ω $\times 10^6$	W	K $\times 10^6$	Ω $\times 10^6$	W
100	1.45	3.9	1.9	1.0	3.4	1.6	1.0
95	1.77	74.2	23.7	12.4	48.8	15.6	9.7
90	2.10	83.4	19.0	10.0	72.1	16.4	10.2
50	4.68	260.6	11.8	6.2	170.2	7.8	4.8
0	7.91	420.9	6.8	3.5	178.0	2.9	1.8

Fig 1. Sketch of an inhomogeneously crosslinked network

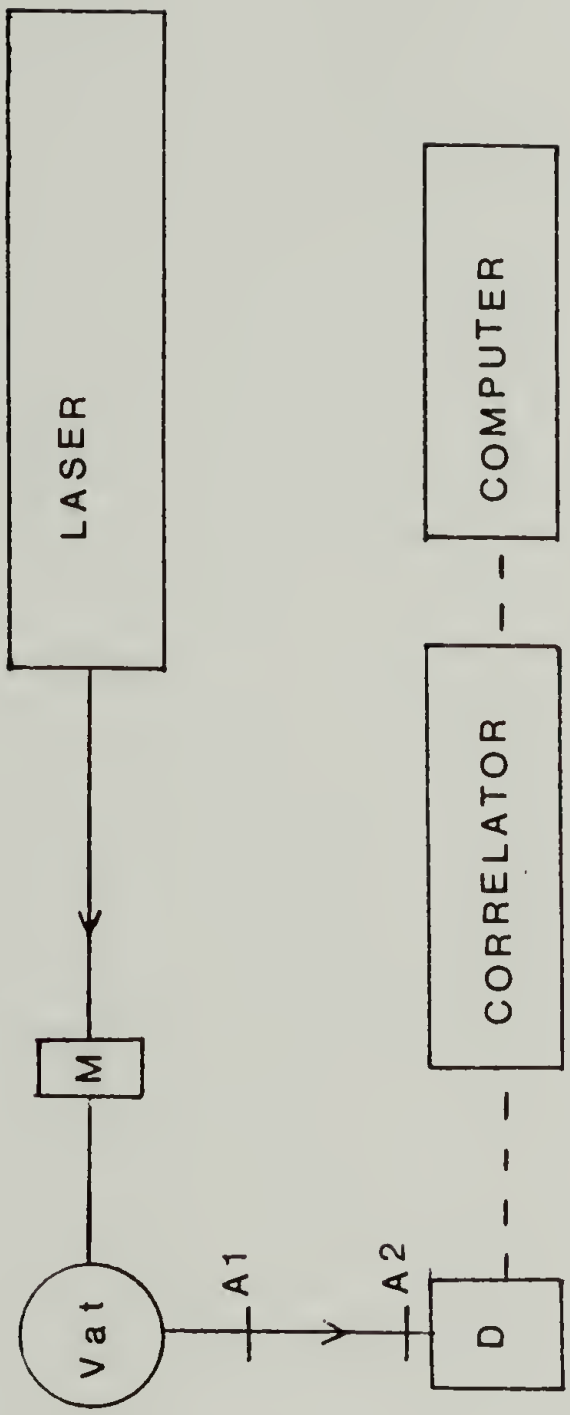

Fig 2. Sketch of the wide angle light scattering apparatus used.

M-MONITOR D-DETECTOR A-APERTURE

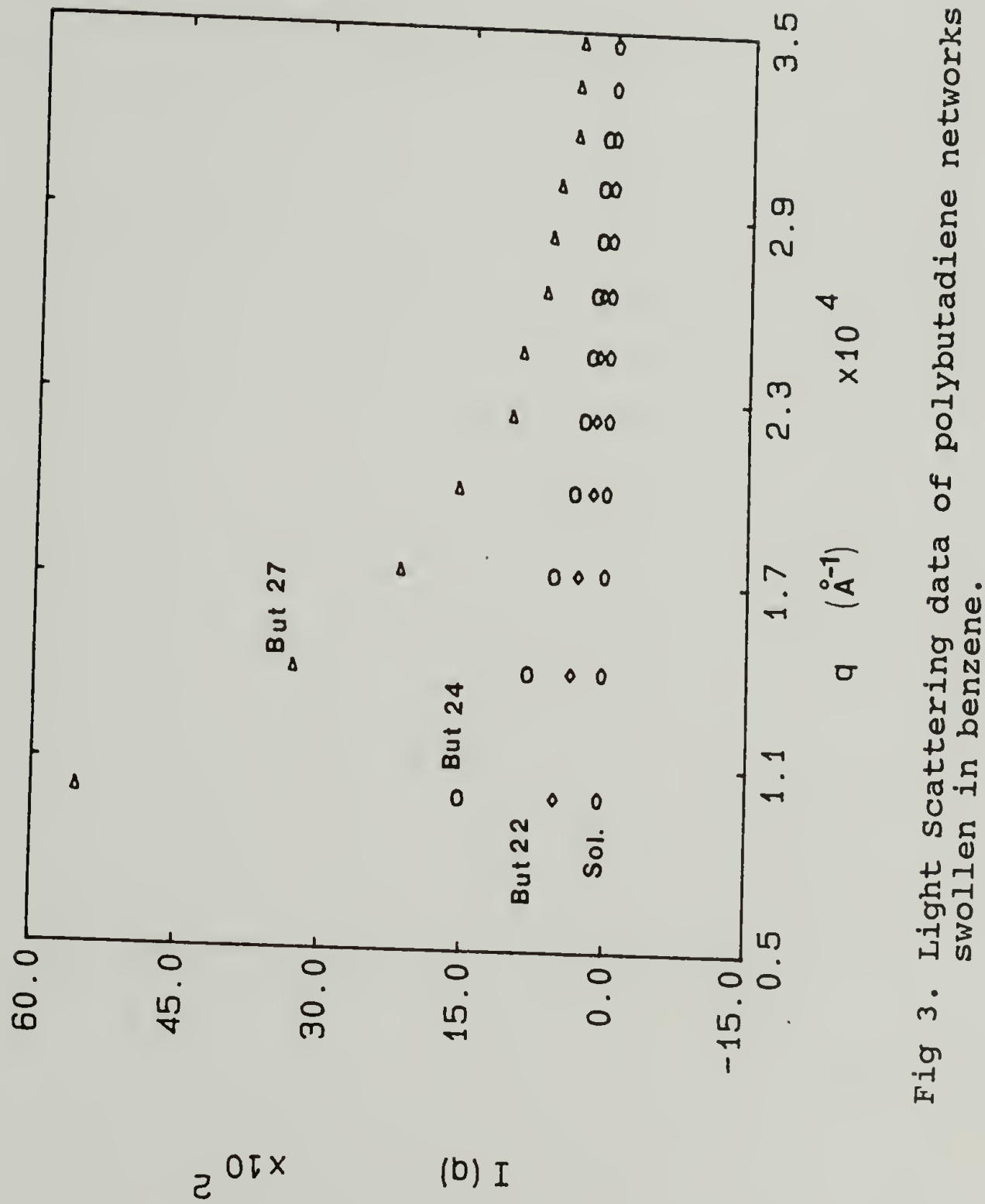

Fig 3. Light scattering data of polybutadiene networks swollen in benzene.

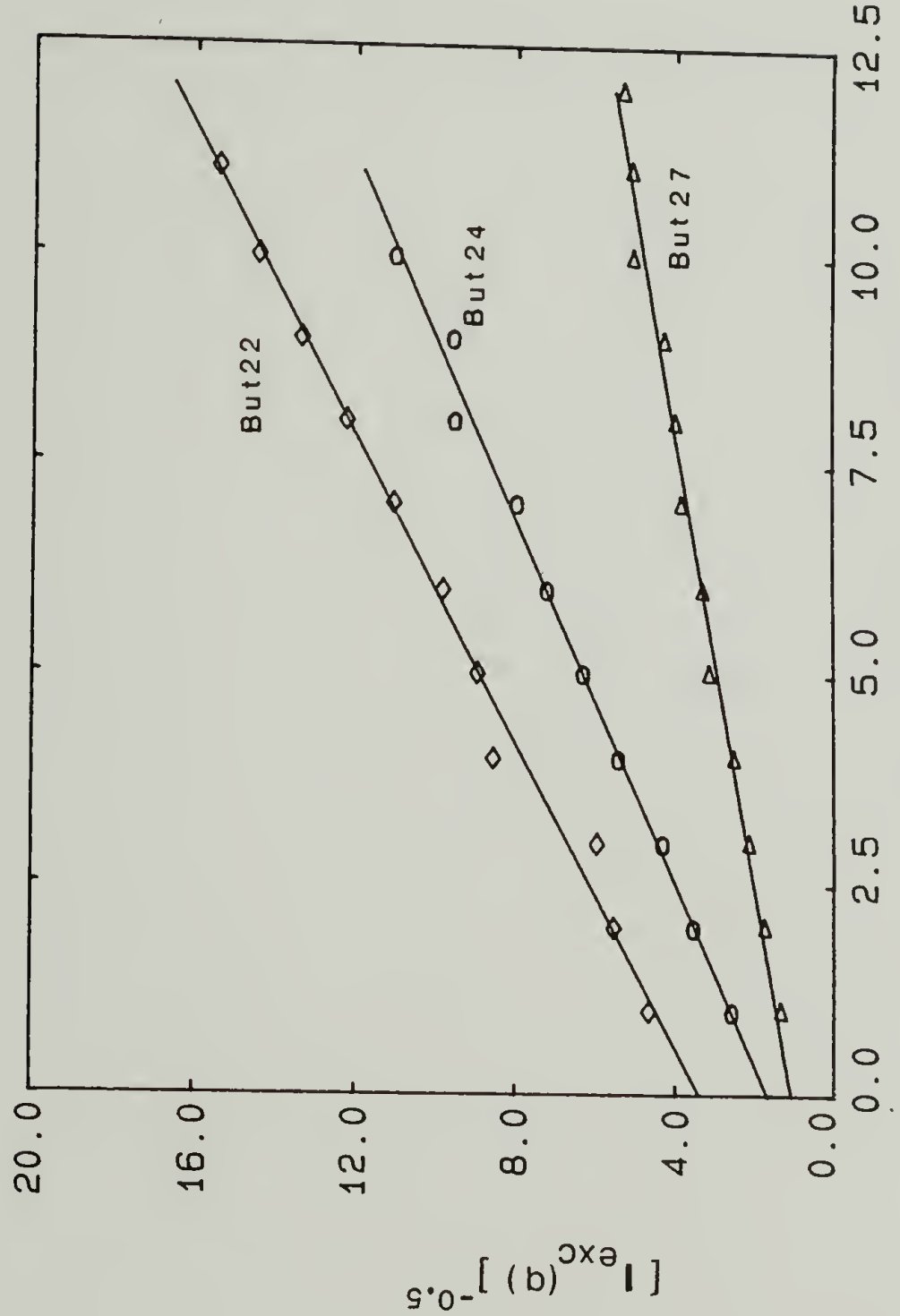

Fig 4. Debye Bueche plots of excess light scattering data from swollen polybutadiene networks.

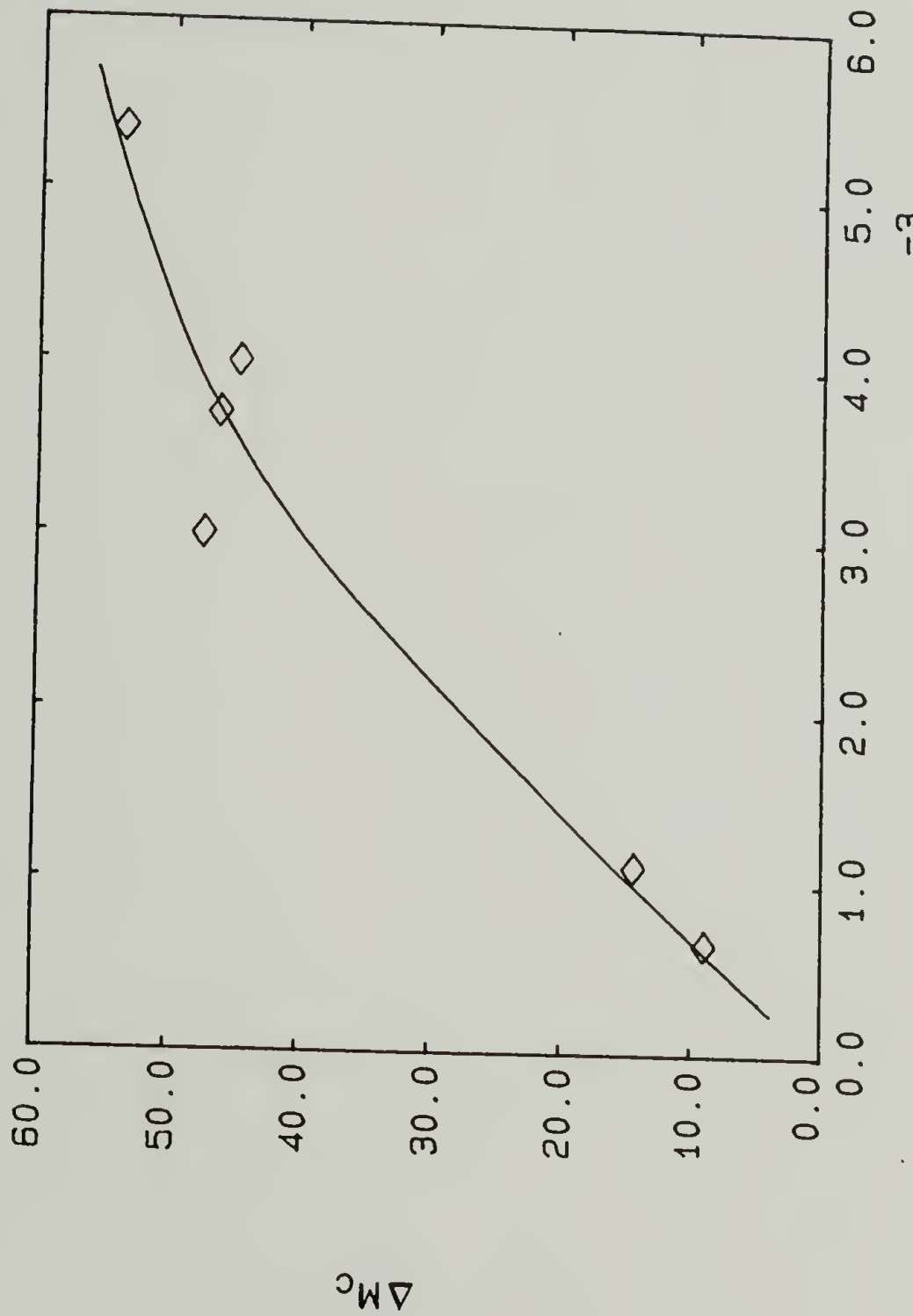

Fig 5. Relative values of ΔM_c vs M_c for polybutadiene networks calculated from SALS results.

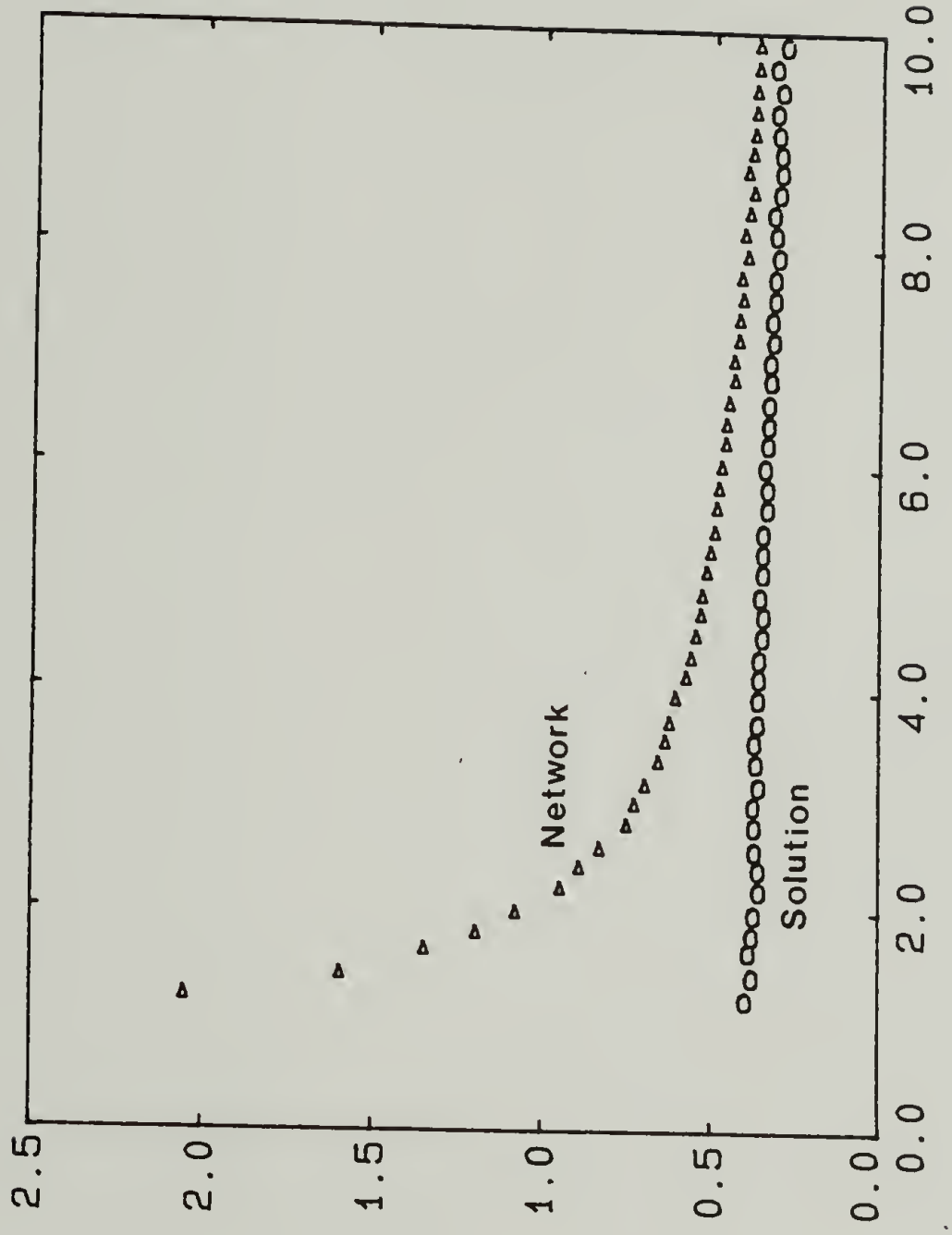

Fig 6. SANS data for But 35 swollen in benzene and the corresponding solution. (SDD = 4.89 m.).

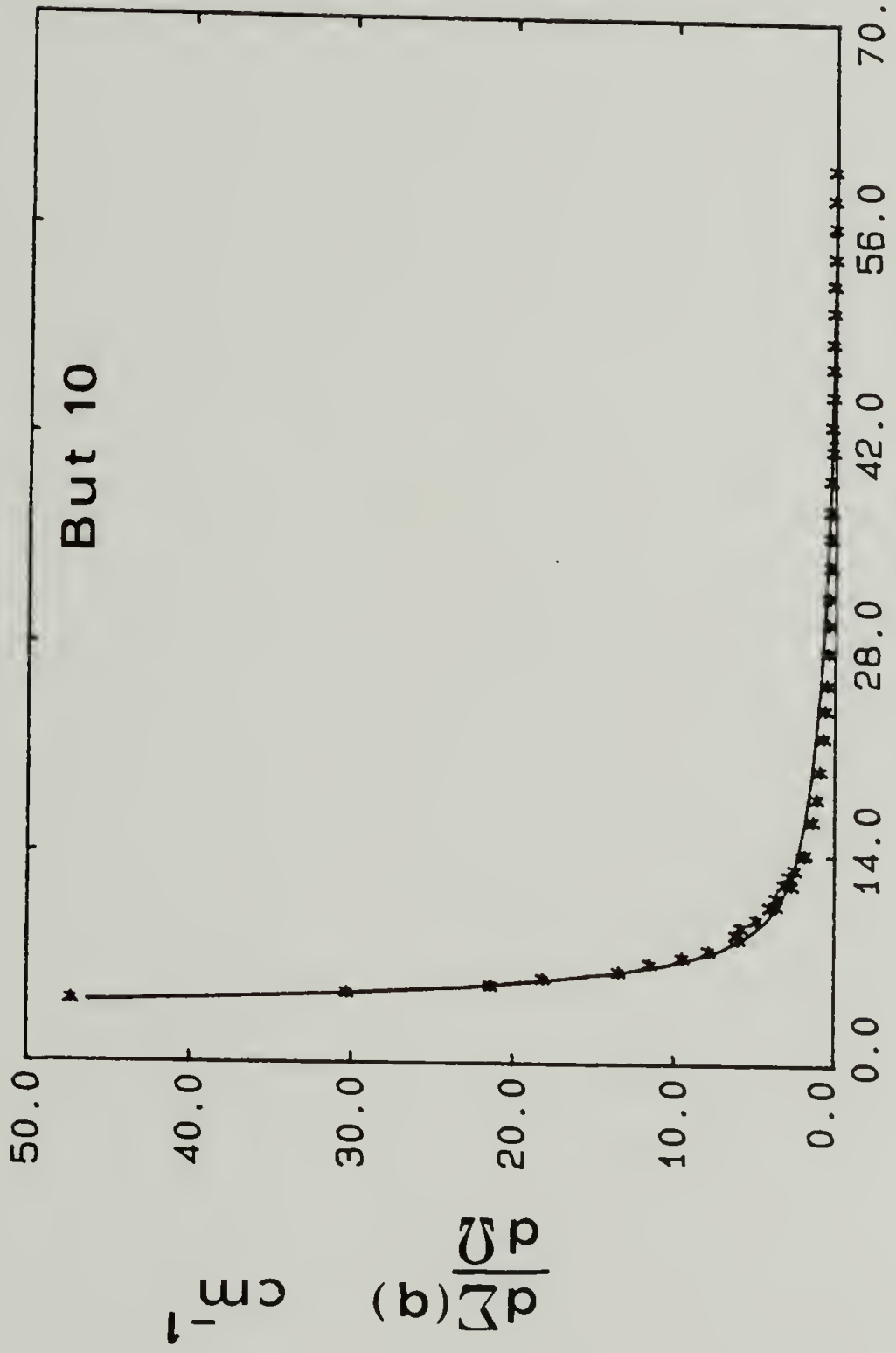

Fig 7. SANS excess scattering curves for But 10 network swollen in benzene. Combined data, SDD 4.89m and 18.9m, and 4 parameter fit.

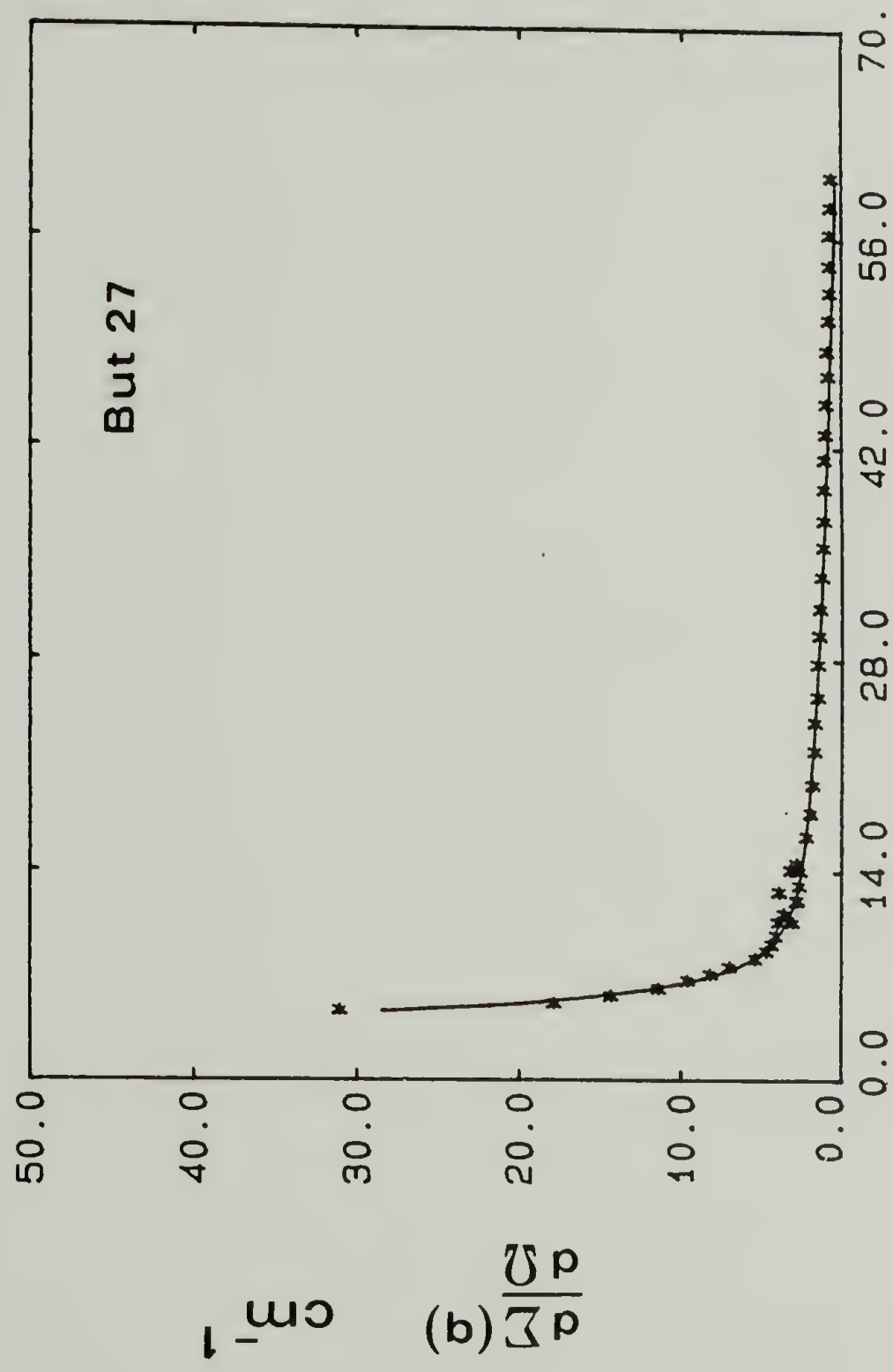

Fig 8. SANS excess scattering curves for But 27 network swollen in benzene. Combined data, SDD 4.89m and 18.9m, and 4 parameter fit.

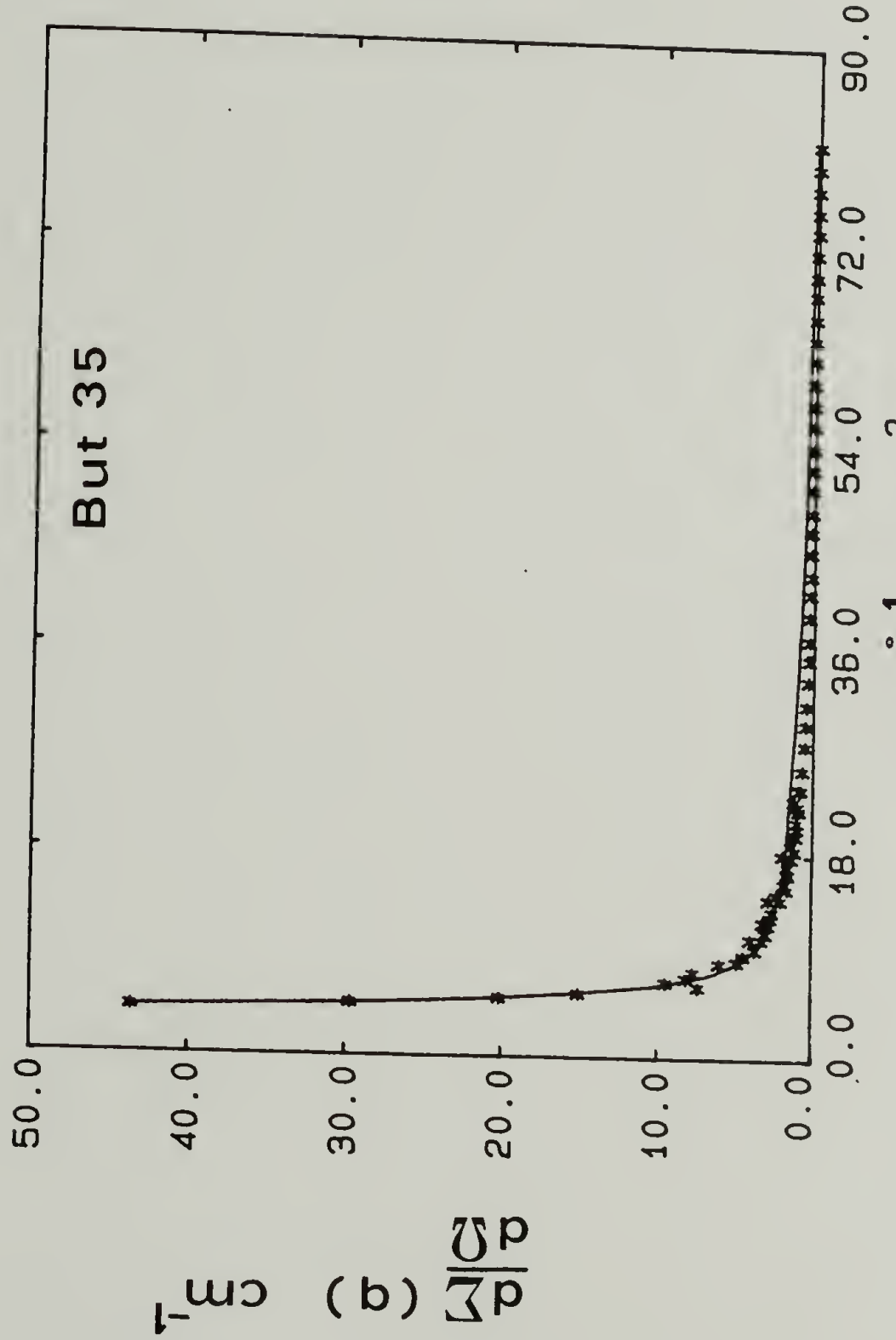

Fig 9. SANS excess scattering curves for But 35 network swollen in benzene. Combined data, SDD 4.89m and 18.9m, and 4 parameter fit.

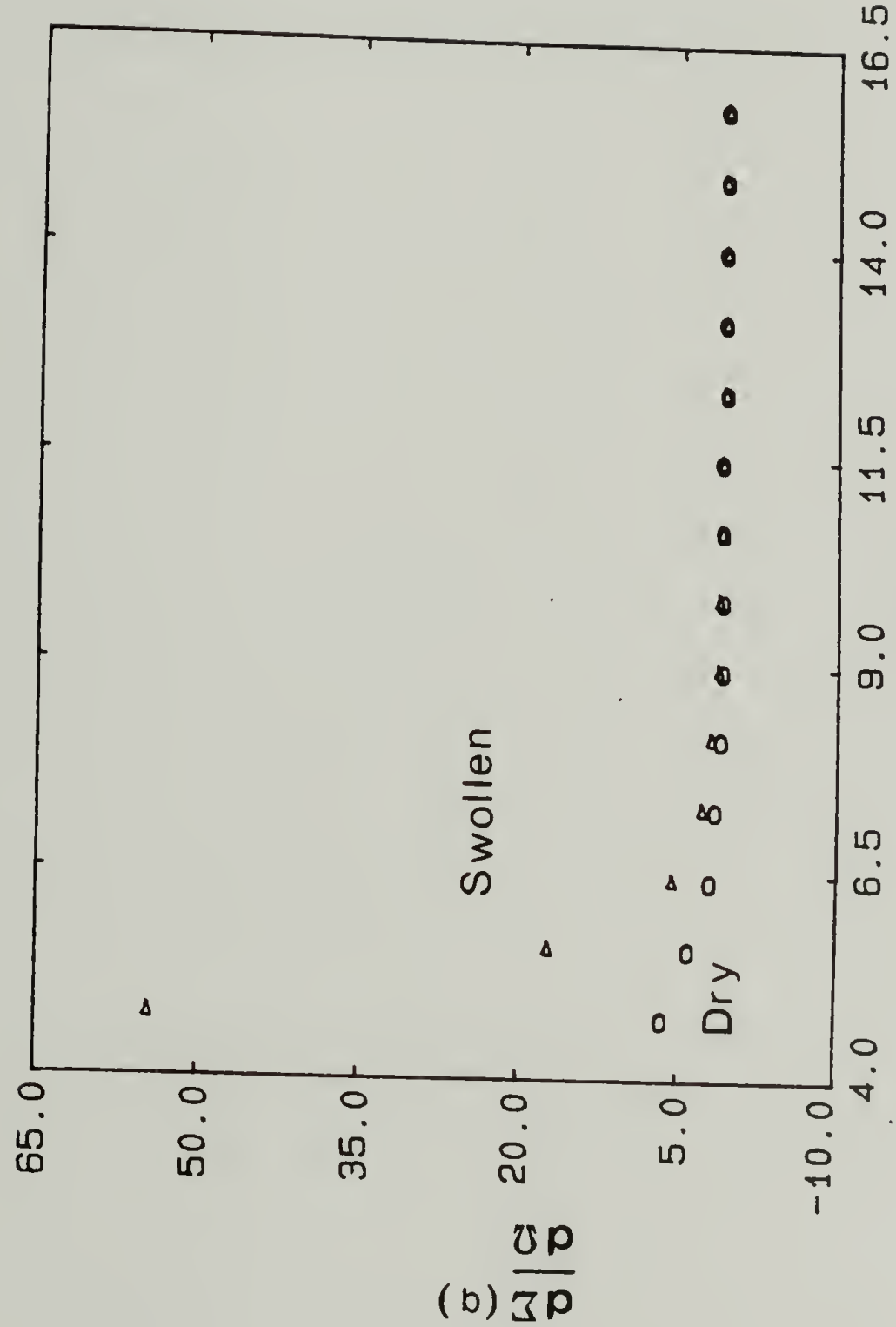

Fig 10. Preliminary SANS experiment on epoxies (D_2O swollen and dry samples).

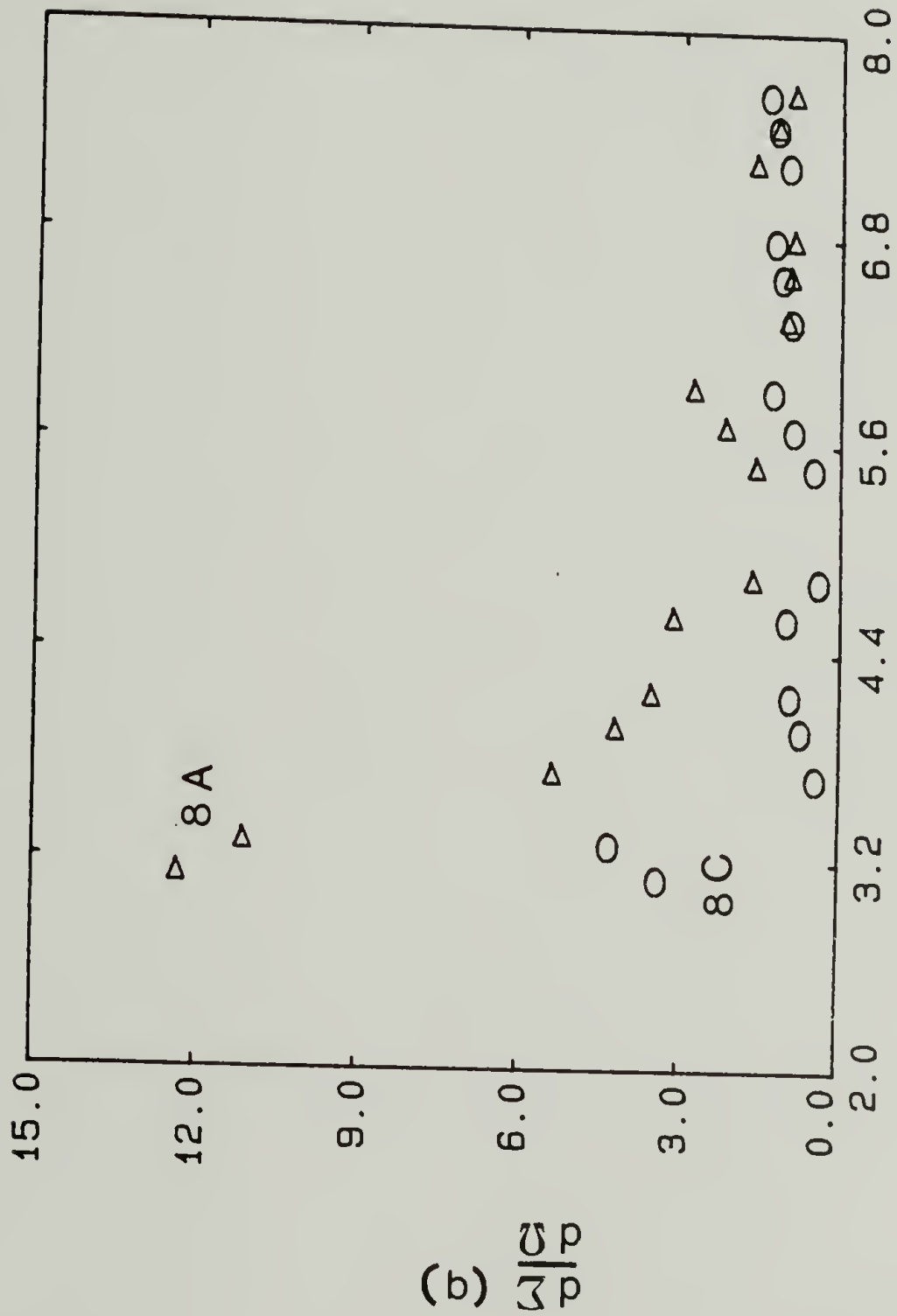

Fig 11. SANS data from swollen (8A) and dry sample (8C) in the second experiment on epoxies.

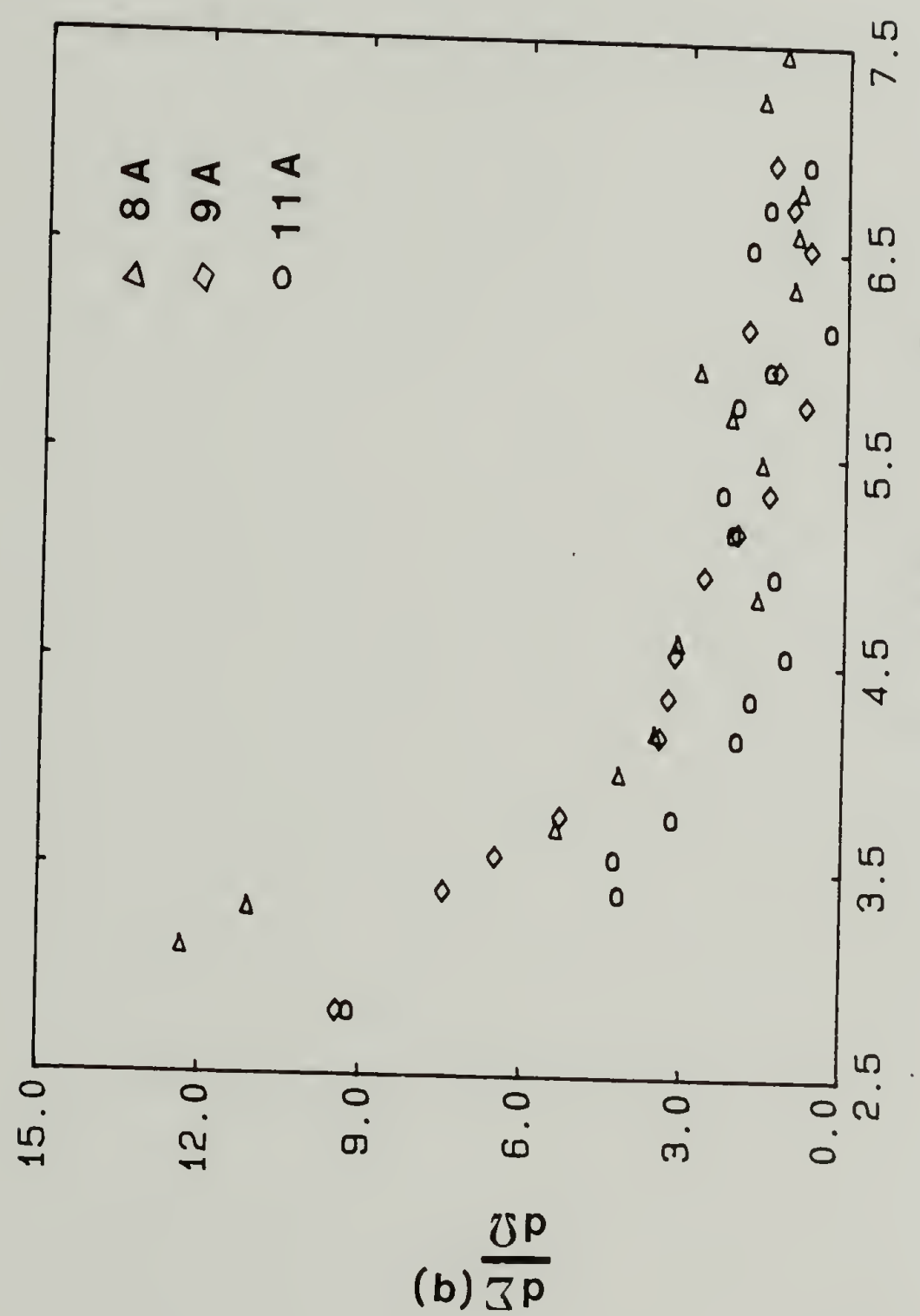

Fig 12. SANS data from epoxy samples cured under different cure conditions and swollen in D_2O in the second experiment (8A, 9A and 11A).

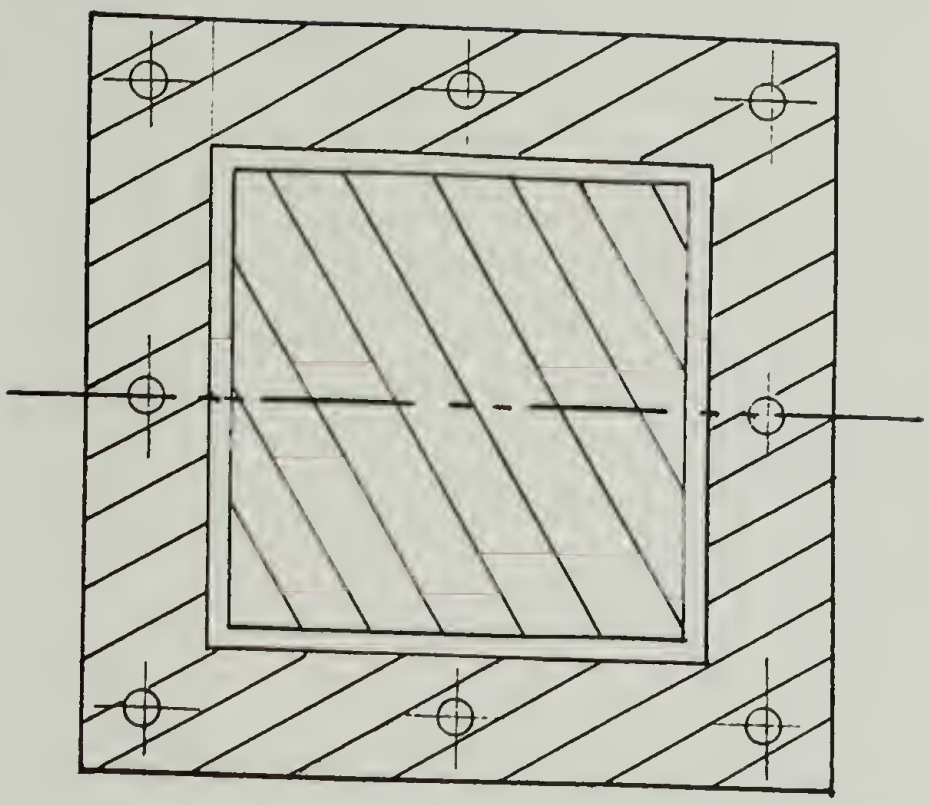

Fig 13. Sketch of mold used for preparing PDMS samples.

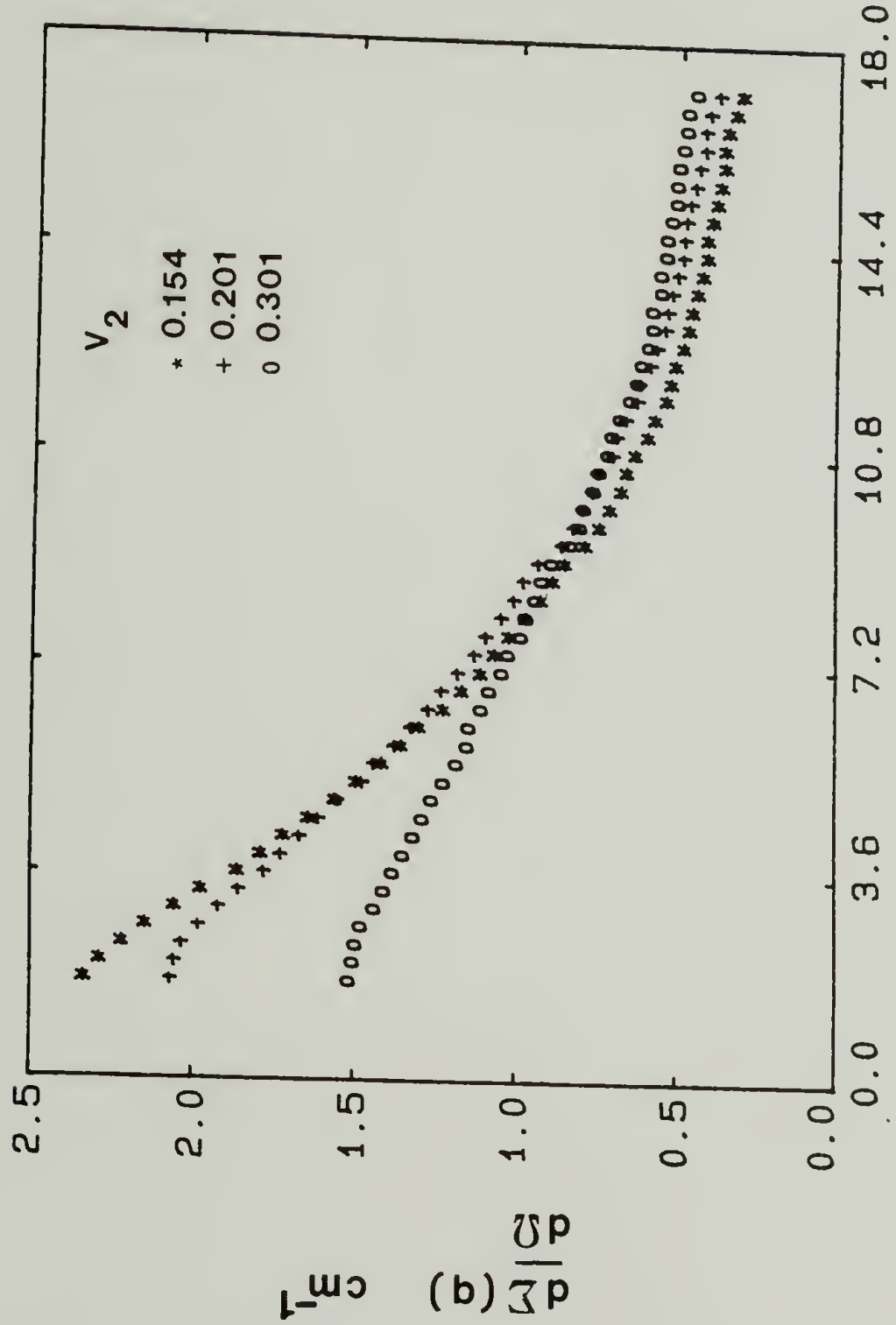

Fig 14. SANS data PDMS 200 solutions in C_6D_6.

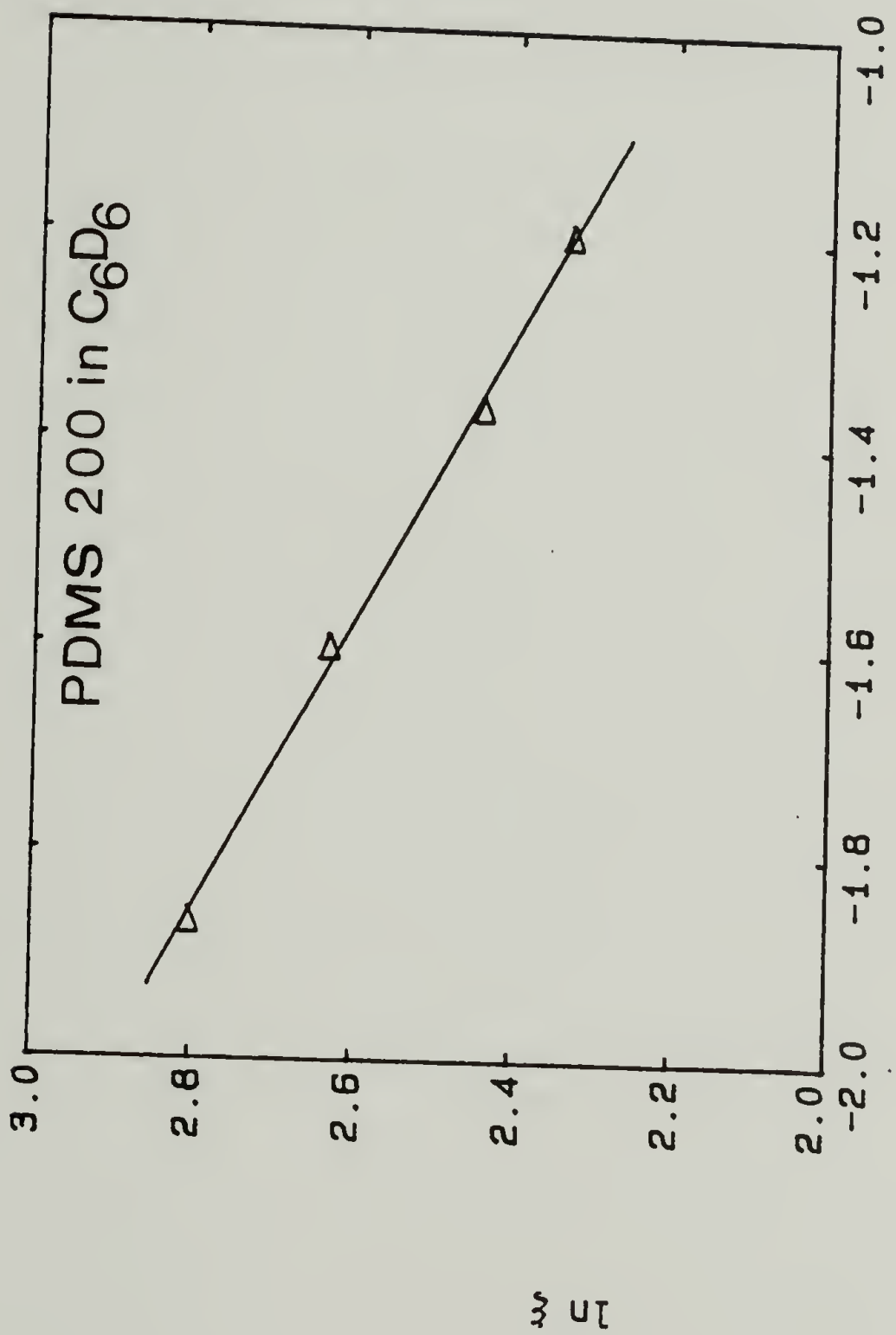

Fig 15. Concentration dependence of mesh size ξ for PDMS 200 solutions in C_6D_6.

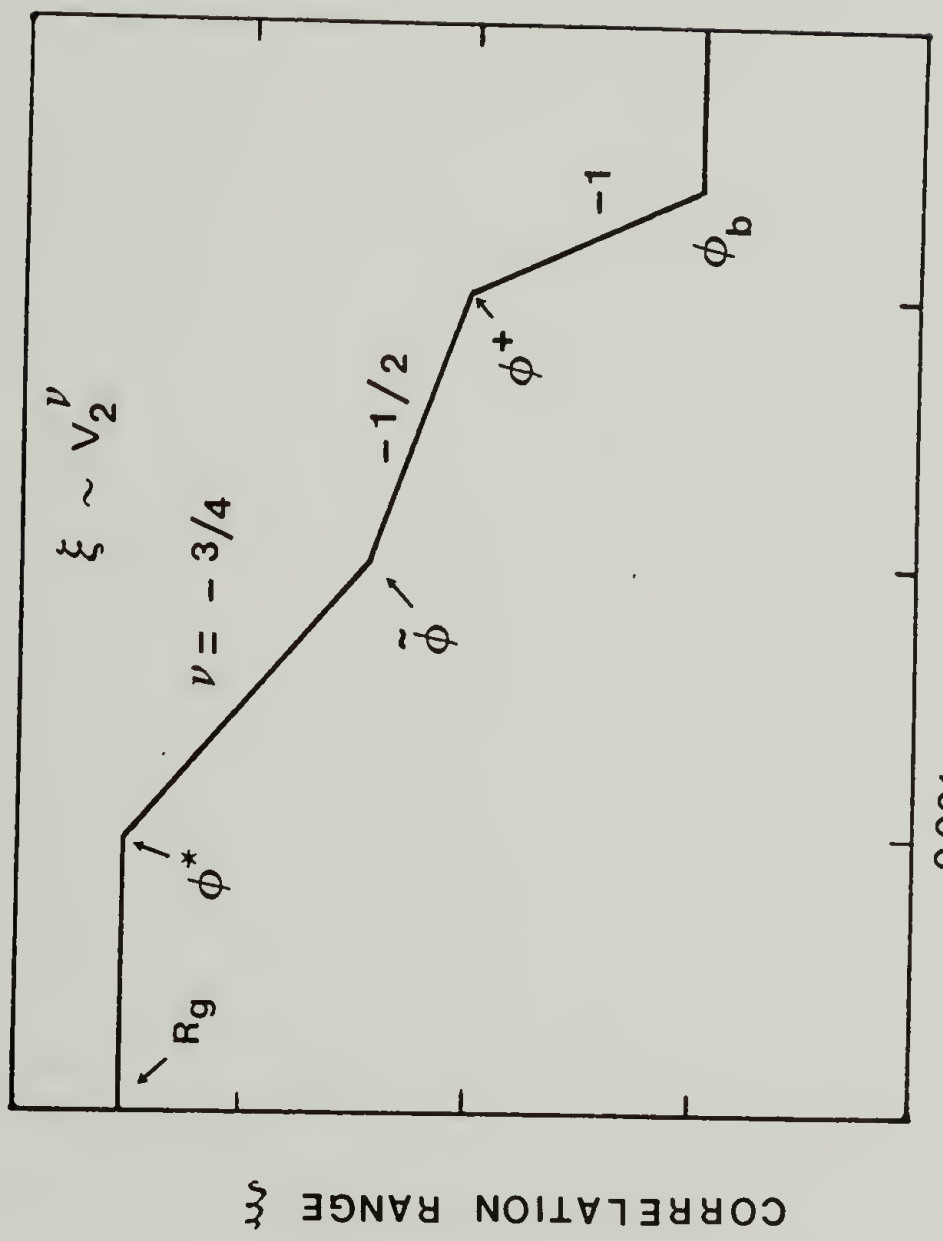

Fig 16. Schaefer's model for different concentration regimes in semi-dilute solutions.

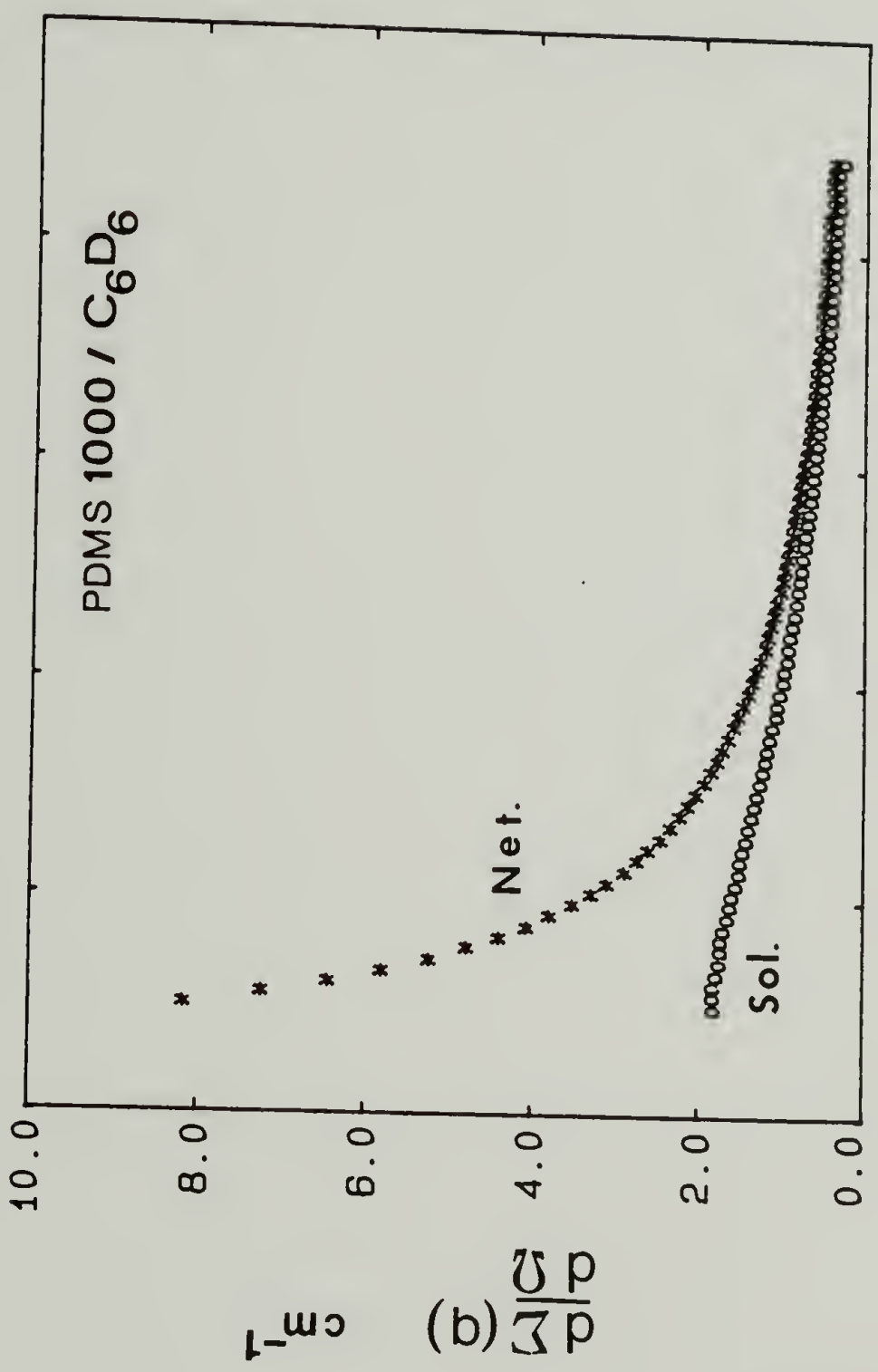

Fig 17. SANS data for swollen PDMS 1000 network and corresponding solution.

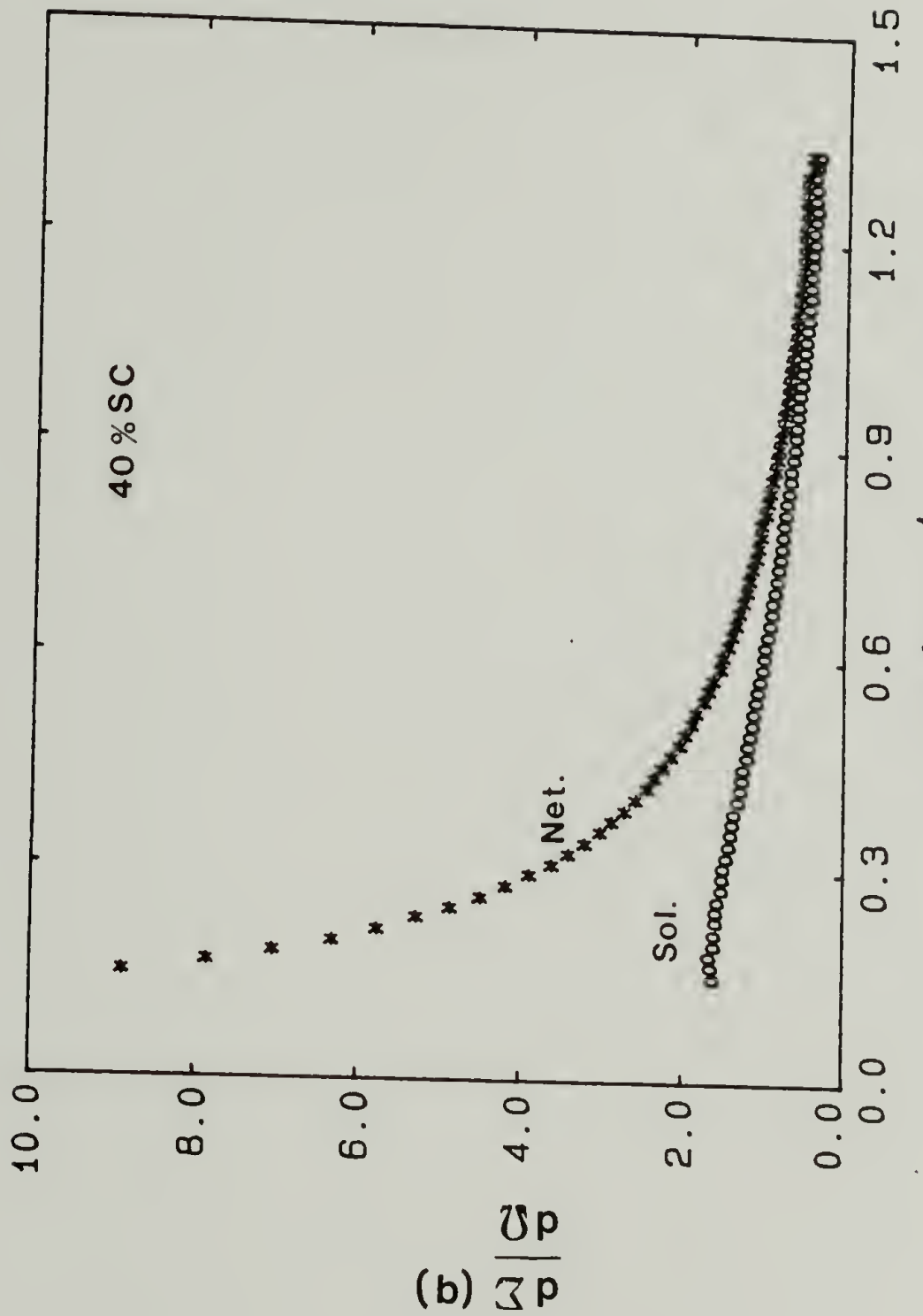

Fig 18. SANS data for swollen bimodal PDMS network (40 % SC) and corresponding solution.

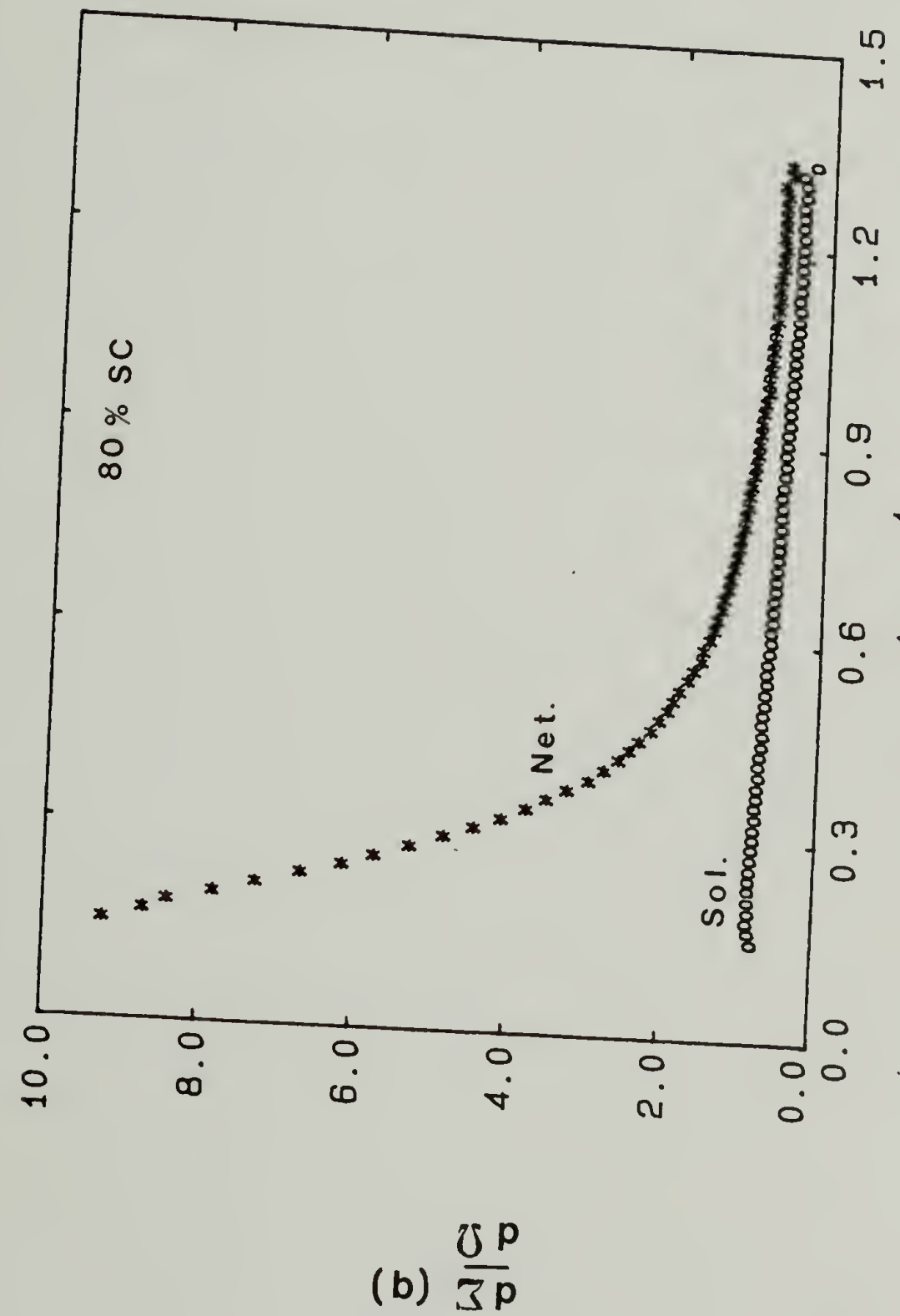

Fig 19. SANS data for swollen bimodal PDMS network (80 % SC) and corresponding solution.

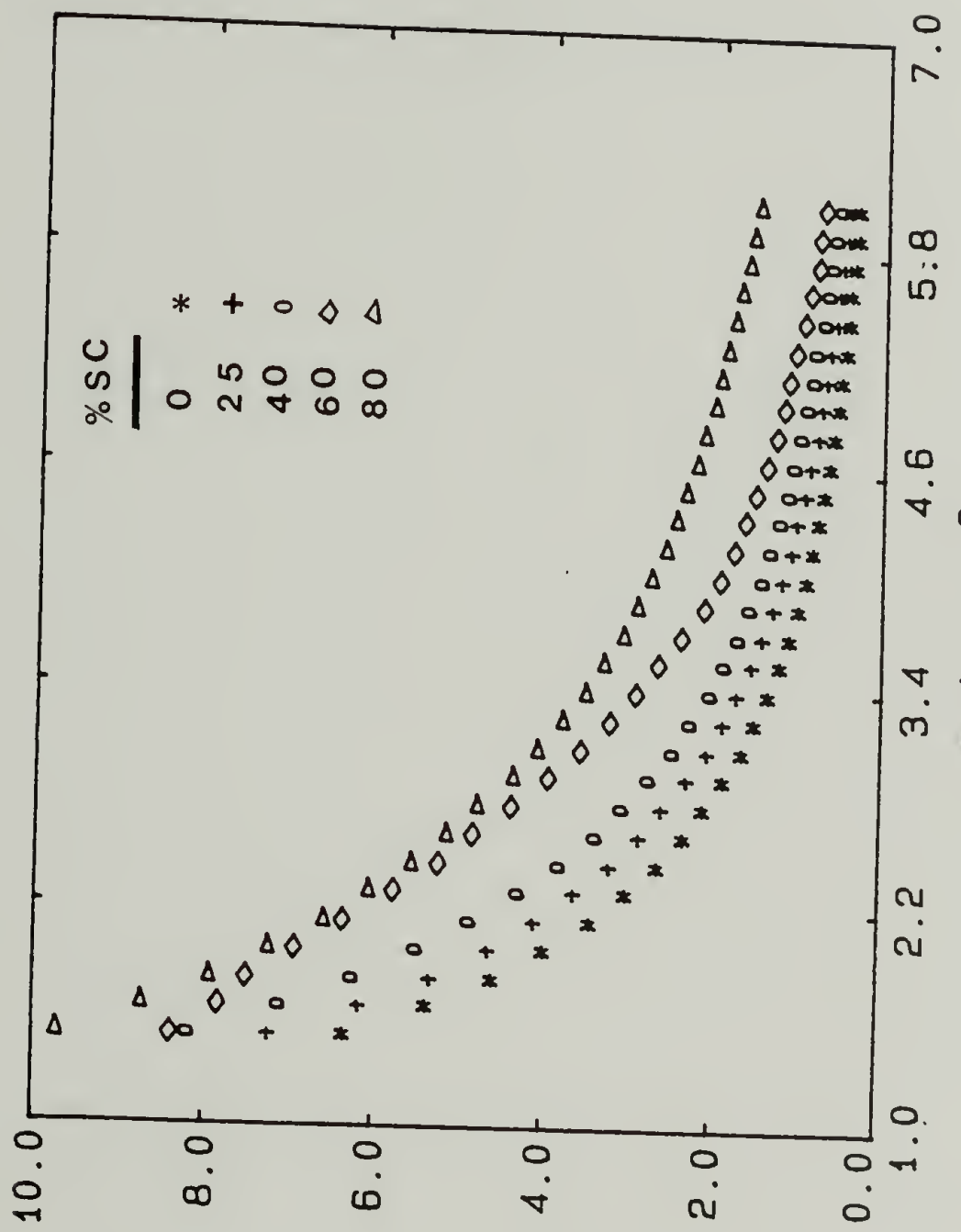

Fig 20. Excess SANS intensities for various swollen bimodal PDMS networks.

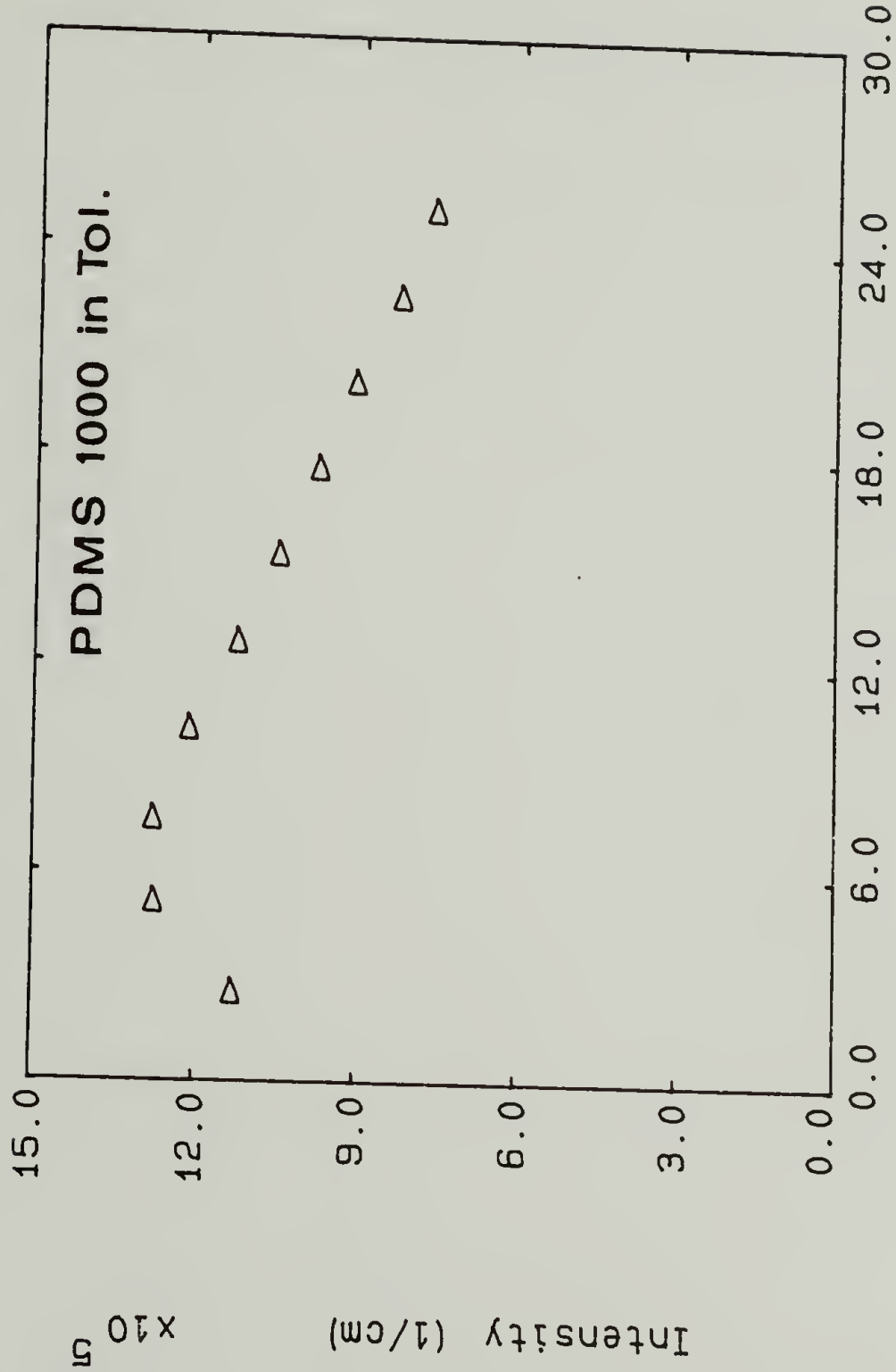

Fig 21. Light Scattering data PDMS 1000 solutions in toluene at 25°C ; Rayleigh Ratio as a function of volume fraction.

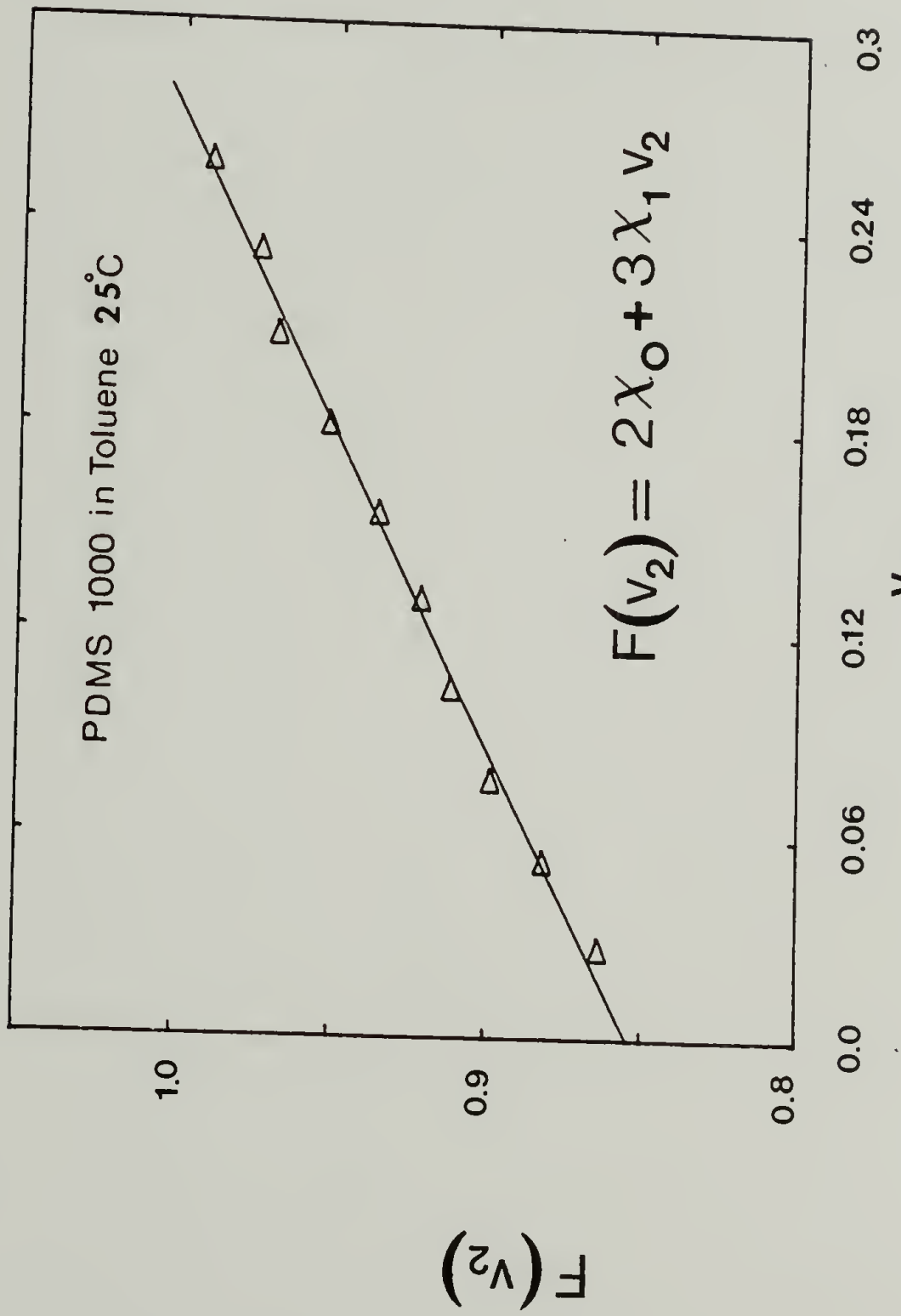

Fig 22. F (v_2) vs v_2 ; PDMS 1000 solutions in toluene at 25°C ; Light scattering data analysis.

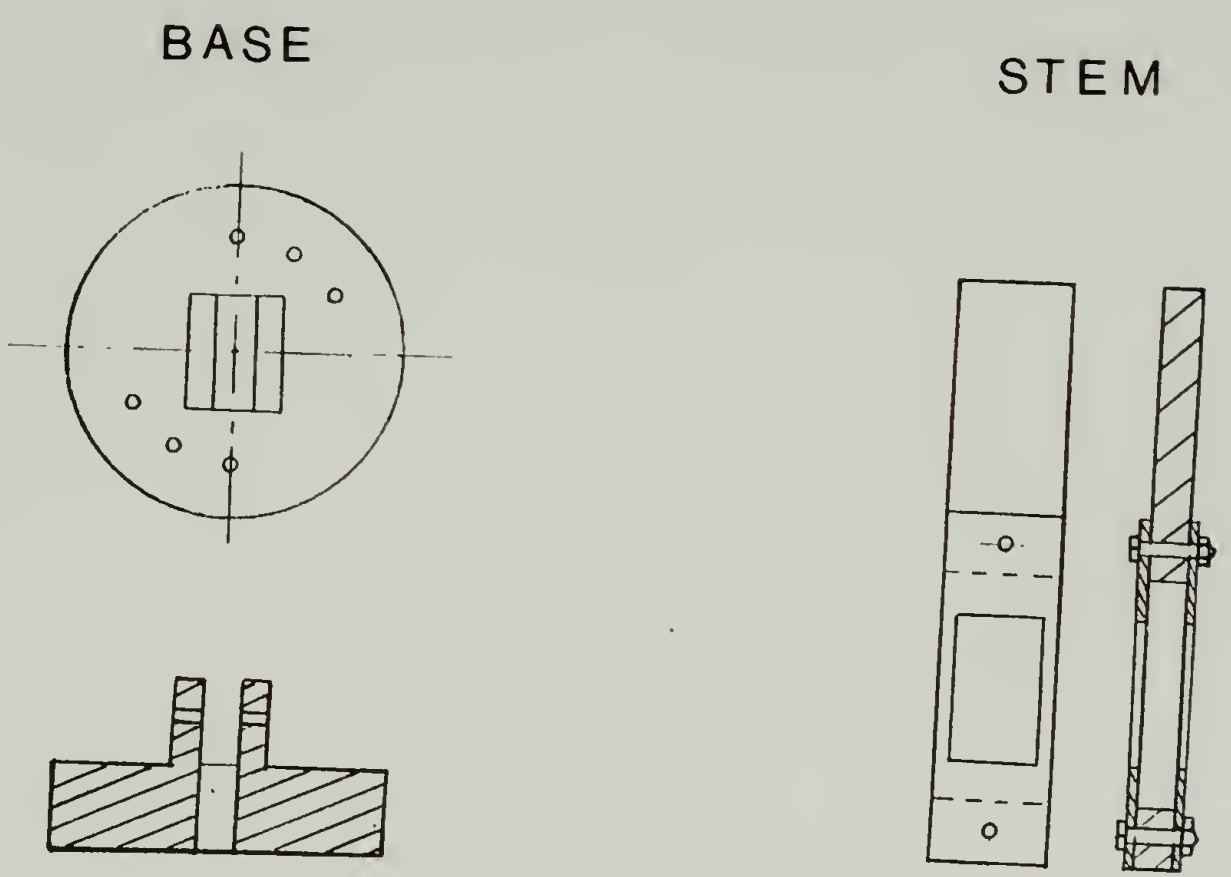

Fig 23. Light scattering sample holder for flat swollen network samples.

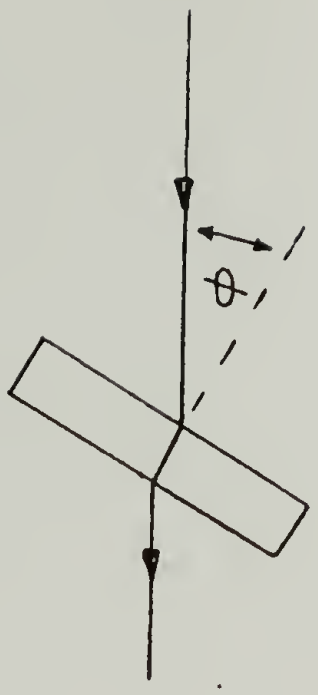

−ve tilt

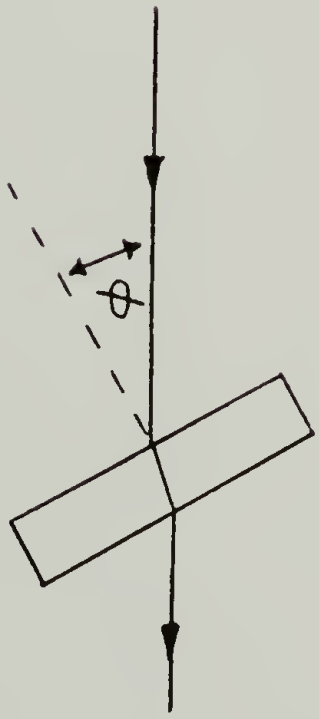

+ve tilt

Fig 24. Sketch of the two types of tilt angles used in the light scattering experiment for networks.

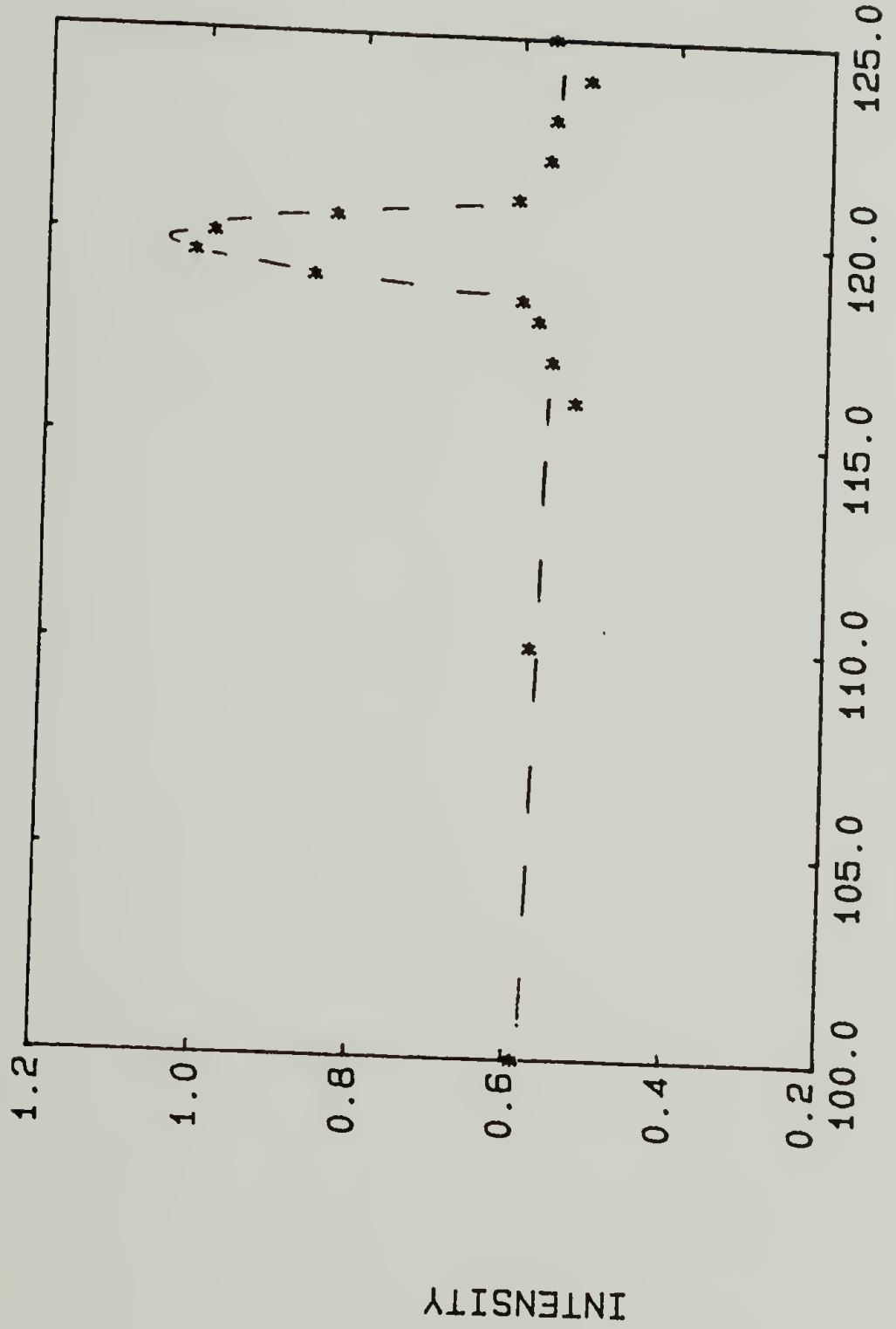

Fig 25. Light scattering data from PDMS 1000 in toluene to show specular reflection at tilt angle = - 30°.

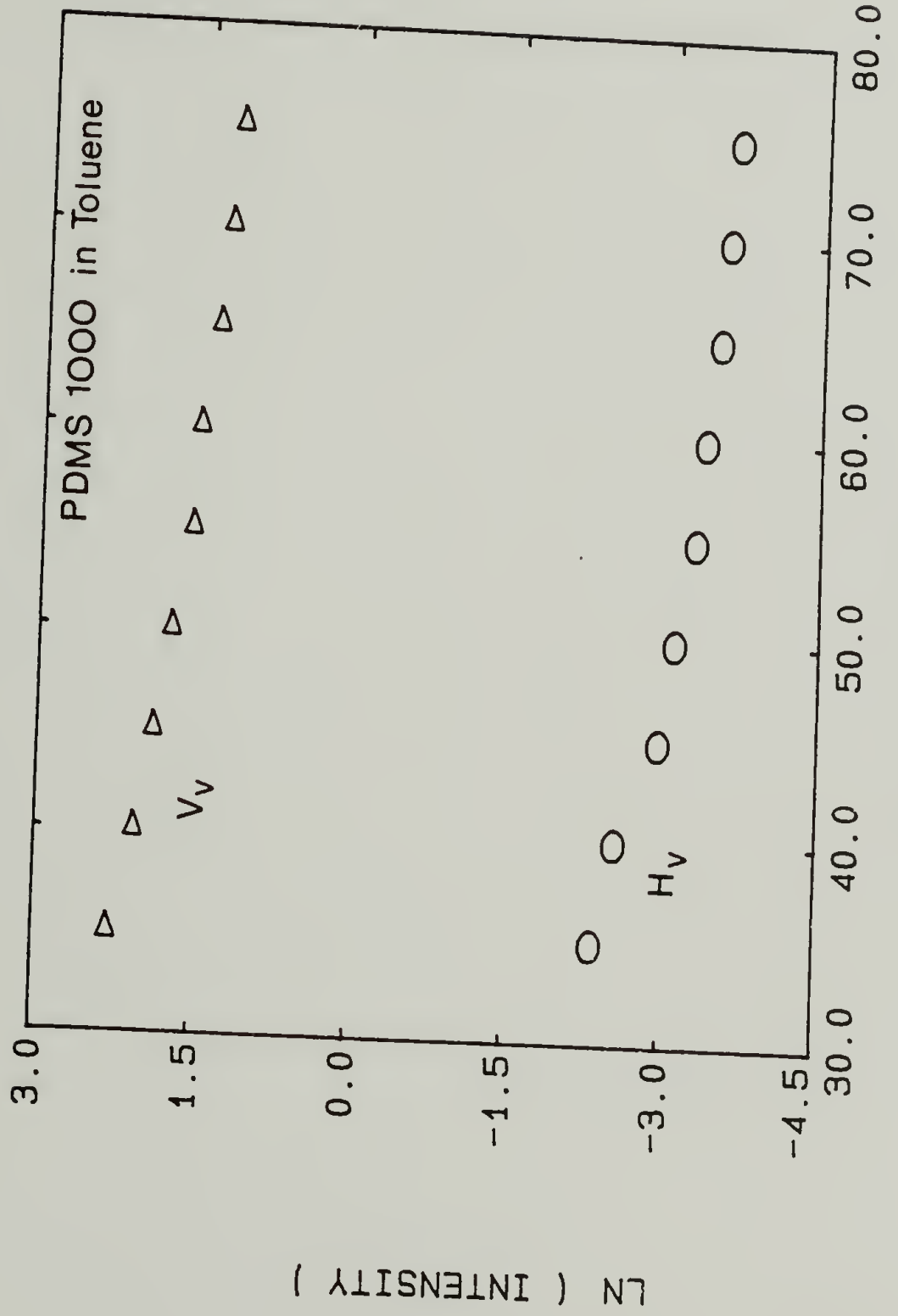

Fig 26. Raw V_v and H_v scattering data from PDMS 1000 in toluene as a function of scattering angle.

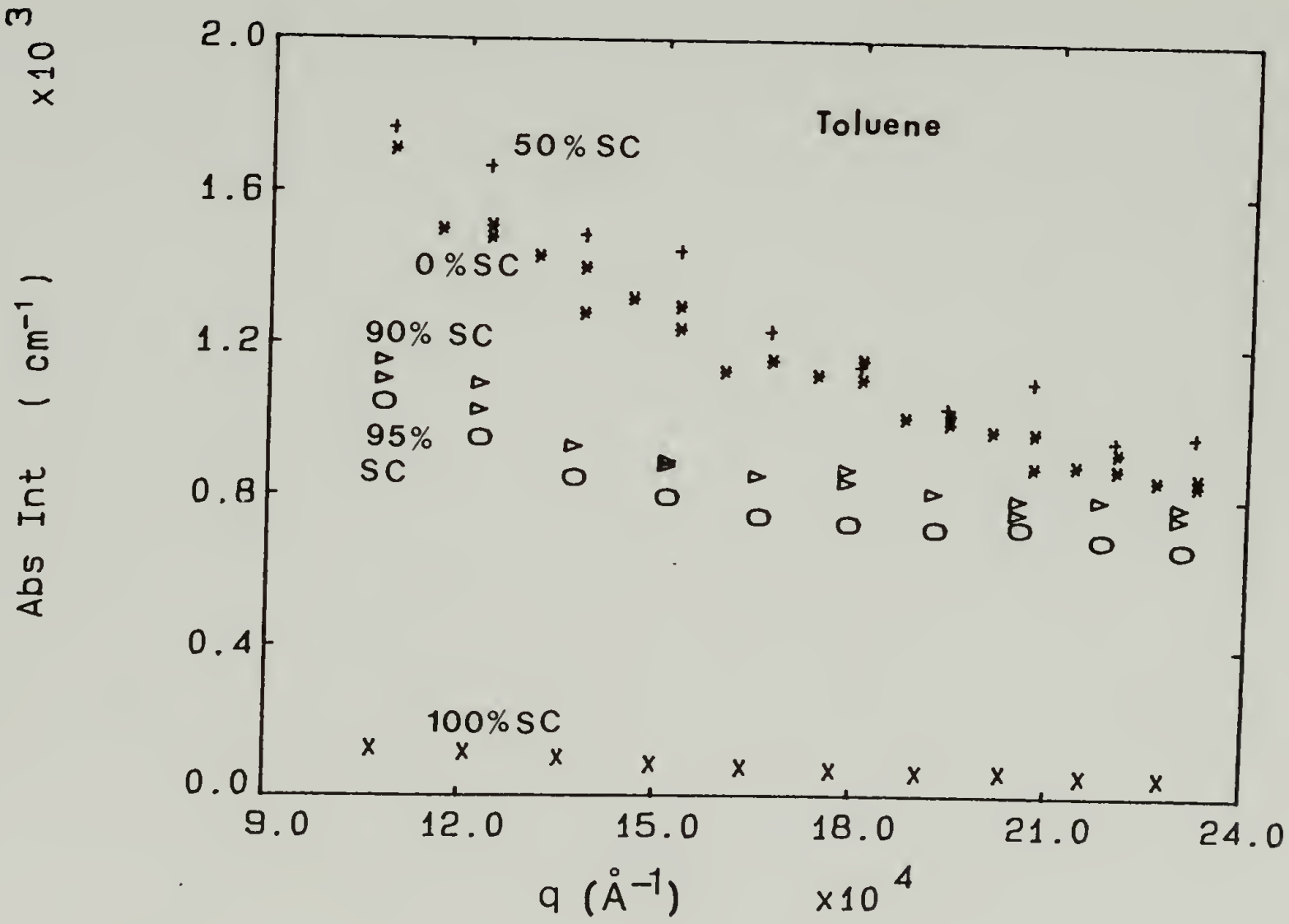

Fig 27. Corrected, absolute intensity light scattering data for bimodal PDMS networks in toluene.

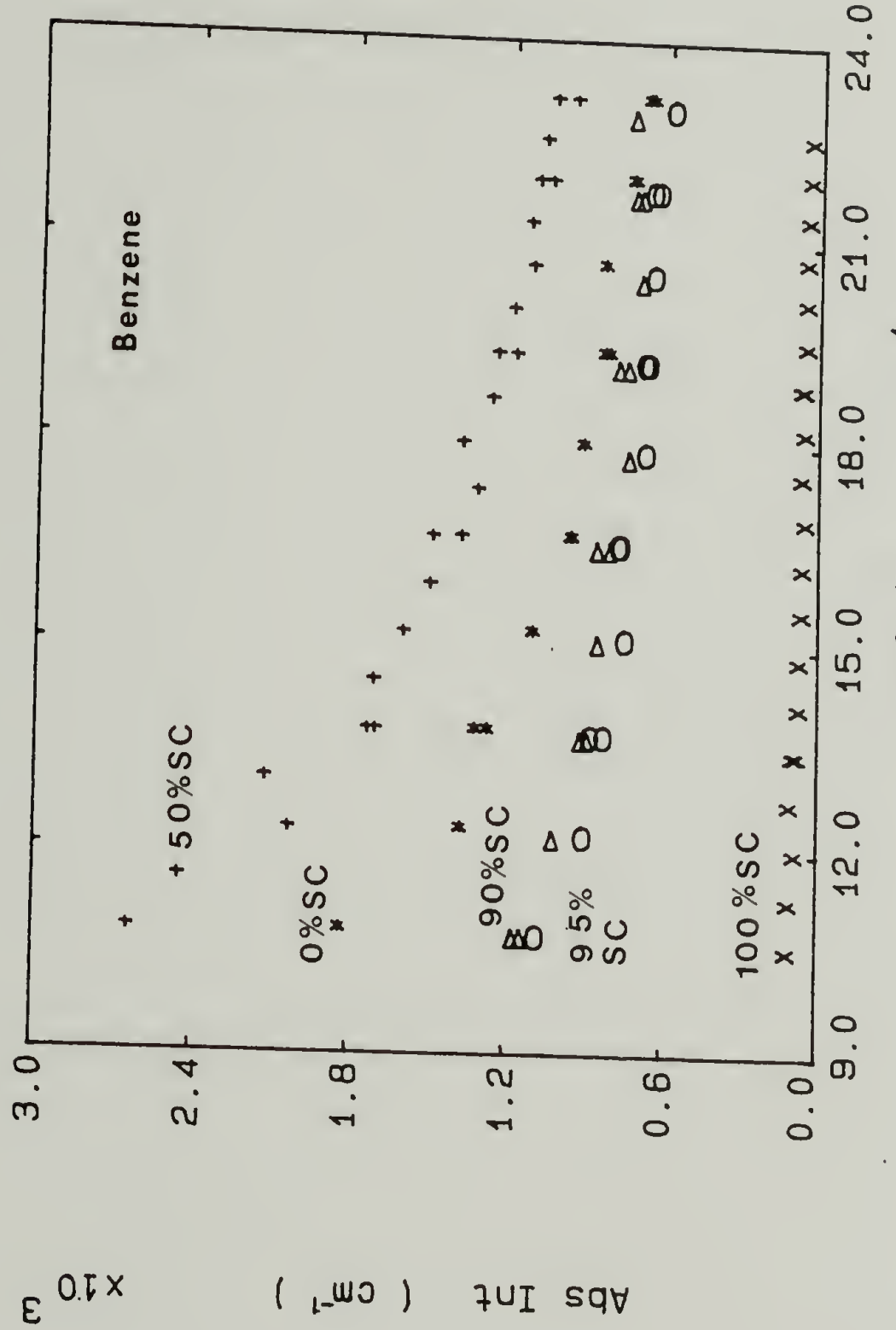

Fig 28. Corrected, absolute intensity light scattering data for bimodal PDMS networks in benzene.

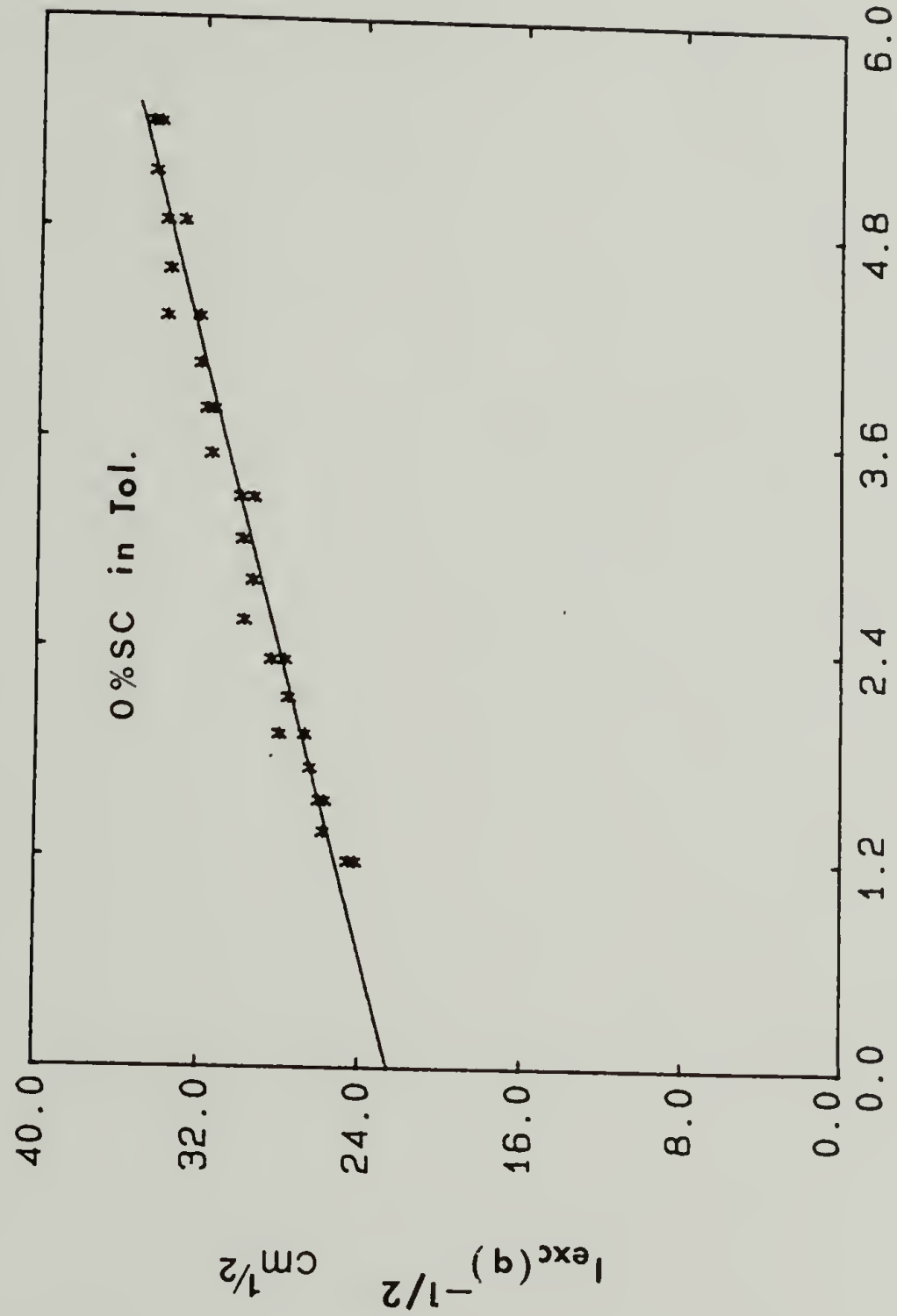

Fig 29. Debye Bueche plot of light scattering data from PDMS 1000 in toluene.

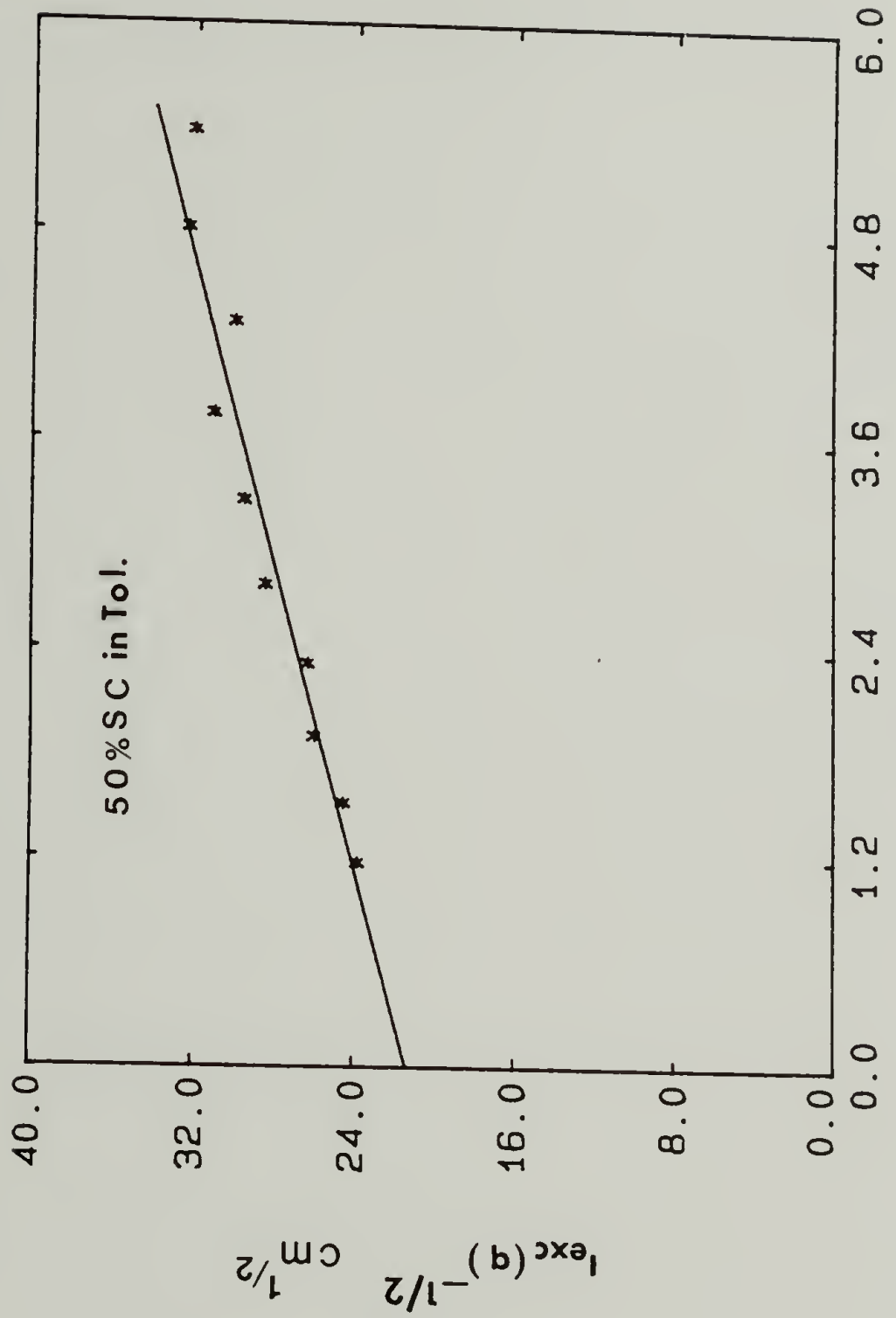

Fig 30. Debye Bueche plot of light scattering data from PDMS 50 % SC in toluene.

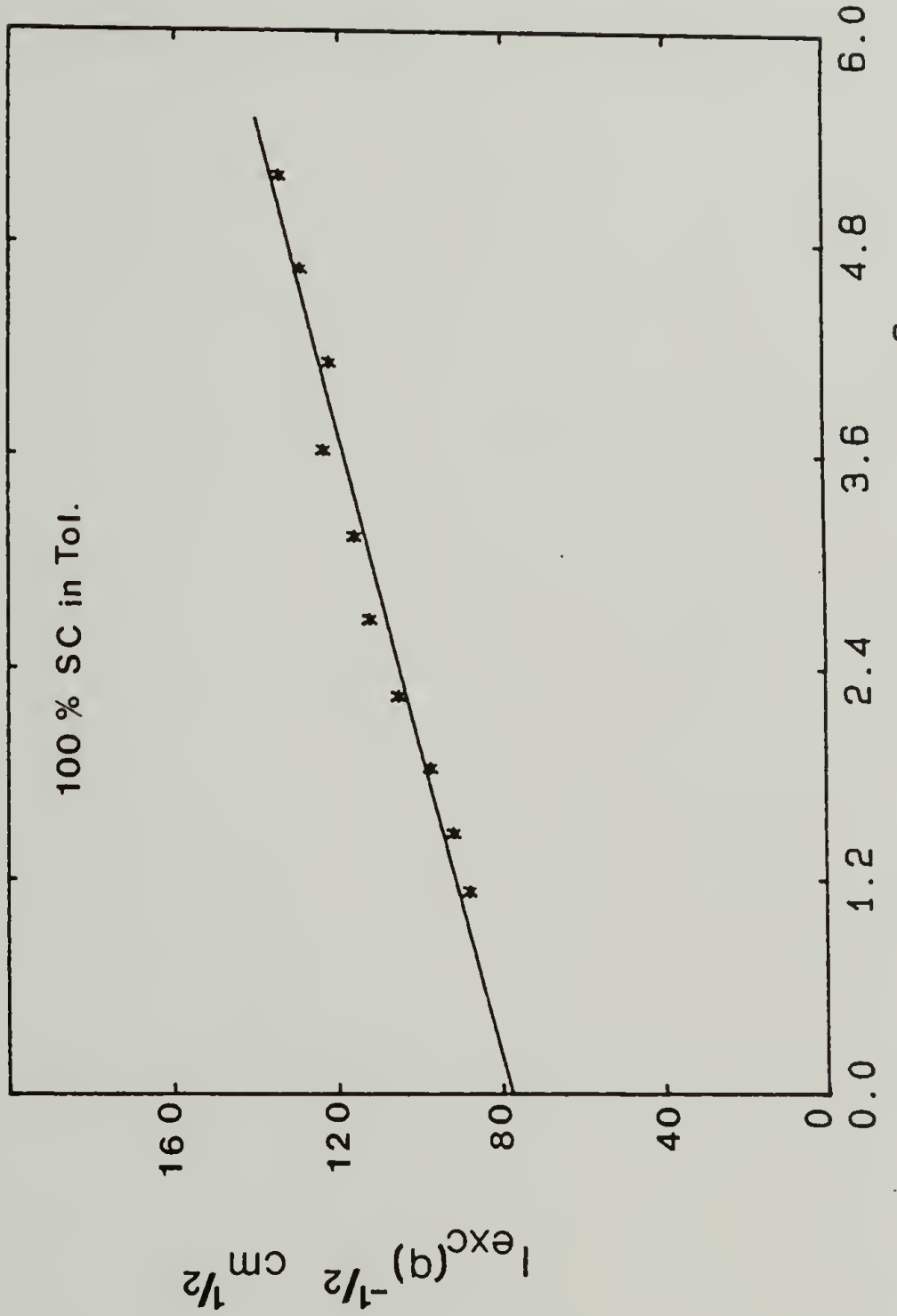

Fig 31. Debye Bueche plot of light scattering data from PDMS 4-6 in toluene.

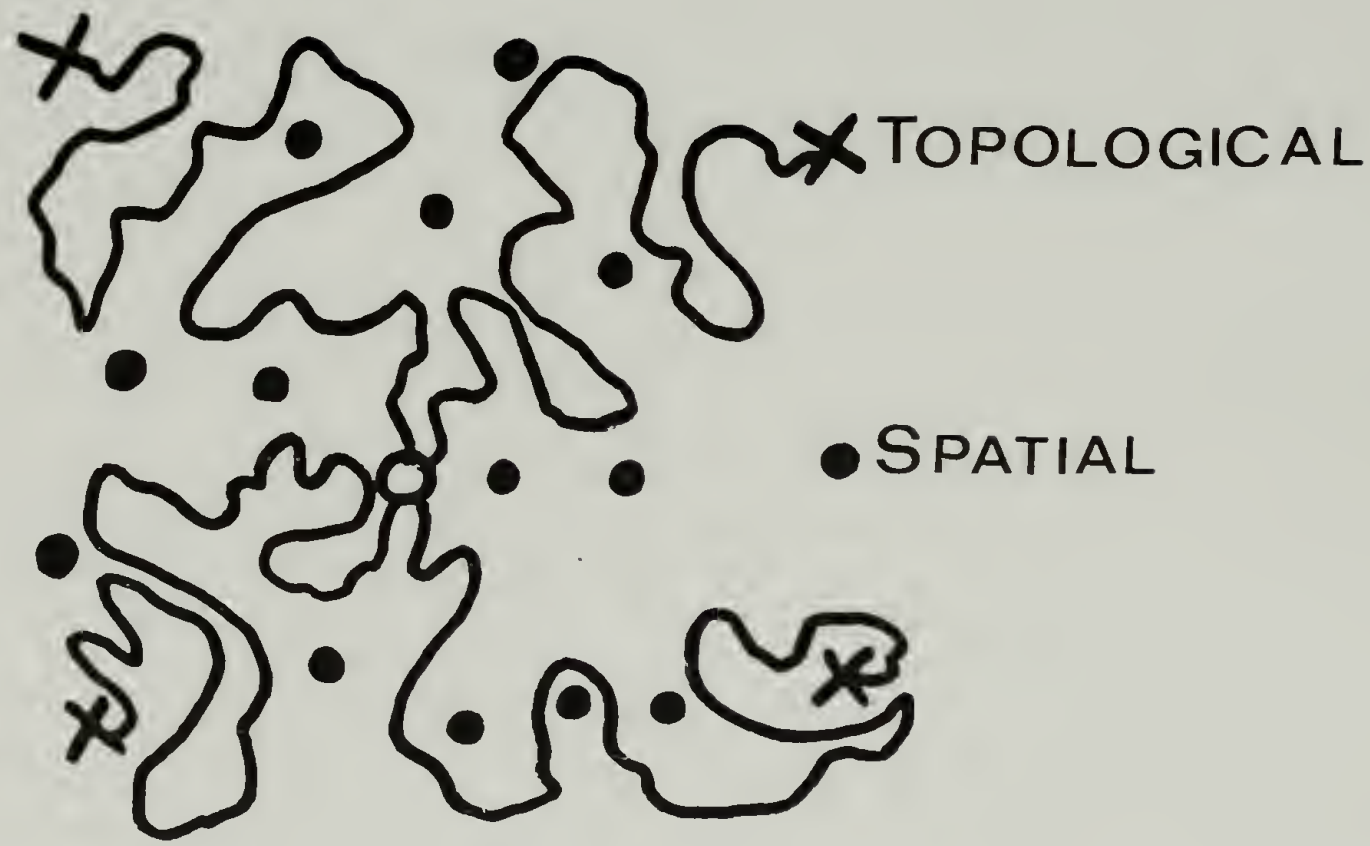

Fig 32. Sketch of topological and spatial neighbouring crosslinks in a network.

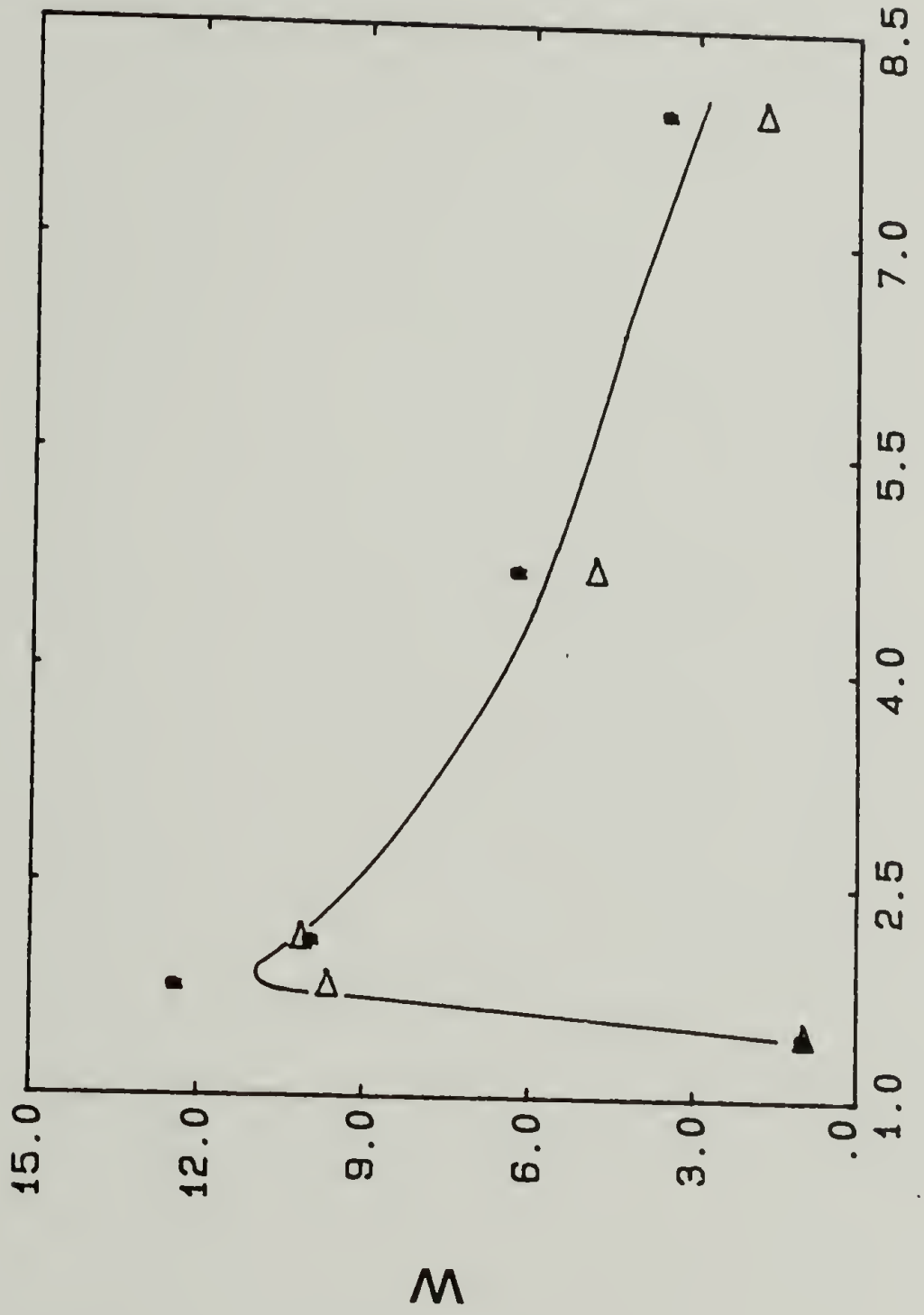

Fig 33. W vs < n / ϕ >

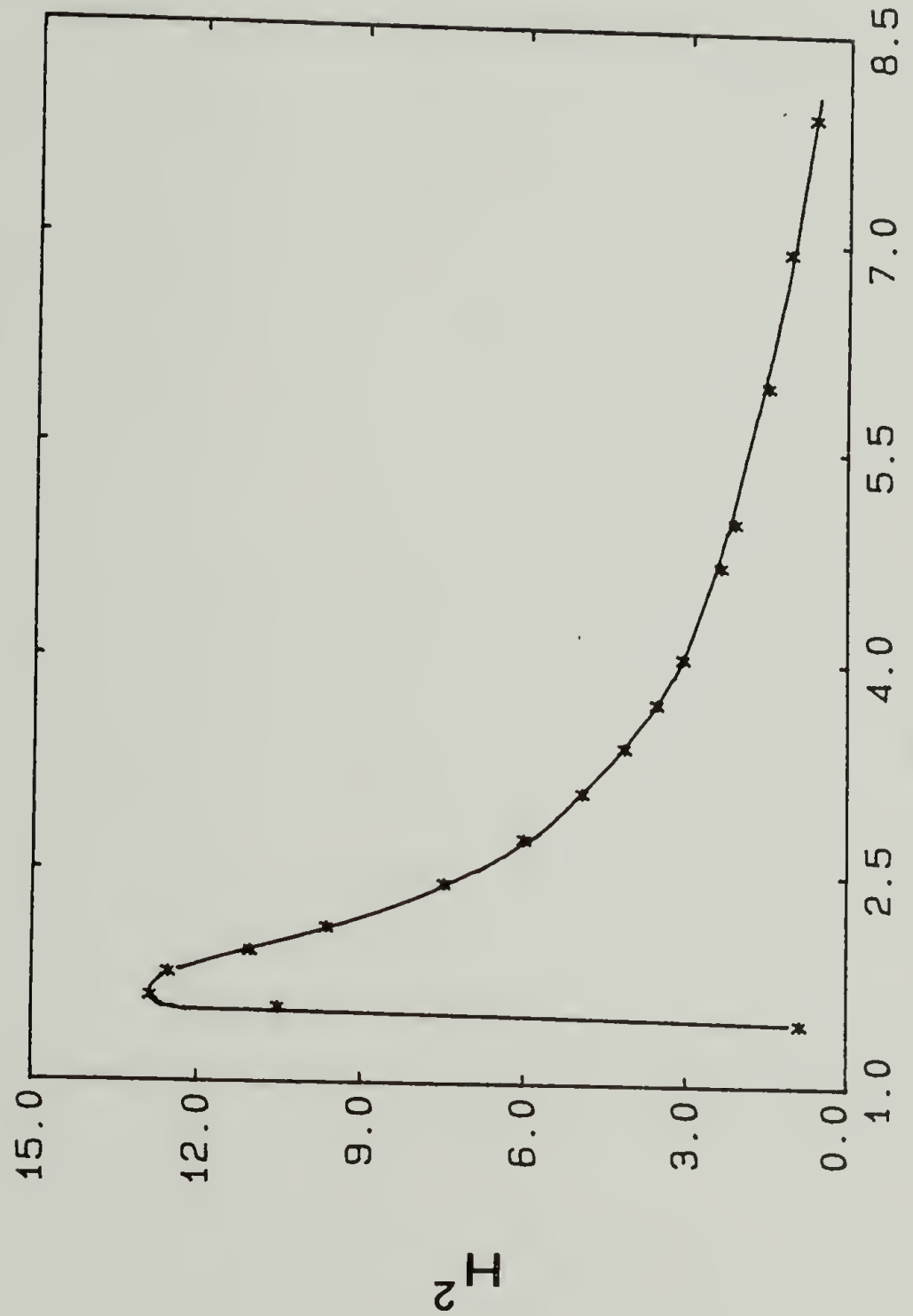

Fig 34. H^2 vs < n / ϕ > for bimodal PDMS networks.

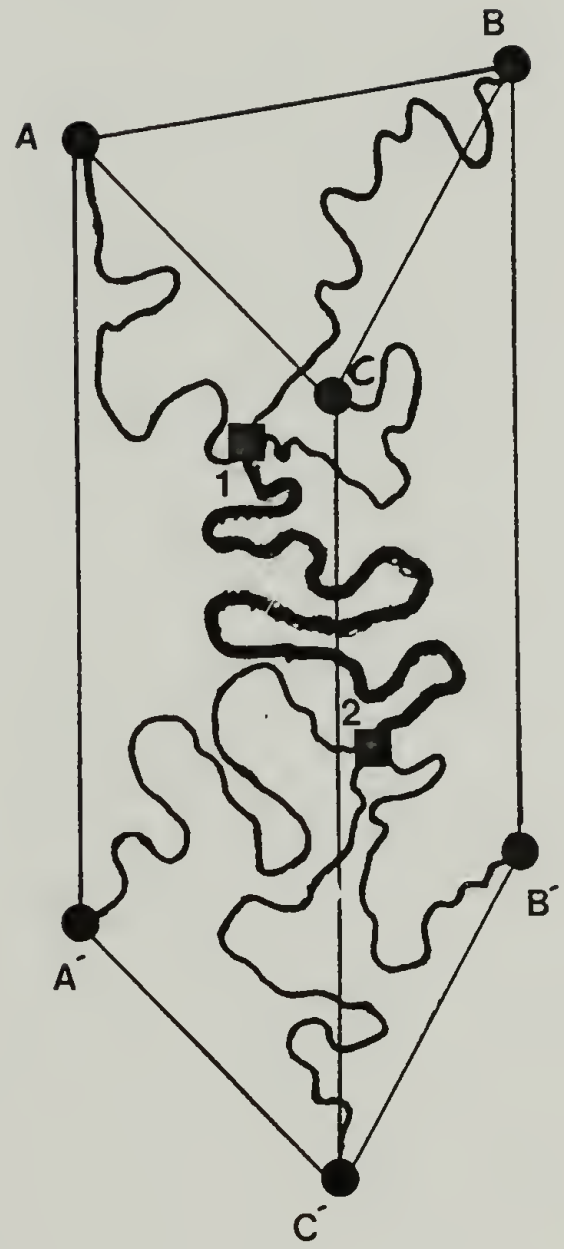

Fig 35. Prism cell model for networks.

BIBLIOGRAPHY

Akcasu A.Z., Summerfield G.C., Jahshan S.N., Han C.C., Kim C.V. and Yu H., J. Polym. Sci., Polym. Phys., Ed., 18, 863 (1980)

Bacon G.E., Neutron Diffraction, 3rd Ed., Oxford University Press, London (1975)

Bastide J., Picot C. and Candau S., J. Macromol. Sci., Phys., B19, 13 (1981)

Bastide J., Dupplesix R., Picot C. and Candau S., Macromolecules, 17, 83 (1984)

Bell J.P., J. Appl. Polym. Sci., 27, 3503 (1982)

Beltzung M., Picot C., Rempp P. and Herz J., Macromolecules, 15, 1594 (1982)

Beltzung M., Herz J. and Picot C., Macromolecules, 16, 580 (1983)

Beltzung M., Herz J. and Picot C., Macromolecules, 17, 663 (1984)

Benoit H. et al, J. Polym. Sci., Polym. Phys. Ed.,14, 2119 (1976)

Brandrup J. and Immergut E.H., Ed., Polymer Handbook John Wiley (1975)

Bueche F., J. Colloid Interface. Sci., 33, 61 (1970)

Bullough R.K., J. Polym. Sci., 46, 517 (1960)

Candau S., Bastide J. and Delsanti M., Adv. Polym. Sci., 44, 27 (1982)

Carpenter R.L., Kan H.-C. and Ferry J.D., Polym. Eng. Sci., 19, 266 (1979)

Curro J.G. and Mark J.E., J. Chem. Phys., 80, 4521 (1984)

Daoud M. and Cotton J.P., J. Phys., Paris, 13, 531 (1982)

Debye P. and Bueche A.M., J. Appl. Phys., 20, 518 (1949)

Debye P. and Bueche A.M., J. Chem. Phys., 1423 (1950)

Debye P., Anderson H.R. and Brumberger H., J. Appl. Phys., 28, 679 (1957)

de Gennes P.G., Scaling Concepts in Polymer Physicis Cornell University Press, Ithaca, New York (1979)

Dole M., The Radiation Chemistry of Macromolecules, Academic Press, New York (1973)

Dossin L.M. and Graessley W.W., Macromolecules, 12, 123 (1979)

Dusek K., Plestil J., Lednicky F. and Lunak S., Polymer, 19, 393 (1978)

Edwards S.F., Proc. Phys. Soc., 88, 265 (1966)

Einstein A., Ann. de Physik., 33, 1275 (1910)

Erman B. and Flory P.J., Macromolcules, 15, 806 (1982)

Flory P.J. and Rehner J., J. Chem. Phys., 11, 512 (1943)

Flory P.J. and Rehner J., J. Chem. Phys., 11, 521 (1943)

Flory P.J., Chem. Revs., 35, 51 (1944)

Flory P.J., Ind. Eng. Chem., 38, 417 (1946)

Flory P.J., J. Chem. Phys., 15, 397 (1947)

Flory P.J., Principles of Polymer Chemistry, Cornell University Press, Ithaca, New York (1953)

Flory P.J., Statistical Mechanics of Chain Molecules, Interscience, New York (1969)

Flory P.J., Proc. R. Soc. London, Ser. A, 351 (1976)

Flory P.J., Macromolecules,12, 119 (1979)

Flory P.J. and Erman B., Macromolcules, 15, 800 (1982)

Funke W., Beer W. and Seitz U., Progr. Coll. & Polym. Sci., 57, 48 (1975)

Golub M.A., J. Polym. Sci., 25, 373 (1957)

Gottlieb M., Macosko C.W., Benjamin G.S., Meyers K.O. and Merrill E.W., Macromolecules, 14, 1039 (1981)

Gottlieb M. and Macosko C.W., Macromolcules, 15, 535 (1982)

Hampton R.R., Anal. Chem., 21, 923 (1949)

Hertz J., Rempp P. and Borchard W., Adv. Polym. Sci. 26, 105 (1978)

Higgins J.S. and Stein R.S., J. Appl. Cryst., 11, 346 (1978)

Hinkley J.A., Han C.C., Mozer B. and Yu H., Macromolecules, 11, 836 (1978)

Huglin M.B., Light Scattering from Polymer Solutions, Academic Press, London (1972)

Huglin M.B. and Sokro M.B., Polymer, 21, 651 (1980)

James H.M. and Guth E., J. Chem. Phys., 15, 651 (1947)

Kaye W. and McDaniel J.B., Appl. Opt., 13, 1934 (1974)

Kenyon A.S. and Nielson L.E., J. Macromol. Sci. (A), 3, 275 (1969)

Kerker M., The Scattering of Light and other Electromagnetic Radiation, Academic Press, New York (1969)

Koberstein J.T., Ph.D. Thesis, University of Massachusetts, Amherst (1979)

Koberstein J.T., Morra B. and Stein R.S., J. Appl. Cryst., 13, 34 (1980)

Kosc M. and Ziabicki A., Macromolecules, 17, 678 (1984)

Kratky O., Pure and Appl. Chem., 12, 483 (1966)

Kreibich U.T. and Schmid R.J., J. Polym. Sci., Polym. Symp., 53, 177 (1975)

Kuhn W., Kolloid Z., 76, 258 (1936)

Kuhn W., Angew. Chem., 51, 640 (1938)

Langley N.R., Macromolcules, 1, 348 (1968)

Langley N.R. and Polmanteer K.E., J. Polym. Sci., Polym. Phys. Ed., 12, 1023 (1974)

Lenz R.W., Organic Chemistry of Synthetic High Polymers, Interscience, New York (1967)

Levy S., Thesis, Universite Louis Pasteur, Strasbourg (1964)

Llorente M.A. and Mark J.E., J. Chem. Phys., 71, 682 (1979)

Llorente M.A. and Mark J.E., Macromolecules, 13, 681 (1980)

Llorente M.A., Andrady A.L. and Mark J.E., J. Polym. Phys., Ed., 19, 621 (1981)

Llorente M.A., Andrady A.L. and Mark J.E., Colloid. Polym. Sci., 259, 1056 (1981)

Loan L.D., J. Appl. Polym. Sci., 7, 2259 (1963)

Luttgert K.E. and Bonart R., Progr. Coll. & Polym. Sci., 64, 48 (1975)

Maconnachie A. and Richards R.W., Polymer, 19, 739 (1978)

Malotky L.O. and Morton M., Polymer Preprints, 15(1), 714 (1974)

Mark J.E. and Sullivan J.L., J. Chem. Phys., 66, 1006 (1977)

Mark J.E., Adv. Polym. Sci., 44, 1 (1982)

Mark J.E., in Elastomers and Rubber Elasticity, Mark J.E. and Lal J. Ed., Am. Chem. Soc., Washington D.C. (1982)

Mark J.E. and Curro J.G., J. Chem. Phys., 79, 5705 (1983)

Meyer K.H. and Ferri C., Helv. Chem. Acta., 18, 570 (1935)

Meyers K.O., Bye M.L. and Merrill E.W., Macromolecules, 13, 1045 (1980)

Miller D.R. and Macosko C.W., Macromolcules, 9, 206 (1976)

Miyake A. and Freed K.F., Macromolecules, 17, 678 (1984)

Mooney M., J. Appl. Phys., 11, 582 (1940)

Moore C.G. and Watson W.F., J. Polym. Sci., 19, 237 (1956)

Moritani M., Inoue T., Motegi M. and Kawai H., Macromolecules, 3, 433 (1970)

Parks C.R. and Lorenz O., J. Polym. Sci., 50, 287 (1961)

Pearson D.S., Skutnik B.J. and Bohm G.G.A., J. Polym. Sci., Polym. Phys. Ed., 12, 925 (1974)

Pearson D.S., Macromolecules, 10, 696 (1977)

Picot C., in Static and Dynamic Properties of the Polymeric Solid State, R.A. Pethric and R.W. Richards, Eds., D. Reichel Publishing Company (1979)

Porod G., Kolloid Z., 124, 83 (1951)

Queslel J.P. and Mark J.E., Adv. Polym. Sci., 65, 135 (1984)

Rowland T.J. and Labun L.C., Macromolecules 14, 1468 (1981)

Schaefer D.W., Joanny J.F. and Pincus P., Macromolecules, 13, 1280 (1980)

Schaefer D.W., Polymer, 25, 387 (1984)

Schultz A.R., in Chemical Reactions of Polymers, E.M. Fettes, Ed., Interscience, New York (1964)

Schulz G.V., Z. Physik. Chem., B43, 25 (1939)

Siemann U. and Ruland W., Colloid Polym. Sci., 260, 999, (1982)

Smith K.J., in Elastomers and Rubber Elasticity, Mark J.E. and Lal J., Eds., Am. Chem. Soc., Washington D.C. (1982)

Sperling L.H., Polymer. Eng. Sci., 24, 1 (1984)

Stein R.S. and Keane J.J., J. Polym. Sci., 17, 21 (1955)

Stein R.S., Wilson P. and Stidham S.N., J. Appl. Phys 34, 46 (1963)

Stein R.S., J. Polym. Sci., Polym. Lett., 7, 657, (1969)

Stein R.S., Farris R.J., Kumar S. and Soni V., in Elastomers and Rubber Elasticity, Mark J.E. and Lal J., Eds., Am. Chem. Soc., Washington D.C. (1982)

Sung P.-H and Mark J.E., Polym. J., 12, 835 (1980)

Sung P.-H and Mark J.E., J. Polym. Sci., Polym. Phys. Ed., 19, 507 (1981)

Takahama T. and Geil P.H., Die Makromol. Chemie, Rapid Commun., 3, 389 (1982)

Toblosky A.V., Properties and Structures of Polymers, John Wiley and Sons, New York (1960)

Treloar L.R.G., The Physics of Rubber Elasticity, 3rd Ed., Clarendon, Oxford (1975)

Ullman R., Macromolecules, 15, 582 (1982)

Valles E.M. and Macosko C.W., Macromolecules, 12, 521 (1979)

Van de Hulst H.C., Light Scattering by Small Particles, John Wiley and Sons, New York (1957)

Van der Hoff B.M.E., Appl. Polym. Symp., 7, 21 (1968)

Wall F.T. and Flory P.J., J. Chem. Phys., 19, 1435 (1951)

Wu W. and Bauer B.J., Polym. Comm., 26, 39 (1985)

Wun K.L. and Prins W., J .Polym. Sci., Polym. Phys., Ed., 12, 533 (1974)

Yang H., Ph.D. Thesis, Univ of Massachusetts, Amherst (1984)

Yuen H.K. and Kinsinger J.B., Macromolecules, 7, 329 (1974).

Zimm B.H., J. Chem. Phys., 16, 1093 (1948)